4) The geothermal structure in the survey area is estimated to be the fault structure from the result of 2-D modeling analysis. The three major faults, which may control geothermal fluid movement and geothermal system in the area, are very important.

II.3.3 Mise-á-la-masse survey

1. Objectives

The Mise-á-la-masse (charged potential) survey was carried out in order to estimate the geothermal structure around the well which was drilled for the heat flow measurement in the most prospective area.

2. Survey procedure

(1) Measuring procedure

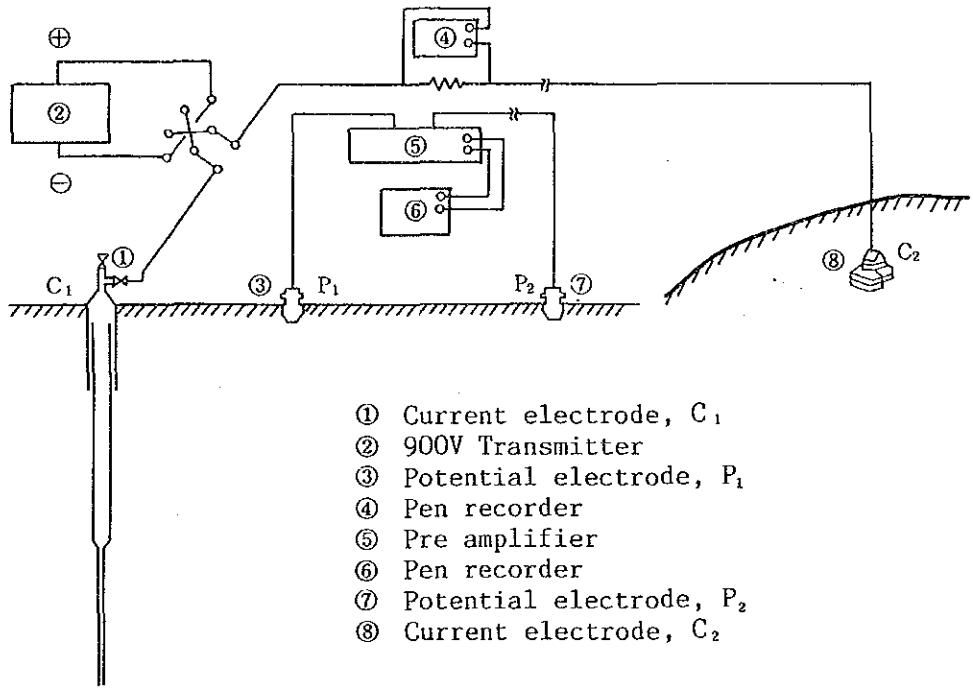

Fig. II.3.47 Equipment layout for Mise-á-la-masse measurement

Fig. II.3.47 shows the equipment layout for Mise-á-la-masse measurement. As shown in the figure, two current electrodes (C_1, C_2) and two potential electrodes (P_1, P_2) were used for the measurement. One of current electrodes, C_2, was earthed at the point as far as possible from the survey area. The potential electrodes, P_1 and P_2, were used for the measurement of the potential difference which was excited by the current flowing into the geothermal reservoir and/or hydrothermally altered zone. One of potential electrodes, P_1, was fixed, and the other, P_2, was movable in the survey area. In this survey, in addition to C_1 which is connected to 200 m casing pipes in DG-1, two other current electrodes were applied such as 500 m casing pipes and a point source. The casing pipes of 500 m length were provisionally installed for the measurement in order to obtain the data concerned with the resistivity distribution caused by depth differences. On the other hand, the point source was also provisionally installed to obtain the resistivity distribution of the shallow part in the survey area. The fixed current electrode, C_2, was installed by burying ten plates of copper and stainless bars in the mud pond near the river. In order to decrease the contact resistance, 20 kg of salt was scattered in the soil as electrolytes. The fixed potential electrode, P_2, was installed in the cotton field to the west far from DG-1, and every morning it was watered to retain the dampness to prevent high contact resistance.

(2) Analysis procedure

Fig. II.3.48 shows the flow of analysis for Mise-á-la-masse measurement. The data obtained from the survey was processed and analyzed according to this flow. The analysis was carried out by calculating the residual resistivities which are obtained by subtracting the theoretical resistivities from the observed resistivities. The apparent resistivities are calculated from the equation based on the theoretical potential which is generated by one line source and one point source. On the other hand, the theoretical resistivities are calculated from the linear equation using the least squared method which is defined by factors such as the observed apparent resistivities and the distance from the well to each point.

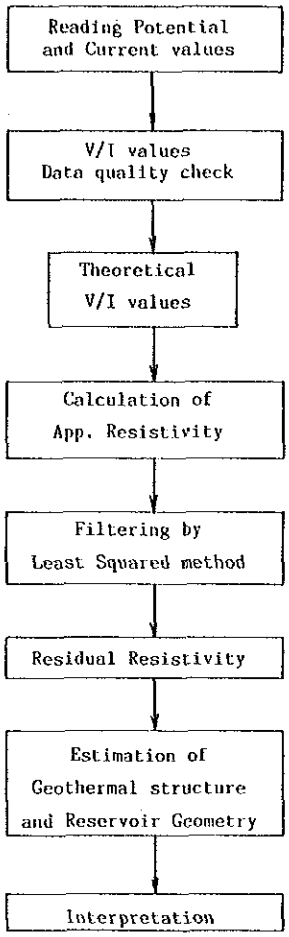

Fig.Ⅱ.3.48 Flow of analysis for Mise-á-la-masse measurement

3. Results and interpretation

(1) V/I map

The patterns of the V/I maps by a point source, 200 m casing pipes and 500 m casing pipes show the same tendency as a whole. And in accordance with seeing the patterns starting from a point source to 500 m casing pipes, the contour distortions become large.

This is based on the principle that a long current line source is more effective in sending the current directly in deeper part of subsurface and to obtain information on the deep electrical structure.

However, the difference in contour distribution between the 200 m and 500 m casing pipes is not so clear, whereas the difference between the point source and the 200 m or 500 m casing pipes is clear.

The features in the V/I map is as follows:

1) V/I map by a point source (Fig. II.3.49)

The measured V/I values range between 0.6 m V/A and 4.2 mV/A. The contours show roughly concentric circles centered around DC-1 which is used as a current electrode C_1. The contours of the northeastern and southwestern parts are distorted outwards, and this shows the existence of resistivity anomalies in and around those distorted parts.

2) V/I map by 200 m casing pipes (Fig. II.3.50)

V/I values range between 0.6 mV/A and 4.2 mV/A. The contour pattern shows a quasi-triangle shape caused by fault-like structures trending NW-SE and NE-SW from the elongation and trend of contours except around DG-1.

Along these directions, the contours have a high density and are distorted, so that faults are estimated to trend those directions as seen in Fig. II.3.51.

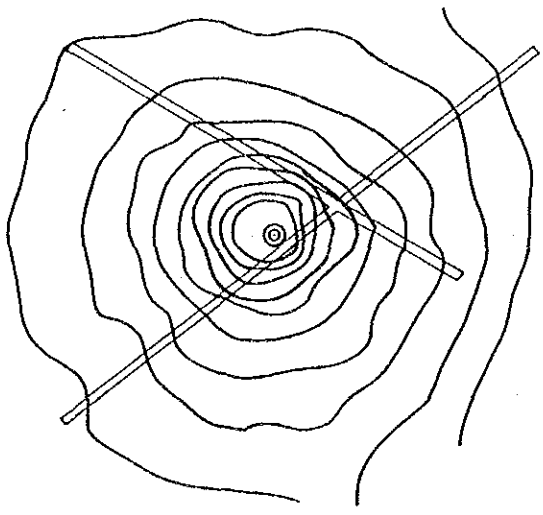

Fig.II.3.51 Lineament estimated from V/I distribution

3) V/I map by 200 m casing pipes (Fig. II.3.52)

The V/I values roughly range between 0.6 mV/A and 4.2 mV/A. The pattern of the V/I distribution is almost the same as the previous one.

The tendency of contour distortion and elongation is more emphasized than those of previous maps.

(2) Theoretical potential map (Fig. II.3.53)

The theoretical potential maps from the point source, 200 m casing pipes and 500 m casing pipes show almost the same distribution patterns, so that the map by 500 m casing pipes will be explained as a representative.

The contours show nearly concentric circles centering DG-1, and the values decrease exponentially in accordance with the distance from DG-1 to each point. The values include the effect by topography and electrode configuration, however the effect of topography is not recognized clearly because there are no distorted parts. The effect of the electrode configuration is not recognized clearly near DG-1, whereas it is recognized as getting larger in proportion to the distance from DG-1.

Hence, contour intervals in the west part of DG-1 increase more than those in the east part in accordance with distance from DG-1. This is because C_2 the fixed current electrode 6 km from DG-1, was installed in the eastern part of the survey area.

(3) Apparent resistivity map (Fig. II.3.54 to II.3.56)

In the distribution patterns of the apparent resistivities using these kinds of current source, those figures show nearly similar distribution. As described previously, the pattern obtained from line source using long casing pipes which can send the current in deeper part directly seems to reflect the deep structure rather than that from a point current source.

The features are explained as follows:

1) The contours show an ellipse form whose major axis trends from the northeast to the southwest, so that a fault-like structure trending in that direction is estimated at Kaynarca.

2) From the elongation of the contours distorted outwards, a fault-like structure trending northwest to southeast is estimated.

3) The contour density in the northeastern part is small, and contours elongate outwards remarkably. This tendency is clear when using 500 m casing pipes.

The northeastern deeper part is considered that low resistivity zone or the sudden changes of resistivities by geological difference may exist.

4) The two fault-like structures trending northwest to southeast and northeast to southwest are inferred in the area where geothermal manifestations are recognized, so that these structures and the intersection of these structures are considered to be closely related to the geothermal structure in the area.

(4) Residual resistivity map

From the residual resistivity map, it is possible to study the geothermal structure and reservoir structure in detail. The features of residual resistivity maps obtained from three kinds of current sources are explained as follows:

1) Residual resistivity map by a point source (Fig. II.3.57)

Residual resistivities range from -2.0×10^{-4} mV/A to 1.5×10^{-4} mV/A. The anomaly pattern seems to be correlated with the pattern of fault-like structures estimated from apparent resistivity maps.

2) Residual resistivity map using 200 m casing pipes (Fig. II.3.58)

Residual resistivities range from -2.5×10^{-4} mV/A to 1.5×10^{-4} mV/A.

The anomaly pattern is almost the same as that of the point source excluding the low anomaly near DG-1. The anomaly center trending northeast to southwest near DG-1 moved to the southern part. It indicates that the fault-like structure trending in that direction is dipping in a southern direction, and DG-1 seems to have been

drilled at the shallower part of that fault.

This tendency is emphasized in the residual map using 500 m casing pipes. Therefore, the fault-like structure trending in that direction is important to study geothermal structure in this area. In the northeastern part, the low residual anomaly is also recognized, and the boundary contour of 0 mV/A between low and high residual anomalies shows a linear structure trending northwest to southeast. This structure is interpreted to be a fault trending in that direction, especially judging from the contour shape.

3) Residual resistivity map using 500 m casing pipes (Fig. II.3.59)

Residual resistivities range from -2.5×10^{-4} mV/A to 2.5 mV/A. The distribution pattern as a whole is nearly the same as that of the 200 m casing pipes. DG-1 is located to the north of the low anomaly zone, so this means that the low residual anomaly zone trending northeast to southwest moved southward. Thus, in accordance with the residual anomaly movement from a point source to the 500 m casing pipes, the low residual anomaly moves southward as if the fault-like structure is dipping to the south. (Fig. II.3.60)

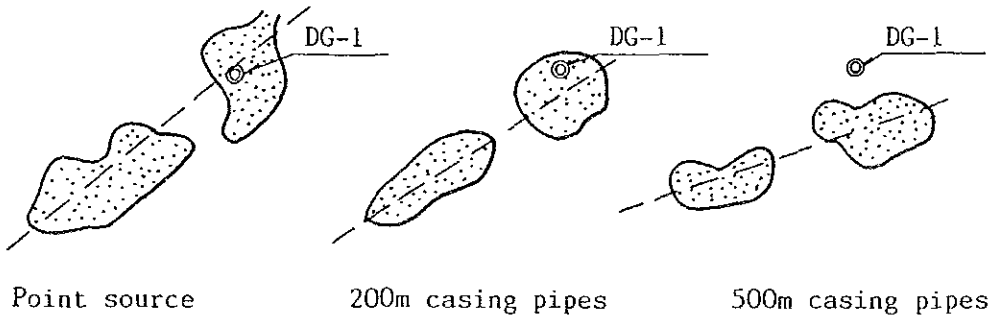

Fig. II.3.60 Difference of low potential anomalies in the case of different current source

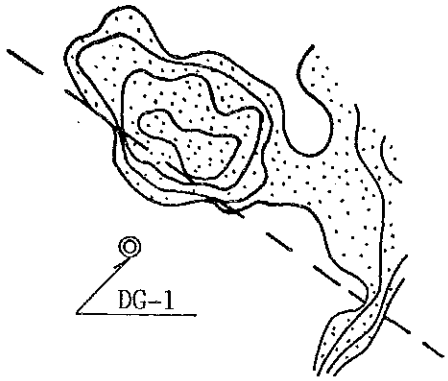

Fig. II.3.61 Fault trending NW-SE direction estimated from low potential anomaly shape in northeastern part of survey area

As described previously, the fault trending northeast to southwest is taking a very important role from the viewpoint of the geothermal structure. If a high temperature geothermal reservoir exists at depth in the area, it is estimated that it may be located further south of DG-1.

Regarding the low residual anomaly in the northeastern part, the fault trending northwest to southeast is inferred from the anomaly shape and contour elongation. (Fig. II.3.61)

(5) Conclusion

The geothermal structure in the Kaynarca geothermal area and the extent of the expected reservoir associated with DG-1 are concluded as follows:

1) Two faults trending northeast to southwest and northwest to southeast are estimated from the shape of the residual anomalies. Hence, these two faults are considered to be major structures which control the geothermal system and thermal structure in the area.

2) The fault trending northeast to southwest is assumed to be dipping southward from the movement of the anomalies near DG-1 when the current source was changed.

3) The geothermal reservoir encontoured by DG-1 may be the shallow part of the fault, so that a deeper reservoir is thought to be located to the south of DG-1.

4) The fault trending northwest to southeast is clearly defined from the CSAMT results, whereas it is estimated from the contour elongation at the boundary between low and high residual anomalies to the northeastern part of DG-1. The area along this fault may be promising from the extent of the low anomaly zone.

(6) Conclusion of electrical surveys

After analysis and interpretation of the two electrical surveys such as CSMAT and Mise-á-la-masse, the conclusion is summarized as follows: (Fig. II.3.62)

1) Estimated faults

The following three major faults are inferred in the survey area.

(a) Fault trending NE-SW direction
..... is recognized remarkably from Mise-á-la-masse results.

(b) Fault trending NW-SE direction
..... is recognized from CSAMT and Mise-á-la-masse results.

(c) Fault trending E-W direction
..... is recognized from CSAMT results.

In these faults, the fault described in (a) shows a relatively good correlation between the two survey results as shown in Fig. II.3.62, but the fault in (b) does not correlate with those two surveys. That is, the fault from CSAMT is located in the Kaynarca geothermal area, whereas the same trending fault from Mise-á-la-masse is located to the northern part of Kaynarca.

Concerning this difference, the Mise-á-la-masse method measures resistivity distribution three-dimensionally, the estimated fault location from CSAMT may be more reliable than that from Mise-á-la-masse.

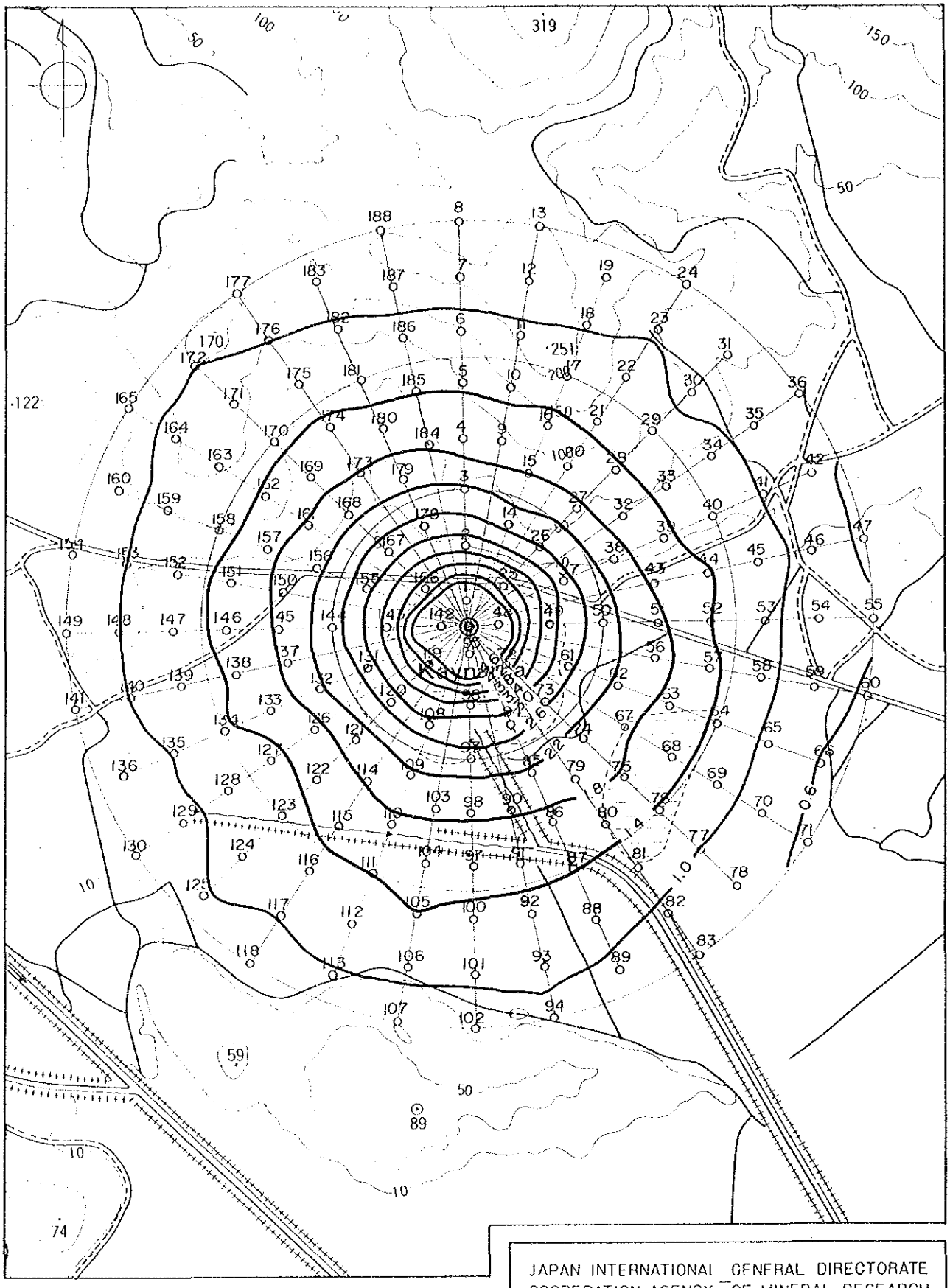

Legend

10
O station number and location

~1.0~ Contour line of V/I (unit : mv/A)

Fig.II.3.49 V/I map (Point source)

JAPAN INTERNATIONAL COOPERATION AGENCY

GENERAL DIRECTORATE OF MINERAL RESEARCH AND EXPLORATION

GEOTHERMAL DEVELOPMENT PROJECT IN DIKILI-BERGAMA FIELD

0 500 1000m

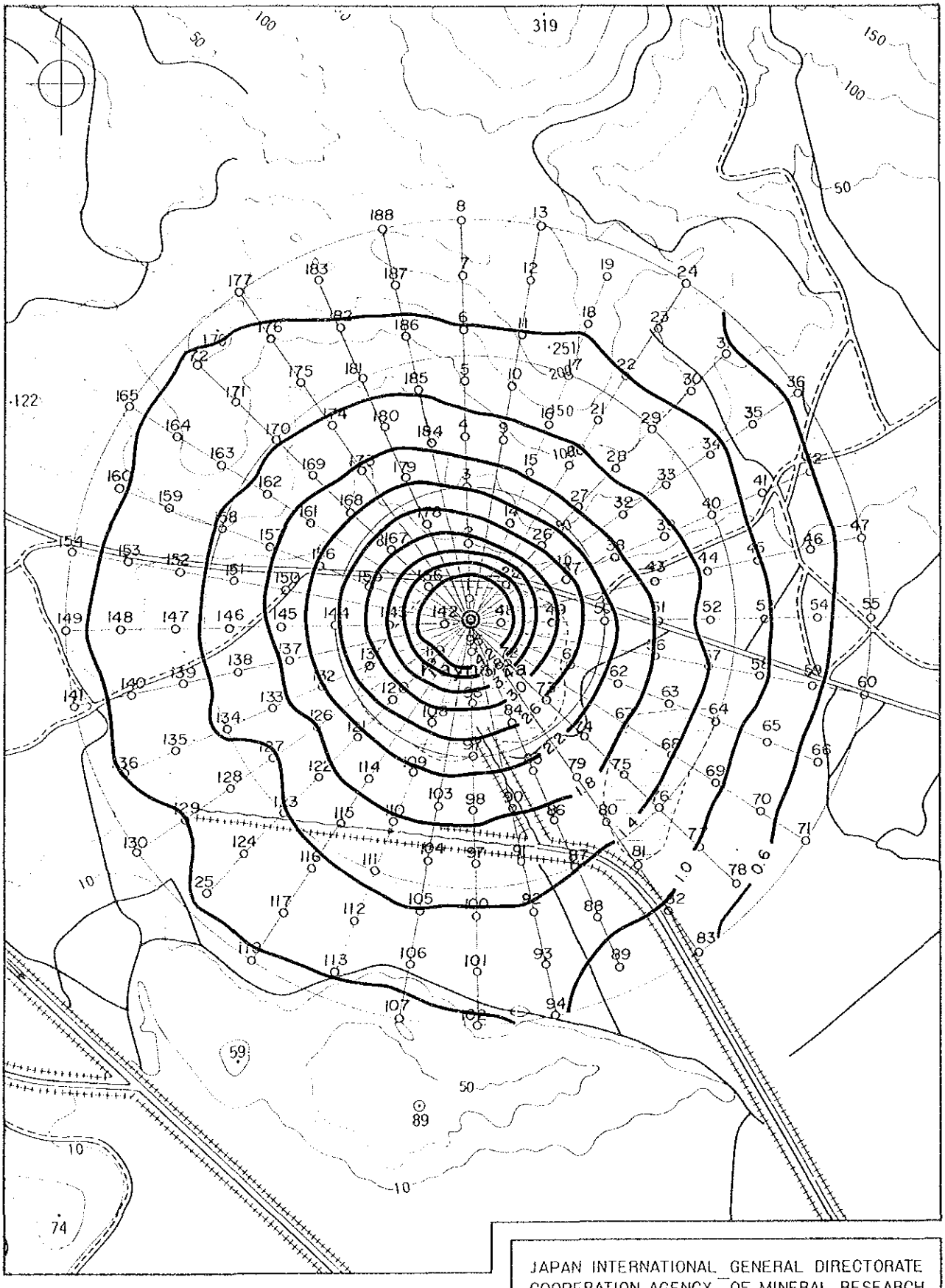

Legend

10
O station number and location

~1.0~ Contour line of V/I (unit : mv/A)

Fig II.3.50 V/I map (200m casing pipe)

JAPAN INTERNATIONAL COOPERATION AGENCY

GENERAL DIRECTORATE OF MINERAL RESEARCH AND EXPLORATION

GEOTHERMAL DEVELOPMENT PROJECT IN DIKILI-BERGAMA FIELD

0 500 1000m

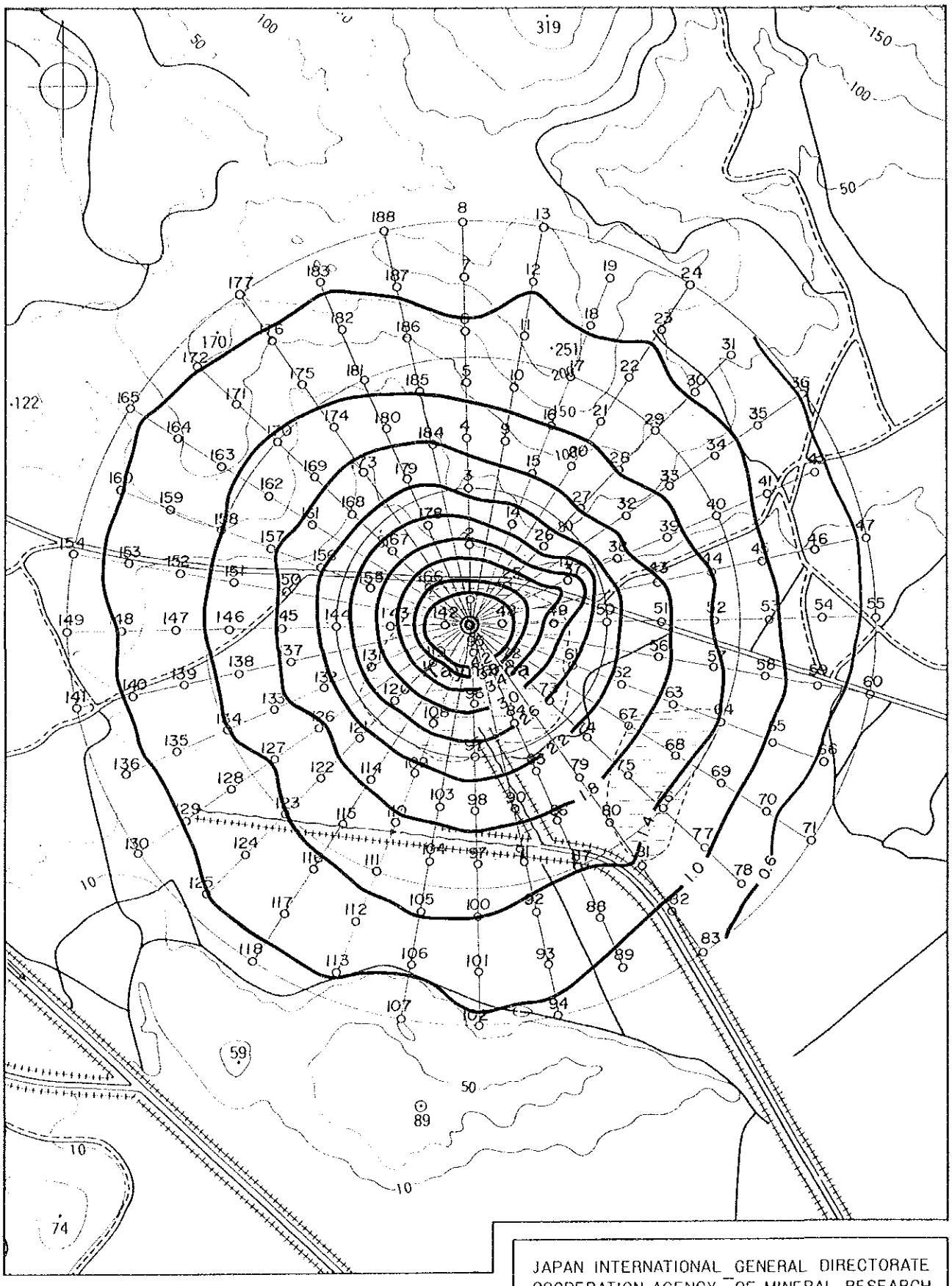

Legend

10
O station number and location

~1.0~ Contour line of V/I (unit : mv/A)

Fig II .3.52 V/I map (500m casing pipe)

JAPAN INTERNATIONAL COOPERATION AGENCY

GENERAL DIRECTORATE OF MINERAL RESEARCH AND EXPLORATION

GEOTHERMAL DEVELOPMENT PROJECT IN DIKILI-BERGAMA FIELD

0 500 1000m

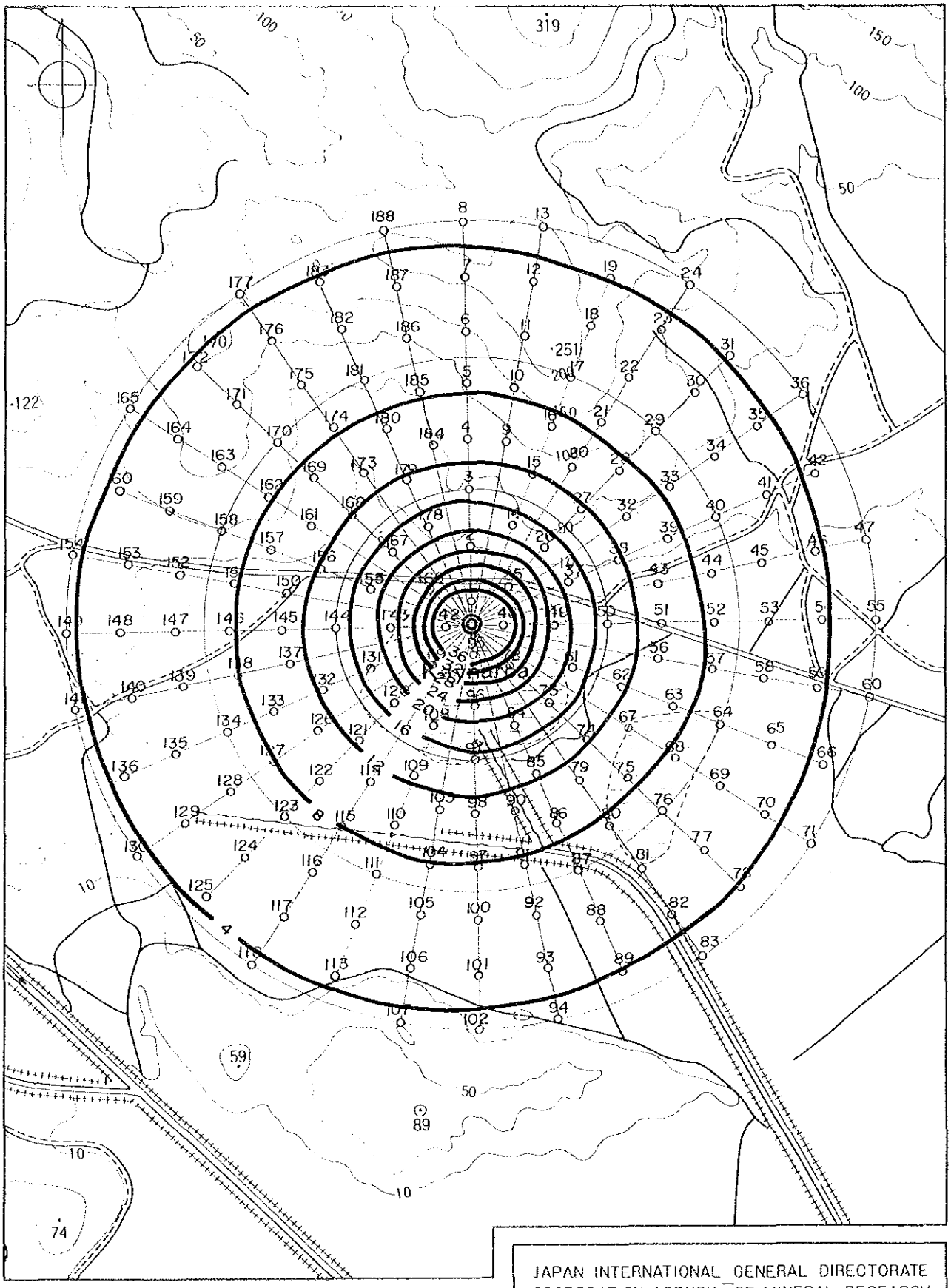

Legend

10 O station number and location

~12~ Contour line of theoretical potential(unit : $10^{-4} \times 1/m$)

Fig.II .3.53 Theoretical potential map

JAPAN INTERNATIONAL COOPERATION AGENCY

GENERAL DIRECTORATE OF MINERAL RESEARCH AND EXPLORATION

GEOTHERMAL DEVELOPMENT PROJECT IN DIKILI-BERGAMA FIELD

0 500 1000m

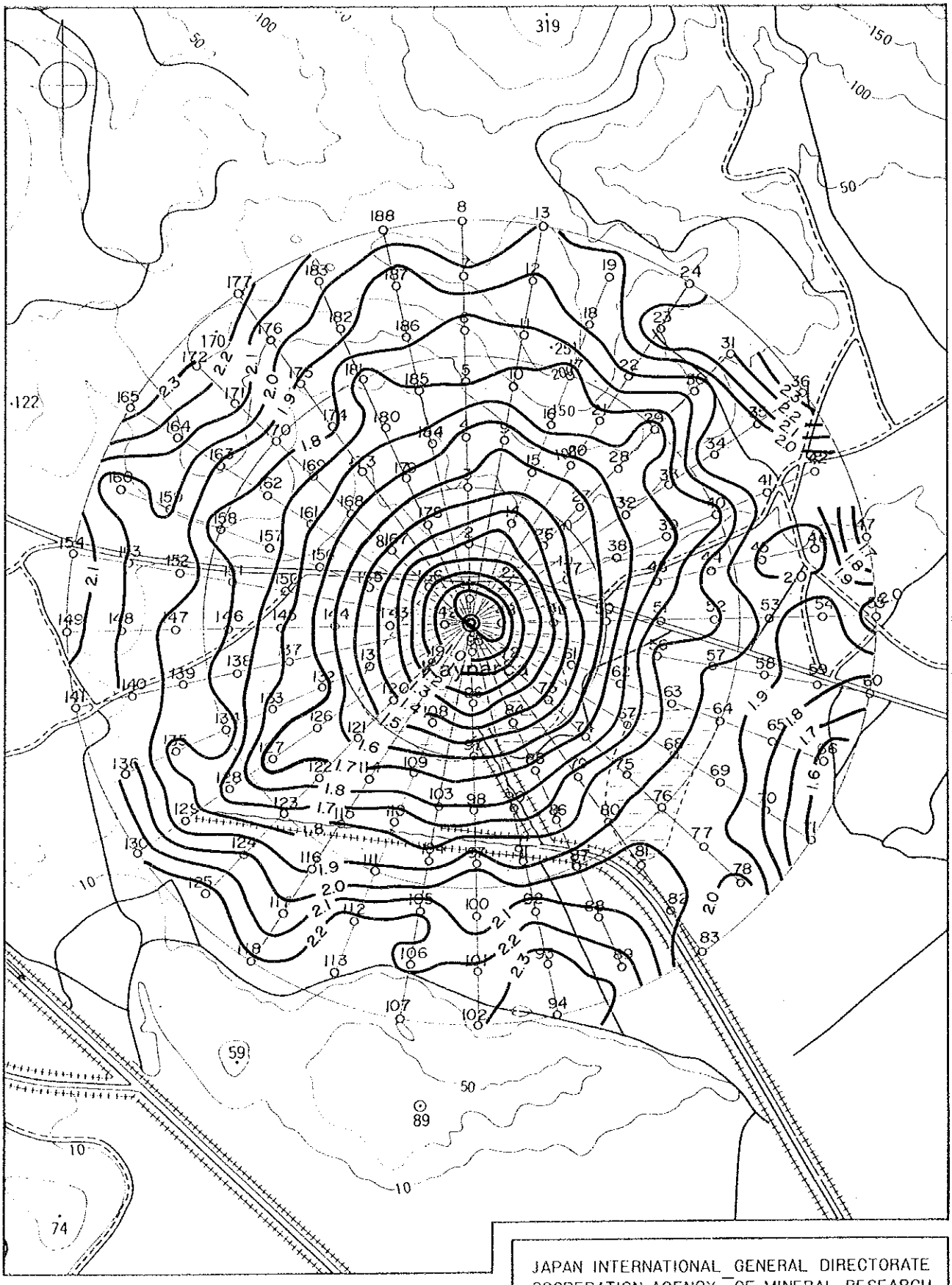

Legend

10
O station number and location

~1.0~ Contour line of apparent resistivity
(unit : 10^{-1} ohm-m)

Fig II.3.54 Apparent resistivity map
(point source)

JAPAN INTERNATIONAL COOPERATION AGENCY

GENERAL DIRECTORATE OF MINERAL RESEARCH AND EXPLORATION

GEOTHERMAL DEVELOPMENT PROJECT
IN
DIKILI-BERGAMA FIELD

0 500 1000m

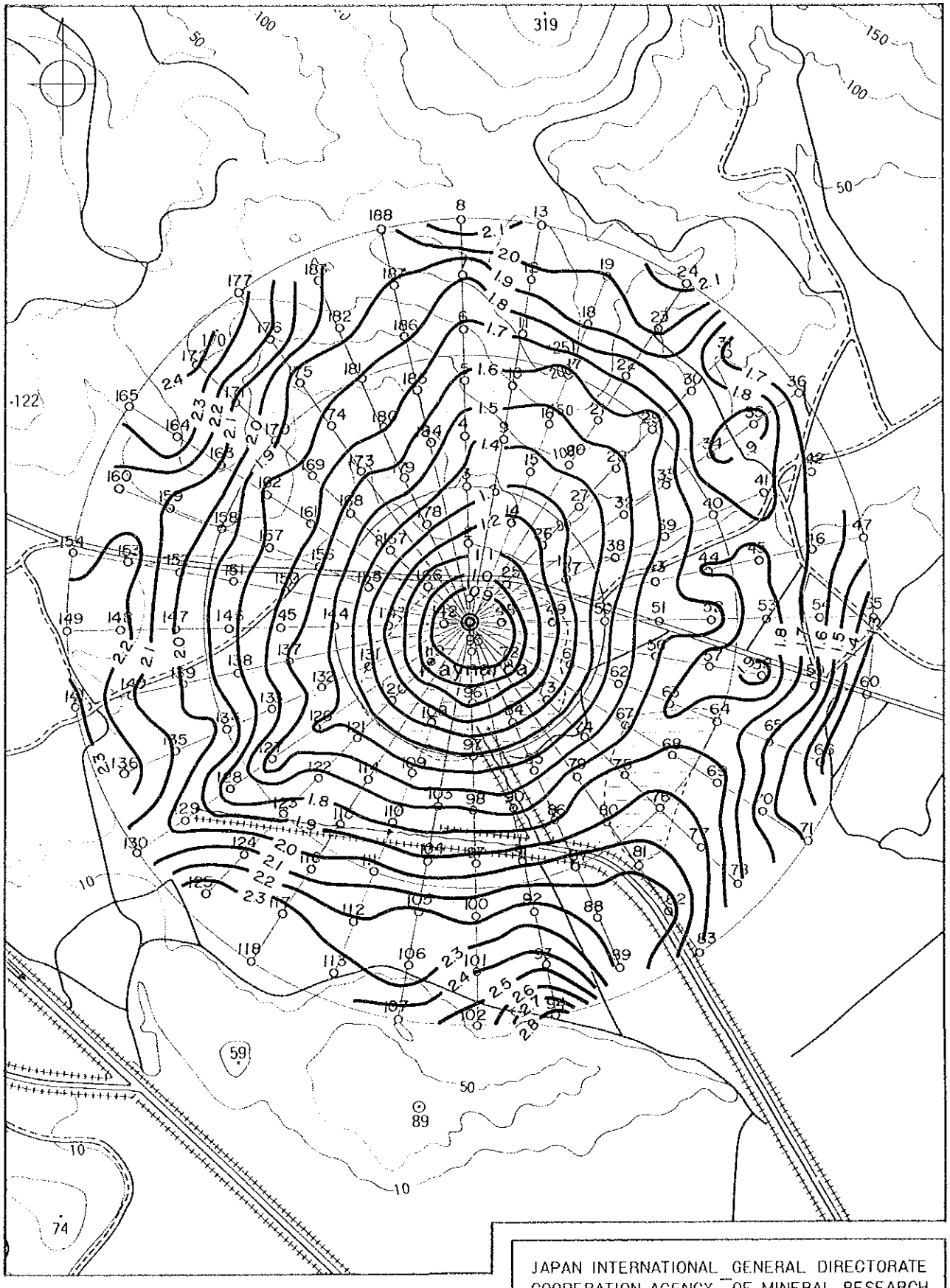

Legend

10
O station number and location

~1.0~ Contour line of apparent resistivity
(unit : 10^{-1} ohm-m)

Fig II.3.55 Apparent resistivity map
(200m casing pipe)

JAPAN INTERNATIONAL COOPERATION AGENCY

GENERAL DIRECTORATE OF MINERAL RESEARCH AND EXPLORATION

GEOTHERMAL DEVELOPMENT PROJECT
IN
DIKILI-BERGAMA FIELD

0 500 1000m

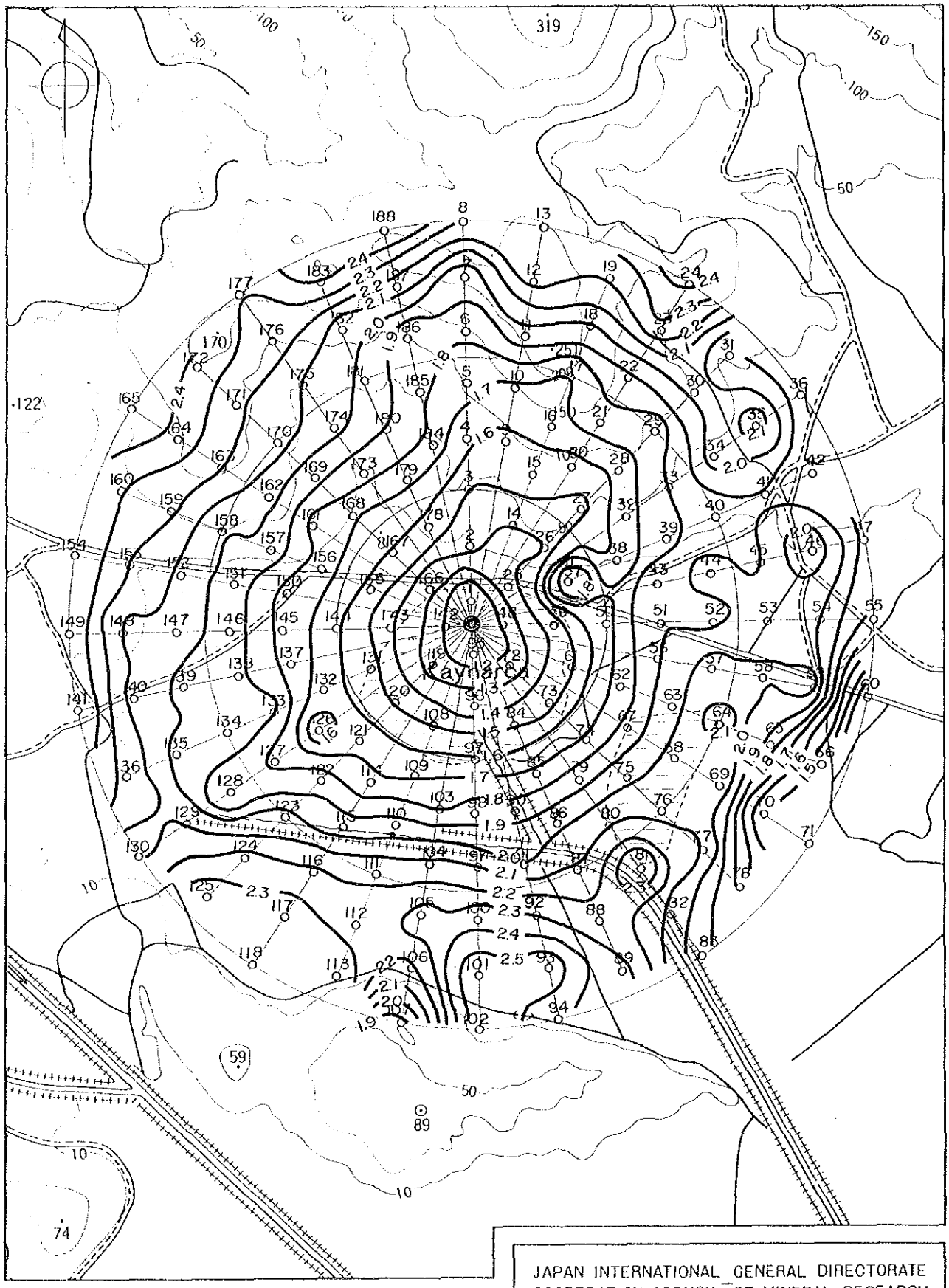

Legend

10 O station number and location

~1.0~ Contour line of apparent resistivity (unit : 10^{-1} ohm-m)

Fig II .3.56 Apparent resistivity map (500m casing pipe)

JAPAN INTERNATIONAL COOPERATION AGENCY

GENERAL DIRECTORATE OF MINERAL RESEARCH AND EXPLORATION

GEOTHERMAL DEVELOPMENT PROJECT IN DIKILI-BERGAMA FIELD

0 500 1000m

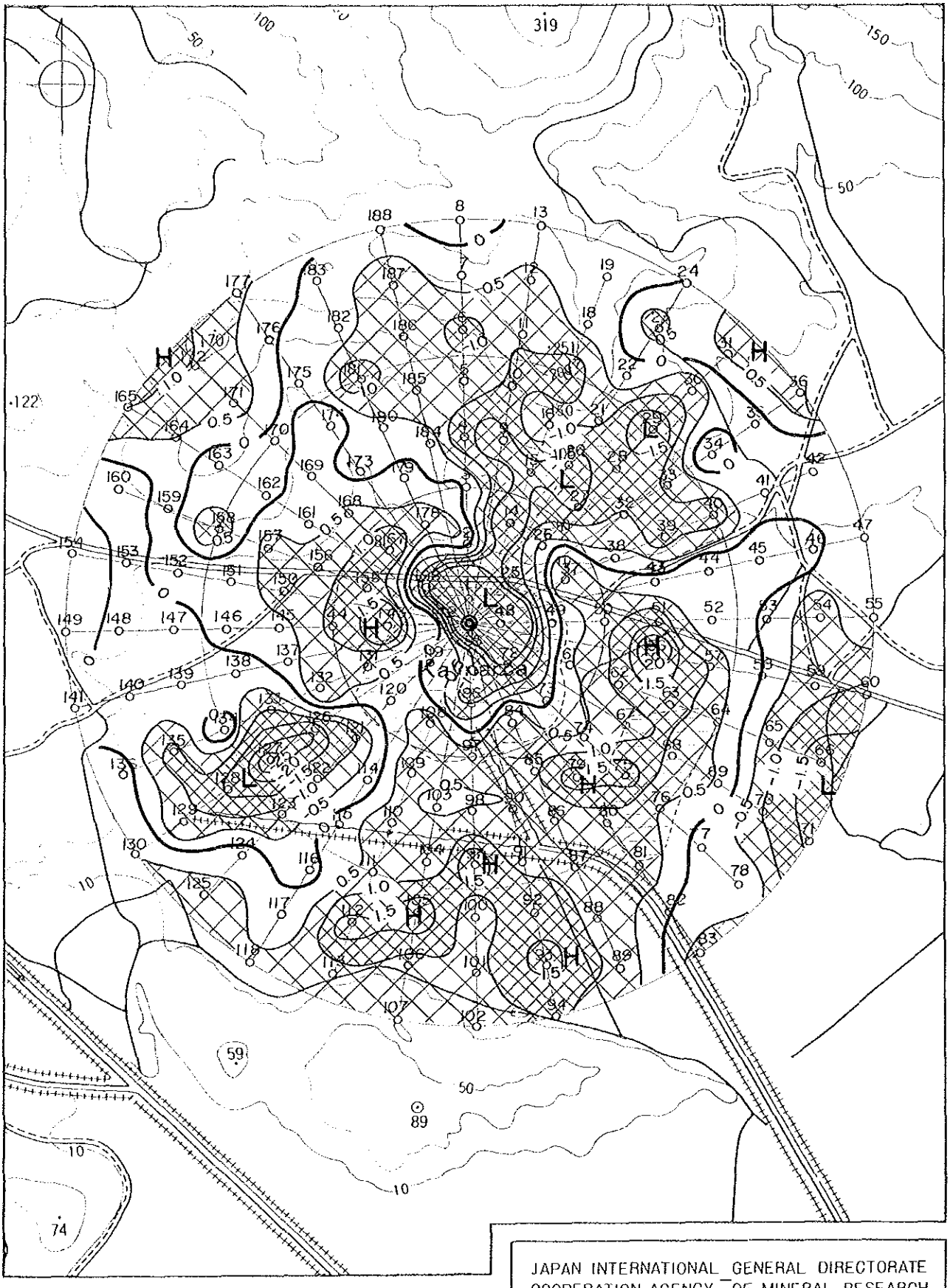

Legend

10 / O station number and location

~O~ Contour line of residual potential (unit : 10^{-4}mv/A)

JAPAN INTERNATIONAL COOPERATION AGENCY

GENERAL DIRECTORATE OF MINERAL RESEARCH AND EXPLORATION

GEOTHERMAL DEVELOPMENT PROJECT IN DIKILI-BERGAMA FIELD

0 500 1000m

Fig II .3.57 Residual potential map (point source)

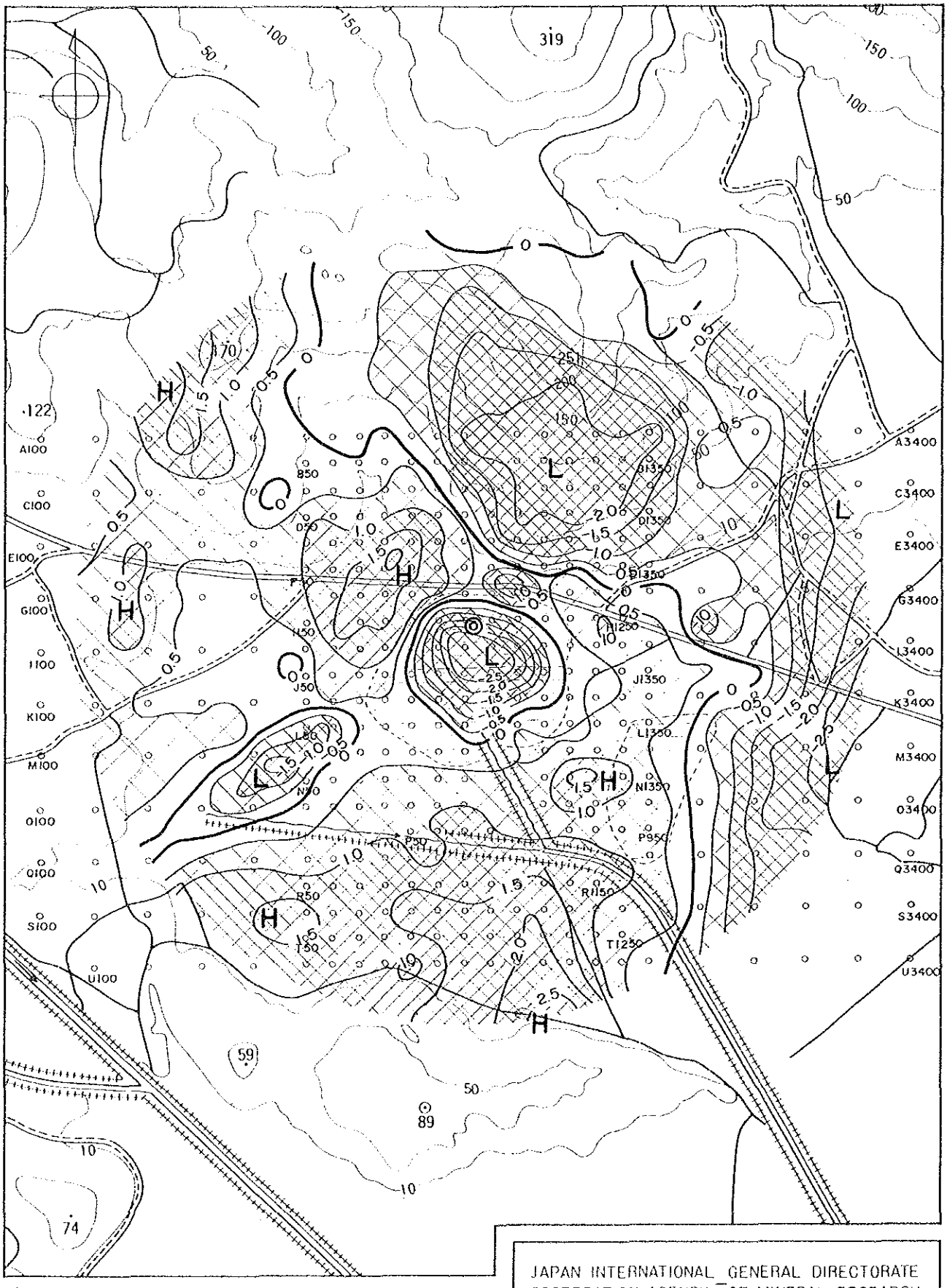

Legend

10
O station number and location

~O~ Contour line of residual potential
(unit : 10^{-4}mv/A)

Fig II.3.58 Residual potential map
(200m casing pipe)

JAPAN INTERNATIONAL COOPERATION AGENCY

GENERAL DIRECTORATE OF MINERAL RESEARCH AND EXPLORATION

GEOTHERMAL DEVELOPMENT PROJECT
IN
DIKILI-BERGAMA FIELD

0 500 1000m

Legend

10
O station number and location

~O~ Contour line of residual potential (unit : 10^{-4}mv/A)

JAPAN INTERNATIONAL COOPERATION AGENCY

GENERAL DIRECTORATE OF MINERAL RESEARCH AND EXPLORATION

GEOTHERMAL DEVELOPMENT PROJECT IN DIKILI-BERGAMA FIELD

0 500 1000m

Fig II .3.59 Residual potential map (500m casing pipe)

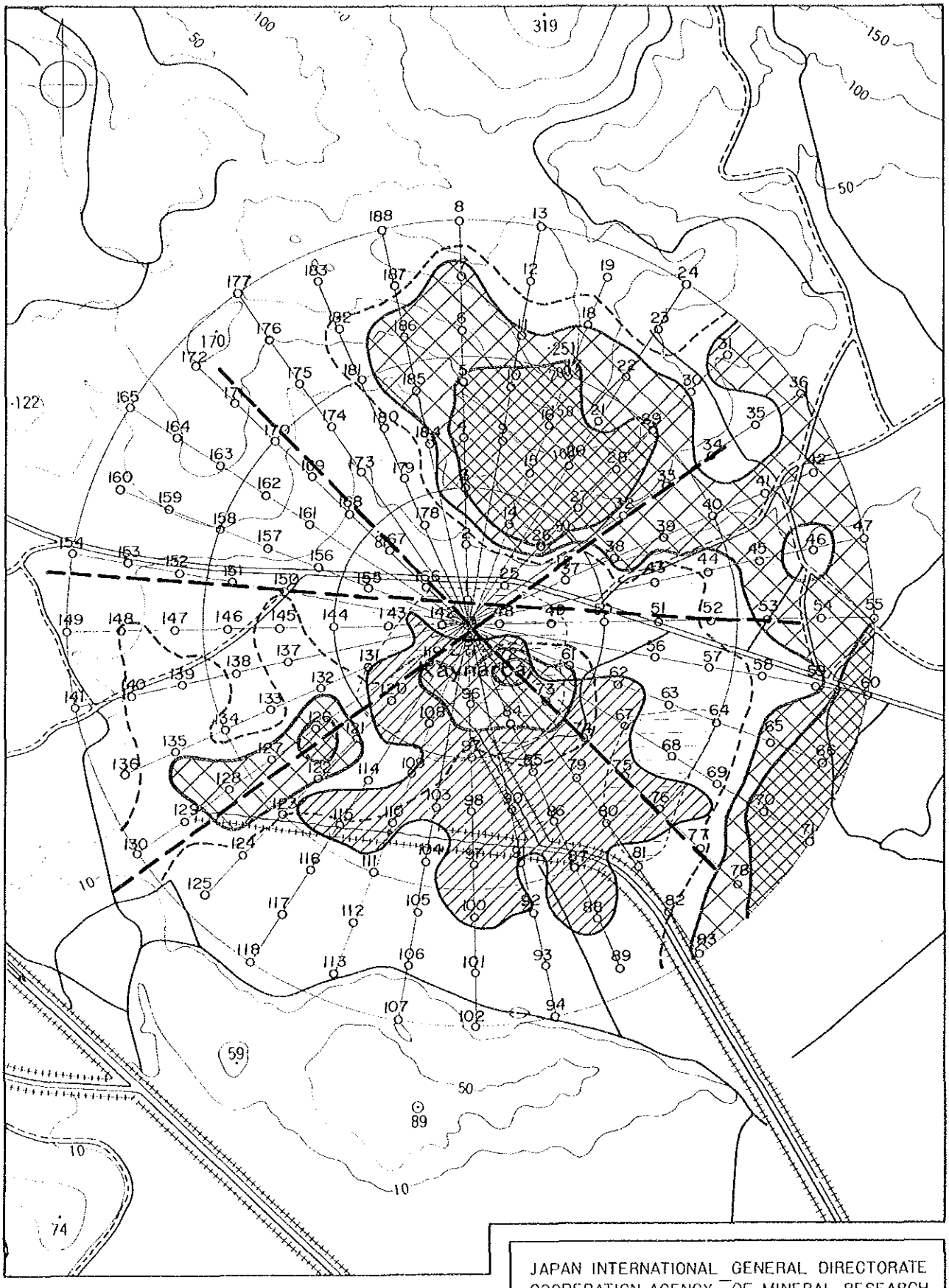

Fig II .3.62 Geothermal structure estimated from electrical surveys

Of these three faults, the faults in (a) and (b) are considered very important by the reason as described below.

2) Geothermal structure

The high longitudinal conductance zone is located in between these two faults near Kaynarca, and the low residual anomaly from the Mise-á-la-masse results is located near the intersection of these two faults.

From the shape of anomaly zones from the electrical surveys, the Kaynarca geothermal area seems to be located at the intersection of these two faults. However, the low residual anomaly zone which is estimated to be related to the reservoir in the area by Mise-á-la-masse measurement, is relatively small (400 m x 300 m) compared with other geothermal fields in the world.

3) Additional comments on residual anomalies

The low residual anomaly located to southwest of DG-1 may be the indication related to the fault structure trending northeast to southwest. The low residual anomaly at northeastern part was detected as a high resistivity zone from CSAMT survey, but it is considered not to be caused by low resistivity zones of the underground but caused by steep resistivity changes because of geological structure. This low residual anomaly might a target for the geothermal exploration. The anomaly spreading at eastern edge is not reliable, because those points are located at the edge of the survey area. Therefore, this anomaly must be checked by the additional survey.

II.3.4 Thermal gradient survey

1. Objectives

The objective of the thermal gradient survey is to estimate the potential of the activity in the Kaynarca geotermal area by drilling thermal gradient holes and temperature logging.

The analysis of cores, cuttings and hotwater is carried out to obtain the basic data to understand the geological structure and construct a geothermal model.

2. Allotment of work

The allotment of work in the thermal gradient survey is as follows:

(1) MTA:

1) Preparation of drilling machine and logging equipment

2) Drilling of thermal gradient hole

3) Sampling of cuttings and core samples

4) Sampling of hot water

5) Temperature logging

6) Management and supervision of work

(2) JICA:

1) Planning of drilling (drilling site, drilling depth, number of holes, casing program)

2) Estimation of heat flow

3) Geological and geophysical analysis of core and cuttings

4) Geochemical analysis of hot water

3. Drilling of the thermal gradient holes

(1) Drilling site

The drilling sites of the thermal gradient holes are shown in Fig. II.3.63.

Hole DG-1: Kaynarca
Hole DG-2: East of Dede Tepe
Hole DG-3: Northwest of Kargın Tepe

(2) Drilling depth

The drilling depth of each thermal gradient hole is as follows:

Hole DG-1: 683.0 m
Hole DG-2: 201.5 m
Hole DG-3: 201.2 m

(3) Casing program

The casing program of the thermal gradient holes is shown in Fig. II.3.64.

From the surface to a depth of 200 m in DG-1, 24 m in DG-2 and 30.7 m in DG-2. The casing pipe was set in order to cut off shallow cold water flowing into the hole.

4. Results of the temperature recovery test

The results of the temperature recovery test from each thermal gradient hole are arranged in Table II.3.2.

The temperature in the hole was measured using a thermister device. Temperature logging was carried out 2 hours after water circulation was stopped and also 12, 24 and 48 hours after. The static formation temperature was estimated using the formulas shown in Appendix A.4.1 and the results are shown in Fig. II.3.64. In order to ascertain the hole temperature, the temperature gradient every 20 m was calculated. The results of the calculation are given in Table II.3.3 and are graphed in Fig. II.3.65.

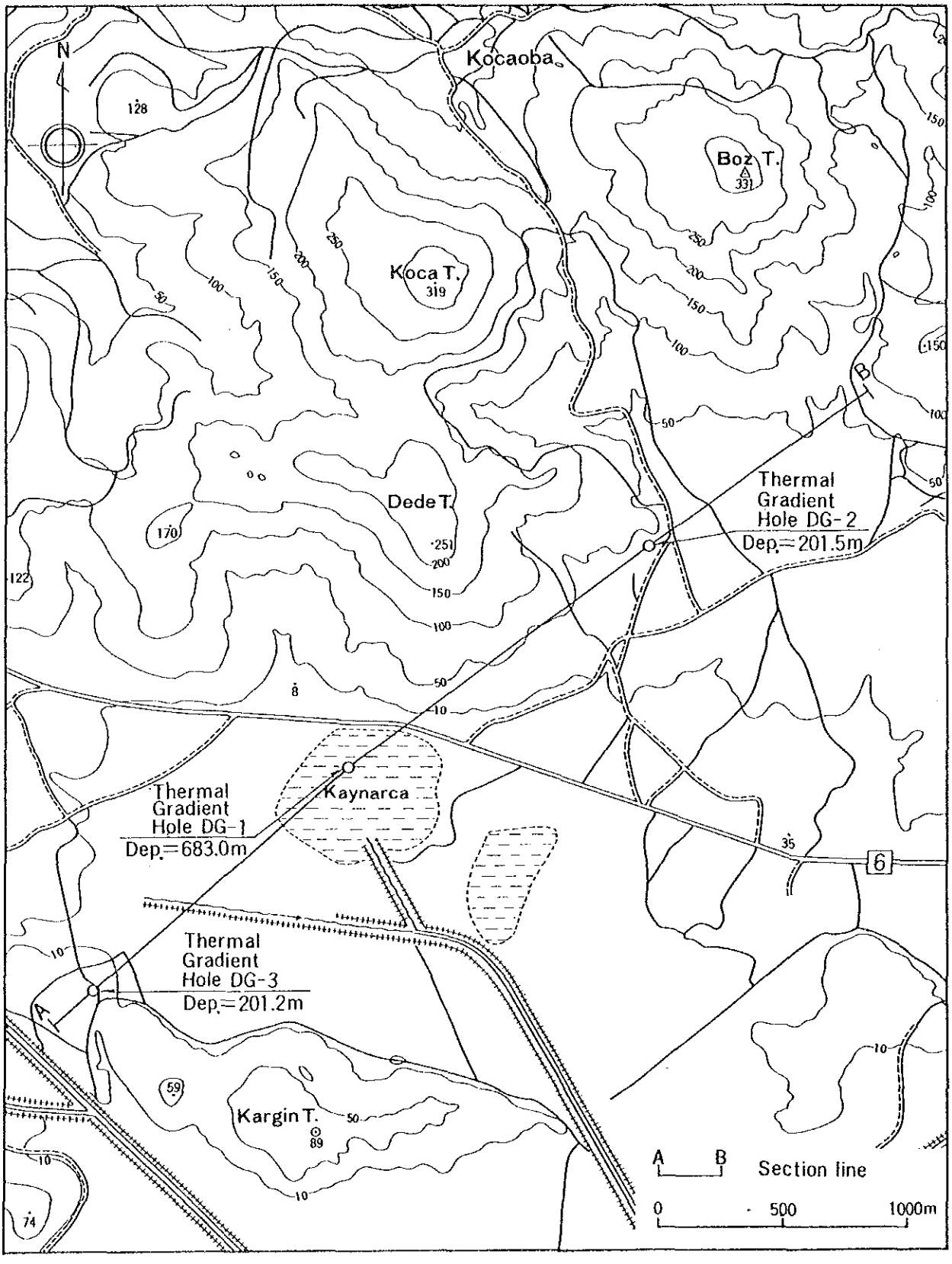

Fig. II.3.63 Location of thermal gradient holes

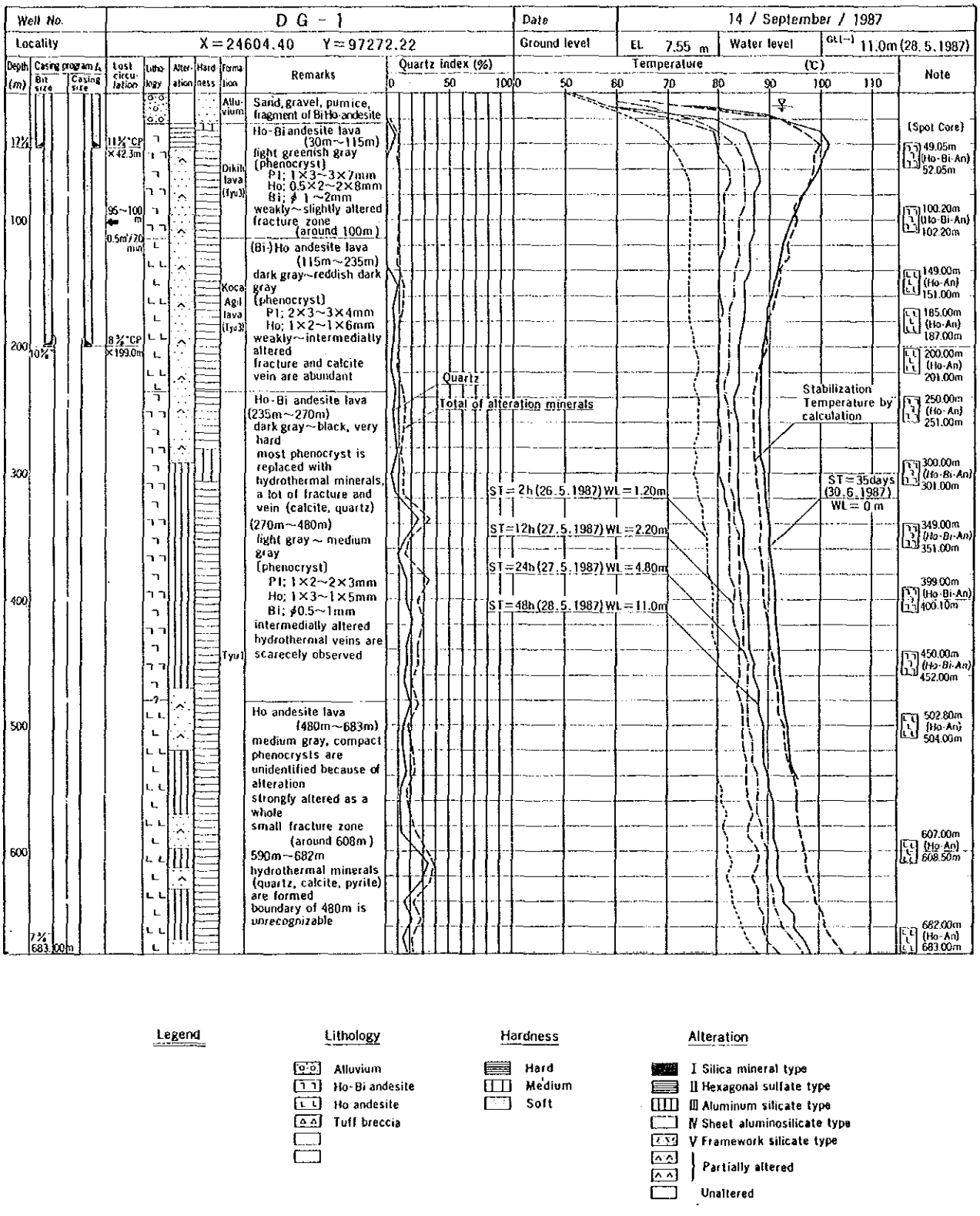

Fig. II.3.64(1) Geologic Column of DG-1

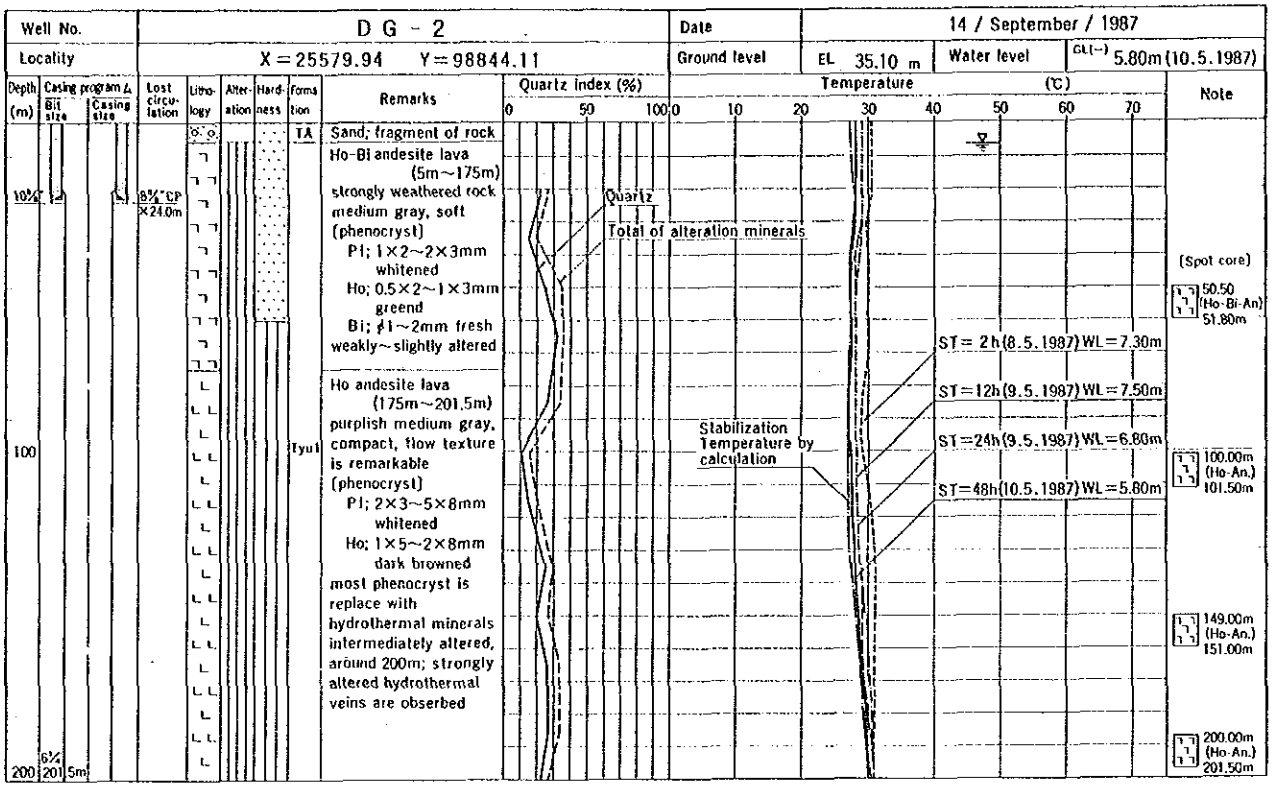

The symbols are as the same as those of geologic column of DG-1

Fig. II.3.64 (2) Geologic Column of DG-2, DG-3

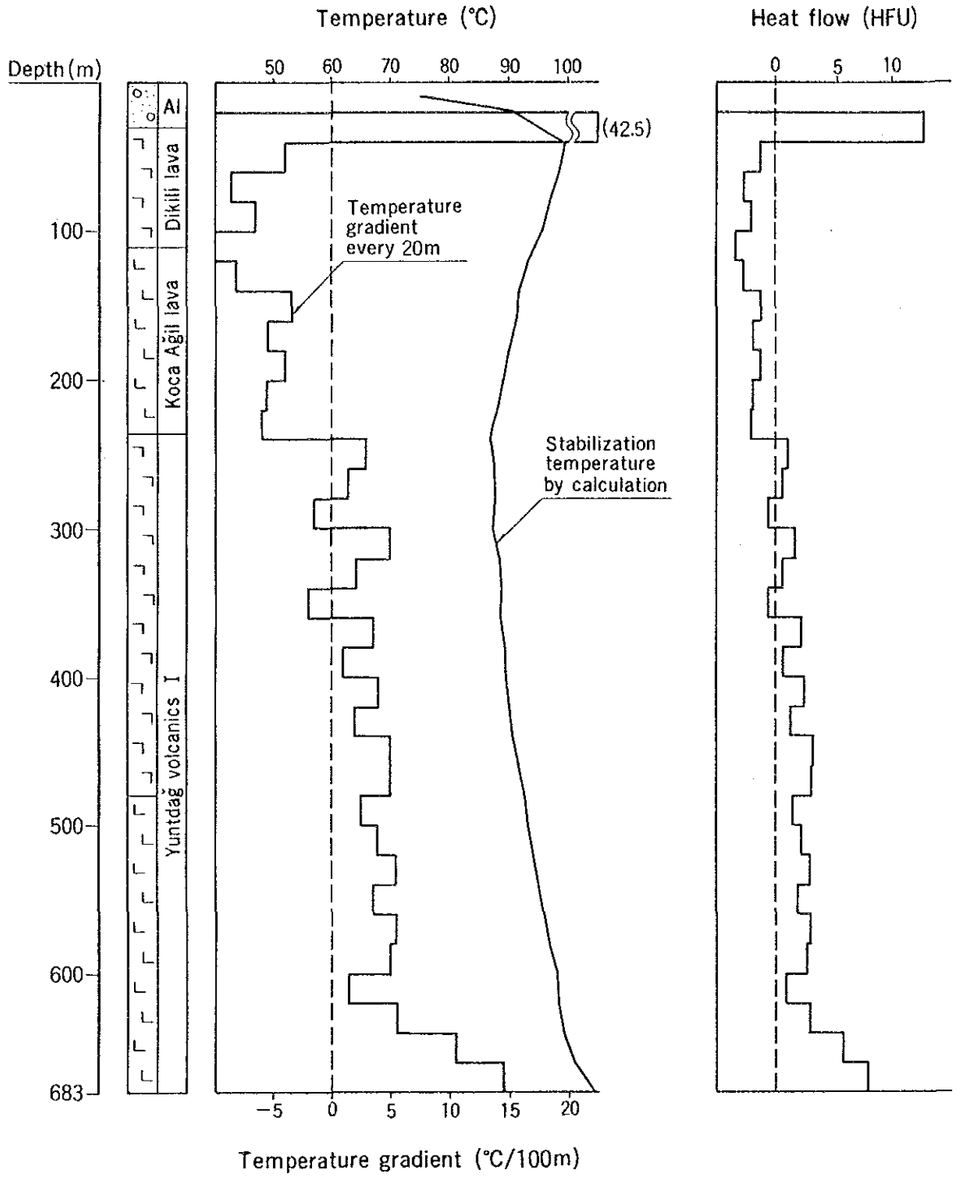

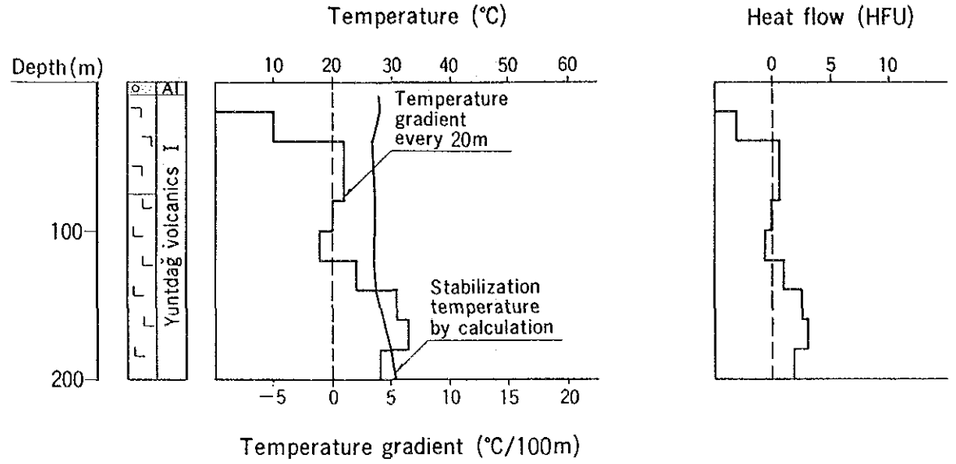

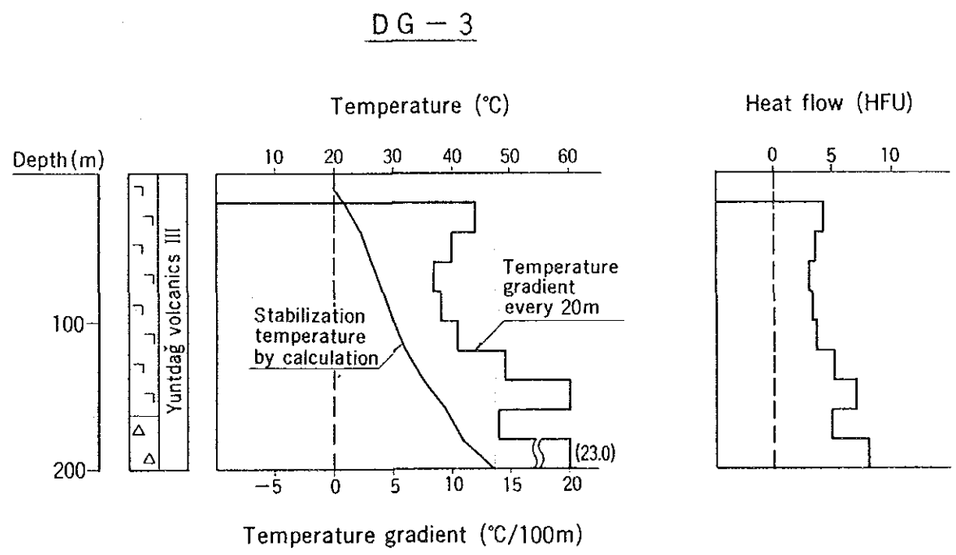

Fig. II.3.65 Heat flow of thermal gradient hole.

Table II.3.2(1) Results of temperature recovery test

Well No. DG-1

	26. 5. 1987 ST= 2hour	27. 5. 1987 ST=12hour	27. 5. 1987 ST=24hour	28. 5. 1987 ST=48hour	Stabilization temperature by calculation	30. 6. 1987 ST=35days
10	55.8	59.0	66.4	59.0	65.1	75.0
20	62.5	70.6	74.7	79.0	90.6	91.1
30	67.6	78.9	78.6	84.9	96.5	99.7
40	69.9	79.6	83.0	86.5	99.1	101.4
50	72.3	80.0	84.5	87.1	98.1	100.0
60	72.9	81.8	85.0	87.3	98.3	98.7
70	74.0	81.8	85.0	87.5	97.1	97.5
80	73.9	81.2	84.9	87.1	96.6	96.3
90	74.5	81.2	84.6	86.5	94.8	95.2
100	74.2	81.0	84.3	86.8	95.3	94.2
110	74.5	81.1	84.0	86.5	94.4	93.5
120	74.8	81.0	83.9	86.0	93.3	92.6
130	74.5	80.5	83.7	86.0	93.4	91.9
140	74.9	80.1	83.0	85.5	91.7	91.2
150	74.9	80.0	83.0	85.5	91.7	90.6
160	74.8	80.0	82.8	85.0	91.0	90.1
170	74.5	80.0	82.5	84.8	90.9	89.6
180	74.9	80.0	82.3	84.5	89.9	89.2
190	75.1	80.0	82.1	84.4	89.4	89.0
200	75.0	80.0	82.0	84.1	89.1	88.9
210	75.5	80.0	82.0	83.9	88.3	88.6
220	75.4	80.0	82.0	83.5	88.0	88.4
230	75.5	79.9	81.6	83.4	87.4	88.4
240	75.8	80.0	81.8	83.0	86.8	88.1
250	75.5	80.0	81.8	83.2	87.4	88.1
260	75.9	80.0	81.9	83.5	87.4	88.1
270	76.0	80.1	81.9	83.5	87.3	88.2
280	75.3	80.0	81.8	83.3	87.7	88.2
290	76.0	80.2	81.9	83.2	86.9	88.3
300	76.0	80.5	82.0	83.5	87.4	88.7
310	76.5	80.8	82.1	84.0	87.6	89.2
320	76.2	81.1	82.5	84.1	88.4	89.5
330	77.0	81.6	83.0	84.5	88.4	89.8
340	77.0	81.7	83.0	84.8	88.8	90.1
350	77.9	81.9	83.4	85.0	88.4	90.3
360	78.0	82.0	83.5	85.0	88.4	90.4
370	77.5	82.0	83.7	85.1	89.2	90.7
380	78.0	82.0	84.0	85.3	89.1	91.0
390	78.9	82.6	84.3	86.0	89.3	91.2
400	79.1	82.9	84.5	86.0	89.3	91.3
410	78.9	83.0	84.5	86.0	89.5	91.6
420	79.0	83.2	84.9	86.3	90.1	91.7
430	79.0	83.4	85.0	86.5	90.4	91.9
440	79.3	83.6	85.1	86.8	90.5	92.0
450	79.4	83.9	85.5	87.0	91.0	92.3
460	79.8	84.0	85.7	87.1	91.5	92.6
470	79.9	84.1	86.0	87.8	91.8	92.9
480	79.5	84.3	86.0	88.0	92.5	93.2
490	80.0	84.5	86.2	88.0	92.1	93.6
500	80.0	84.7	86.5	88.5	93.0	93.9
510	80.2	84.9	86.8	88.5	93.0	94.2
520	80.0	85.0	86.9	88.9	93.8	94.5
530	80.0	84.9	87.0	89.1	94.1	94.9
540	80.0	85.5	87.6	89.3	94.9	95.3
550	80.3	85.4	88.0	90.0	95.7	
560	81.0	86.0	88.2	90.4	95.6	
570	81.8	86.5	88.2	90.9	95.4	
580	81.2	86.4	88.9	91.0	96.7	
590	81.5	86.5	89.0	91.2	96.7	
600	82.1	87.8	89.9	91.8	97.7	
610	83.0	87.2	90.0	92.0	96.8	
620	82.0	87.1	90.0	92.0	98.0	
630	83.0	87.9	91.1	92.9	98.9	
640	83.1	88.7	91.2	93.0	99.1	
650	84.5	89.0	92.0	95.0	100.6	
660	84.9	89.5	93.0	95.2	101.2	
670	85.7	90.1	95.1	96.7	103.8	
680	87.9	93.0	96.3	97.9	104.1	
690	88.0	95.0	97.0	98.2	105.3	

Table II.3.2(2) Results of temperature recovery test

Well № DG-2

Depth	8. 5. 1987 ST= 2hour	9. 5. 1987 ST=12hour	9. 5. 1987 ST=24hour	10. 5. 1987 ST=48hour	Stabilization temperature by calculation
10	30.5	29.0	28.5	28.0	27.6
20	30.5	29.0	29.0	28.0	27.8
30	29.5	28.5	29.0	27.5	27.9
40	30.0	28.0	28.5	27.0	26.8
50	30.0	28.0	28.5	27.0	26.8
60	30.0	28.0	28.0	27.5	27.0
70	30.0	28.0	28.0	27.5	27.0
80	29.0	28.0	28.0	27.0	27.2
90	29.0	28.0	28.0	27.0	27.2
100	29.0	28.0	28.0	27.0	27.2
110	30.0	28.0	28.0	27.5	27.0
120	30.5	28.5	28.5	27.5	27.0
130	31.0	28.5	28.5	28.0	27.1
140	31.0	28.5	29.0	28.0	27.4
150	31.0	29.0	29.5	28.5	28.2
160	31.0	29.0	30.0	28.5	28.5
170	31.0	29.5	30.5	29.0	29.3
180	31.0	30.0	30.5	29.5	29.8
190	31.0	30.5	30.5	29.5	29.9
200	31.0	31.0	31.0	30.0	30.6

Well № DG-3

Depth	20. 4. 1987 ST= 2hour	21. 4. 1987 ST=12hour	21. 4. 1987 ST=24hour	22. 4 1987 ST=48hour	Stabilization temperature by calculation
10	28.0	23.5	23.0	22.0	19.9
20	27.5	24.6	23.9	23.0	22.0
30	27.5	25.5	24.7	24.0	23.5
40	27.5	25.8	25.4	24.5	24.4
50	28.0	26.2	26.0	25.5	25.3
60	28.5	26.4	27.2	26.5	26.4
70	28.8	26.8	28.2	27.0	27.2
80	29.0	27.7	28.5	28.0	28.1
90	29.5	28.6	29.0	29.0	29.0
100	30.0	29.5	29.8	30.0	29.9
110	30.4	30.4	30.5	31.0	30.6
120	30.8	31.2	31.5	32.5	32.0
130	31.5	32.1	32.7	34.0	33.5
140	32.0	33.0	34.0	35.0	34.9
150	32.9	34.0	35.4	37.0	36.9
160	32.8	35.1	36.8	38.0	38.9
170	32.1	36.5	38.3	39.0	41.7
180	35.3	37.7	39.6	40.5	41.7
190	35.9	39.1	41.1	42.0	43.8
200	36.8	40.7	42.7	44.0	46.3

Table II.3.3(1) Results of heat flow calculation

Well No. DG－1

Depth (m)	Stabilization temperature by calculation (℃)	Temperature gradient (℃／100 m)	Thermal conductivity ($\times 10^{-3}$ cal／cm・sec・℃)	Heat flow (HFU)
20	90.6	—	3.00 (Alluvivm)	—
40	99.1	+ 42.5		12.75
60	98.3	− 4.0	3.08	− 1.23
80	96.6	− 8.5		− 2.62
100	95.3	− 6.5		− 2.00
120	93.3	− 10.0	3.42	− 3.42
140	91.7	− 8.0		− 2.74
160	91.0	− 3.5		− 1.20
180	89.9	− 5.5		− 1.88
200	89.1	− 4.0		− 1.37
220	88.0	− 5.5		− 1.88
240	86.8	− 6.0		− 2.05
260	87.4	+ 3.0		1.03
280	87.7	+ 1.5	3.31	0.50
300	87.4	− 1.5		− 0.50
320	88.4	+ 5.0		1.66
340	88.8	+ 2.0		0.66
360	88.4	− 2.0		− 0.66
380	89.1	+ 3.5	6.17	2.16
400	89.3	+ 1.0		0.62
420	90.1	+ 4.0		2.47
440	90.5	+ 2.0		1.23
460	91.5	+ 5.0		3.09
480	92.5	+ 5.0	5.36	2.68
500	93.0	+ 2.5		1.34
520	93.8	+ 4.0		2.14
540	94.9	+ 5.5		2.95
560	95.6	+ 3.5		1.88
580	96.7	+ 5.5		2.95
600	97.7	+ 5.0		2.68
620	98.0	+ 1.5		0.80
640	99.1	+ 5.5		2.95
660	191.2	+ 10.5		5.63
680	194.1	+ 14.5		7.77

Table II.3.3(2) Results of heat flow calculation

Well No. DG－2

Depth (m)	Stabilization temperature by calculation (℃)	Temperature gradient (℃/100 m)	Thermal conductivity ($\times 10^{-3}$ cal/cm·sec·℃)	Heat flow (HFU)
20	27.8	—	6.28	—
40	26.8	− 5.0		− 3.14
60	27.0	+ 1.0		0.63
80	27.2	+ 1.0		0.63
100	27.2	0		0
120	27.0	− 1.0		− 0.63
140	27.4	+ 2.0	4.83	0.97
160	28.5	+ 5.5		2.67
180	29.8	+ 6.5		3.14
200	30.6	+ 4.0		1.93

Well No. DG－3

Depth (m)	Stabilization temperature by calculation (℃)	Temperature gradient (℃/100 m)	Thermal conductivity ($\times 10^{-3}$ cal/cm·sec·℃)	Heat flow (HFU)
20	22.0	—	3.56	—
40	24.4	+ 12.0		4.27
60	26.4	+ 10.0		3.56
80	28.1	+ 8.5		3.03
100	29.9	+ 9.0		3.20
120	32.0	+ 10.5		3.74
140	34.9	+ 14.5		5.16
160	38.9	+ 20.0		7.12
180	41.7	+ 14.0		4.98
200	46.3	+ 23.0		8.19

(1) Thermal characteristics of DG-1

The temperature data of DG-1 shows that the distribution of the well temperatures can be classified roughly into three patterns, upper (0 m to 240 m, middle (240 m to 500 m) and lower (500 m to 683 m) section.

1) Upper section (0 m to 240 m)

In the upper section, from the surface to a depth of 40 m the gradient (42.5°C/100 m) is very high and has a comparatively high temperature of 90 to 100°C.

As shown in Fig. II.3.64 (1), at around 40 m the degree of recovery is high. The temperature at 40 m, 101.4°C was obtained from temperature logging 35 days after water circulation was stopped. The hole temperature decreases gradually from 40 m to 240 m.

2) Middle section (240 m to 500 m)

In the middle section, from 240 m to 500 m, the gradient is ±5°C/100 m and the temperature of the hole is fixed at about 90°C.

3) Lower section (500 m to 683 m)

In the lower section, at a depth of more than 500 m, the gradient (3 to 15°C/100 m) is high compared with the standard gradient (3°C/100 m) and increases with depth. The temperature recovery degree is high too. The static formation temperature by calculation at the bottom of the well (683 m) is about 105°C.

(2) Thermal characteristics of DG-2

In DG-2, the temperature recovery is very small, and the gradient (2 to 5°C/100 m) is almost the same value as the standard gradient. The static formation temperature at the bottom (200 m) is about 31°C.

(3) Thermal characteristics of DG-3

The temperature in DG-3 increases linearly. The gradient (5 to 17°C/100 m) is high. The static formation temperature at the bottom (200 m) is about 46°C.

5. Estimation of heat flow

Underground heat flows from high temperature zones to low temperature zones in proportion to the thermal gradient. The quantity of heat flow is controlled by the thermal conductivity of the rock. The heat flow in each thermal gradient hole was calculated from the static formation temperature and the thermal conductivity measurement of the core. From this the vertical distribution of the heat flow in the Kaynarca geothermal area can be elucidated. The results of the calculation are shown in Table II.3.3 and Fig. II.3.65. The formulas for the calculation are given in the Appendix A.4.2.

The mechanism for the supply of heat in the geothermal field is basically thermal conduction and transfer of hot geothermal fluid. A large quantity of heat is quickly carried by the geothermal fluid compared with heat supply from thermal conductivity.

(1) Characteristics of the heat flow in DG-1

The basic flow is presented in Fig. II.3.65. At around 40 m in depth it is remarkably high. It is difficult to explain the supply of heat using only thermal conduction. It is presumed that hot water of 100°C is flowing into the area. The value of the heat flow from 60 m to 240 m are negative. This shows that the heat moves from shallow depths to greater depths. The values of the heat flow at a depth of 240 m to 640 m are -0.66 to 3.09 HFU and they are roughly even. There is no disturbance in the area, the heat seems to be moving only by thermal conduction. The values of heat flow at depths greater than 640 m are as high as 5.63 to 7.77 HFU. There is a high possibility that this area is heated by hydrothermal fluid from below because the value of heat flow increase with depth.

(2) Characteristics of the heat flow in DG-2

The heat flow from the surface to 120 m is often a negative value. This indicates that the shallow part of DG-2 is influenced by cold shallow

water. From 120 m to the bottom (200 m), the values of the heat flow were fixed between -3.14 and 3.14. These values are the same as the mean value (1.65 HFU) in the continent.

(3) Characteristics of the heat flow in DG-3

The values of the heat flow are high (4.27 to 8.19 HFU) and increases with depth. This suggests the existence of hydrothermal fluid at depth around DG-3.

6. Analysis of core and cuttings

(1) Stratigraphy of the thermal gradient holes

The stratigraphy was deduced from the observation of the core and cuttings which were sampled from the thermal gradient holes. Microscopic observation was made on 21 thin sections. The stratigraphy is shown in Table II.3.4 and the results of the microscopic observation are shown in Table II.3.5.

The geological columns of the holes are drawn in Fig. II.3.64. As shown in the geological column, the stratigraphy of DG-1 in descending order is as follows: Alluvium, Dikili lava, Koca Agıl lava and Yuntdağ volcanics I. The Dikili lava and Koca Agıl lava belong to the Yuntdağ volcanics III.

The stratigraphy of DG-2 is composed of talus deposit of 5 m in thickness and Yuntdağ volcanics I.

In DG-3, the stratigraphy is composed of Dikili lava and 1 m of talus deposit.

(2) Occurrence of hydrothermal veins

Hydrothermal veins are dominant at depths of 150 m to 200 m in DG-1. The occurrence of hydrothermal veins coincides with that of the fractures. These fracture seem to be accompanied by faults. In most cases, the hydrothermal veins are filled with calcite and quartz of 0.1 cm to 2 cm in width, and frequently they are accompanied by druse. The druse is composed of well developed calcite and quartz crystals. The rocks in DG-1 were subjected to hydrothermal alteration at an older time, however, these hydrothermal veins appear to have been formed

Table II 3. 4 Stratigraphy of thermal gradient holes

DG－1

Distribution depth (m)	Elevation (m)	Thickness (m)	Formation
0 ～ 30	7.6～ −22.4	30	Alluvium
30 ～ 115	− 22.4～-107.4	85	Yuntdağ volcanics III (Dikili lava)
115 ～ 235	−107.4～-227.4	120	Yuntdağ volcanics III (Koca Ağıl lava)
235 ～ 683	−227.4～-675.4	448	Yuntdağ volcanics I

DG－2

Distribution depth (m)	Elevation (m)	Thickness (m)	Formation
0 ～ 5	35.1～ 30.1	5	Talus deposit
5 ～ 201.5	30.1～-166.4	196.5	Yuntdağ volcanics I

DG－3

Distribution depth (m)	Elevation (m)	Thickness (m)	Formation
0 ～ 1	9.3 ～ 8.3	1	Talus deposit
1 ～ 201.2	8.3～-200.2	200.2	Yuntdağ volcanics III (Dikili lava)

Table II 3.5(1) Petrography of Rock-forming Minerals

Well No. DG − 1

Depth (m)	Rock name	Rock-forming minerals: Phenocryst									Rock-forming minerals: Ground mass								Alteration Minerals										Remarks
		Cpx	Opx	Ho	Bi	Ol	Op	Pl	Af	Qz	Cpx	Opx	Bi	Op	Pl	Af	Si	Gl	Tr	Cr	Qz	Al	Ka	Mo	Ch	Mi	Ah	Ca	Ep	
49.7	Ho-Bi andesite			▲	○			○						×						△				◎						Weakly altered
100.5	〃			▲	○			○						△						△				○						〃
149.3	〃			▲	▲			▲						△							△			△				×			Intermediatly altered
186.2	〃			▲	▲			▲						×							△			○							〃
200.7	〃			▲	▲			▲						△							○			○							Strongly altered
250.4	〃			▲	△			○						×							△			△				◎		×	Strongly altered Qz, Ca veins are dominant
300.3	〃			▲	○			○						×							△		×	×							Weakly altered
349.5	〃			▲	○			○						×							○		△	×						×	〃
399.1	〃			?	▲			▲						×							○		×			×				△	Strongly altered
450.9	?				?			▲						×						×	○		○	△		×				◎	Strongly altered Do veins are dominant

LEGEND : ◎ Abundant ○ Intermediate △ Small amount × A very small amount ▲ Pseudomorph

CPx : Clinopyroxene OPx : Orthopyroxene Ho : Hornblende Bi : Biotite Ol : Olivine Op : Opaque mineral
Pl : Plagioclase Af : Alkali feldspar Qz : Quartz Si : Silica mineral Gl : Glass Tr : Tridymine Cr : Cristobalite
Al : Alunite Ka : Kaolinite Ch : Chlorite Mo : Montmorillonite Mi : Mica An : Anhydrite Ca : Calcite Ep : Epidote Do : Dolomite

Table II 3.5(2) Petrography of Rock-forming Minerals

Well No. DG－1

Depth (m)	Rock name	Rock-forming minerals: Phenocryst Cpx	Opx	Ho	Bi	Ol	Op	Pl	Af	Qz		Ground mass Cpx	Opx	Bi	Op	Pl	Af	Si	Gl		Alteration Minerals Tr	Cr	Qz	Al	Ka	Mo	Ch	Mi	An	Ca	Ep	Do	Remarks
503.5					?			▲							×								○					×				○	Strongly altered
608.0				▲	?			▲							×								◎		×			×					〃
682.3					?			▲							×								○					×				○	〃

LEGEND : ◎ Abundant ○ Intermediate △ Small amount × A very small amount ▲ Pseudomorph

CPx : Clinopyroxene OPx : Orthopyroxene Ho : Hornblende Bi : Biotite Ol : Olivine Op : Opaque mineral

Pl : Plagioclase Af : Alkali feldspar Qz : Quartz Si : Silica mineral Gl : Glass Tr : Tridymite Cr : Cristobalite

Al : Alunite Ka : Kaolinite Ch : Chlorite Mo : Montmorillonite Mi : Mica An : Anhydrite Ca : Calcite Ep : Epidote Do : Dolomite

No. 3

Table II 3.5(3) Petrography of Rock-forming Minerals

Well No. DG－2

Depth (m)	Rock name	Rock-forming minerals: Phenocryst										Rock-forming minerals: Ground mass									Alteration Minerals											Remarks
		Cpx	Opx	Ho	Bi	Ol	Op	Pl	Af	Qz		Cpx	Opx	Bi	Op	Pl	Af	Si	Gl		Tr	Cr	Qz	Al	Ka	Mo	Ch	Mi	Ah	Ca	Ep	Do	
50.7	Ho - Bi andesite			▲	△			▲							×		·						○		△	×				△		△	Intermediatly altered
101.0	〃			▲	×			▲							×								○		×	×						○	Strongly altered
150.0	〃			▲	×			▲							×								◎		×			×				○	〃
201.5	?			?	?			?							×								◎		×			×				○	〃

LEGEND : ◎ Abundant ○ Intermediate △ Small amount × A very small amount ▲ Pseudomorph

CPx : Clinopyroxene OPx : Orthopyroxene Ho : Hornblende Bi : Biotite Ol : Olivine Op : Opaque mineral
Pl : Plagioclase Af : Alkali feldspar Qz : Quartz Si : Silica mineral Gl : Glass Tr : Tridymite Cr : Cristobalite
Al : Alunite Ka : Kaolinite Ch : Chlorite Mo : Montmorillonite Mi : Mica An : Anhydrite Ca : Calcite Ep : Epidote Do : Dolomite

Table II 3.5 (4) Petrography of Rock-forming Minerals

Well No. D G − 3

Depth (m)	Rock name	Rock-forming minerals																		Alteration Minerals												Remarks
		Phenocryst										Ground mass																				
		Cpx	Opx	Ho	Bi	Ol	Op	Pl	Af	Qz		Cpx	Opx	Bi	Op	Pl	Af	Si	Gl		Tr	Cr	Qz	Al	Ka	Mo	Ch	Mi	Ah	Ca	Ep	Do	
550.7	Bi-Ho andesite			○	○			◎							×				○							×							Fresh Flow texture is remarkable
101.0	〃			▲	○			○							×											○							Weakly altered
150.0	〃			?	▲			○							×							○				○							〃
201.5	Tuff breccia			?	○			○							×							○										○	〃

-163-

LEGEND : ◎ Abundant ○ Intermediate △ Small amount × A very small amount ▲ Pseudomorph

CPx : Clinopyroxene OPx : Orthopyroxene Ho : Hornblende Bi : Biotite Ol : Olivine Op : Opaque mineral
Pl : Plagioclase Af : Alkali feldspar Qz : Quartz Si : Silica mineral Gl : Glass Tr : Tridymite Cr : Cristobalite
Al : Alunite Ka : Kaolinite Ch : Chlorite Mo : Montmorillonite Mi : Mica An : Anhydrite Ca : Calcite Ep : Epidote Do : Dolomite

by more recent geothermal activity because the boundary between the hydrothermal veins and the wall rocks is clear.

In the rocks of DG-2 and DG-3, hydrothermal veins are sparse.

(3) X-ray analysis

In order to know the characteristics and degree of hydrothermal alteration in the Kaynarca geothermal area, alteration zones were evaluated using the classification of alteration type and the quartz index. Their principles are outlined in Appendix A.4.3.

X-ray analysis was carried out on 65 samples, collected at intervals of about 15 m. The results of the X-ray analysis are shown in Table II.3.6 and alteration zones and the depth at which alteration of minerals appear are drawn in Fig. II.3.66.

1) Hydrothermal alteration in DG-1

The following features of hydrothermal alteration of DG-1 become apparent from the results of X-ray analysis.

(a) Silica minerals: Low-cristobalite is identified from 20 m to 170 m. Quartz occurs at 35 m and deeper than 149 m. As a whole, the Quartz-Index is less than 34 and a notable silicified zone (Type I) is not found.

(b) Clay minerals: Montmorillonite formed in weakly acidic or neutral conditions is found at less than 300 m. At more than 415 m, mica clay minerals occur intermittently. Conversely, kaoline formed by acidic hydrothermal alteration is found at depths greater than 300 m.

(c) Carbonate minerals: Much clacite and dolomite are formed from 215 m to 682 m.

(d) Other minerals: At a depth of 35 m, alunite formed in sulfate acidic conditions is identified. Pyrite is distributed at all depths in DG-1.

From the occurrence of these hydrothermal minerals, the follow-

Well No. DG-1

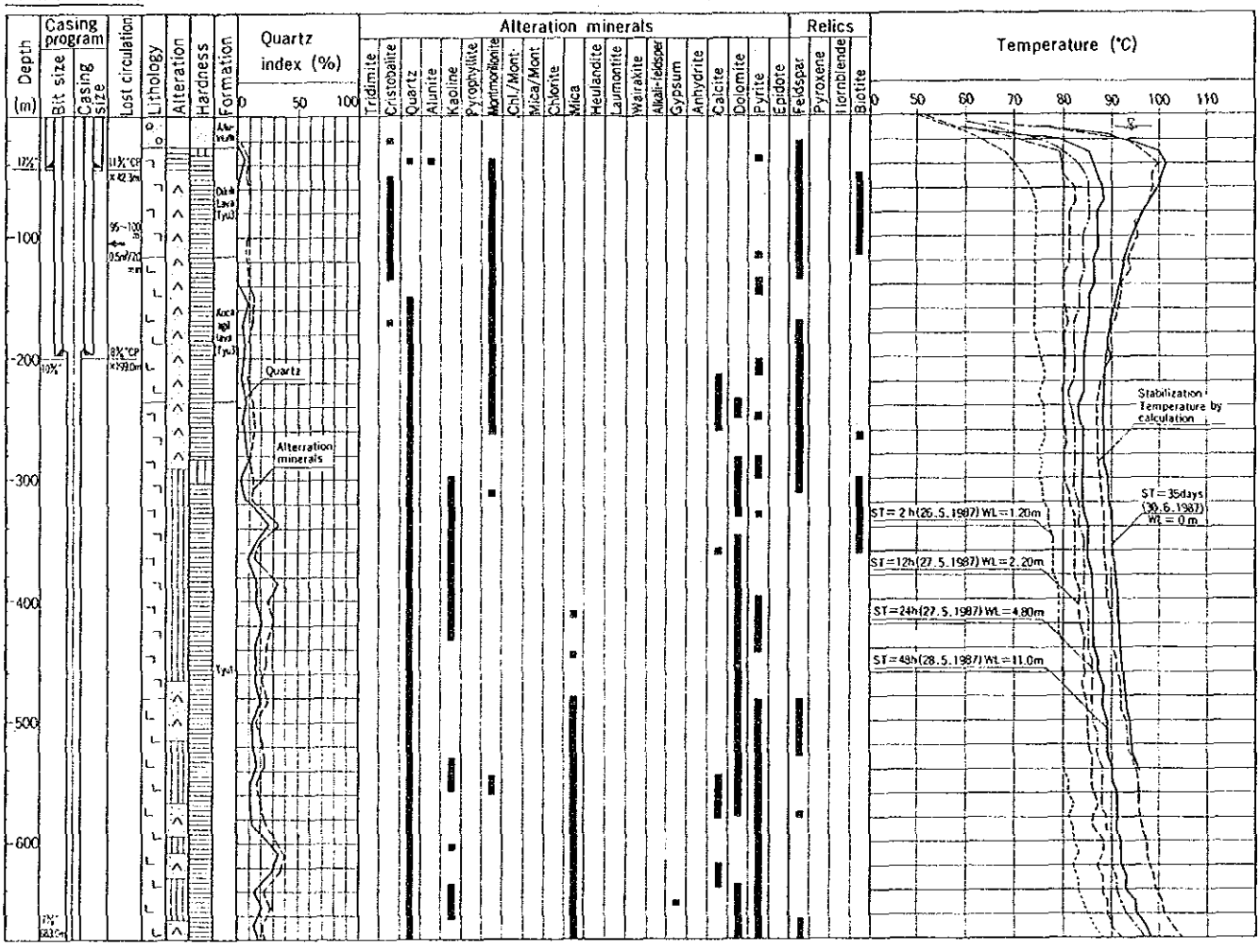

Fig. II.3.66 (1) Distribution of alteration in thermal gradient hole.

Well No. DG-2

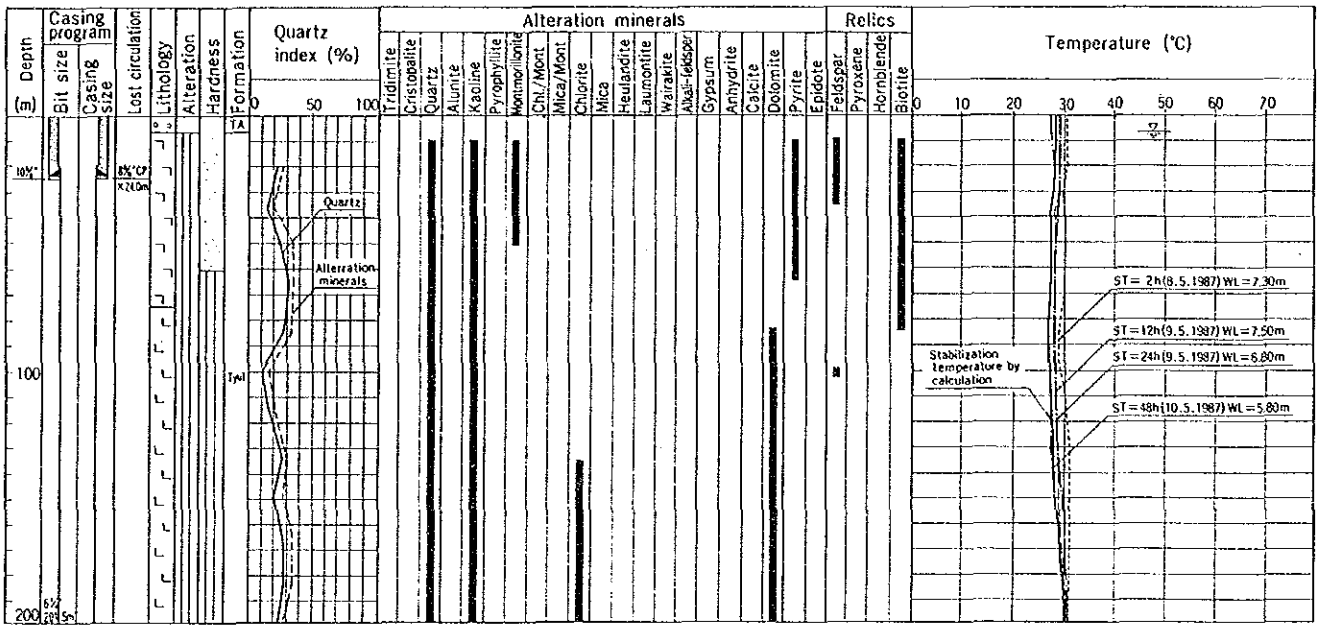

Well No. DG-3

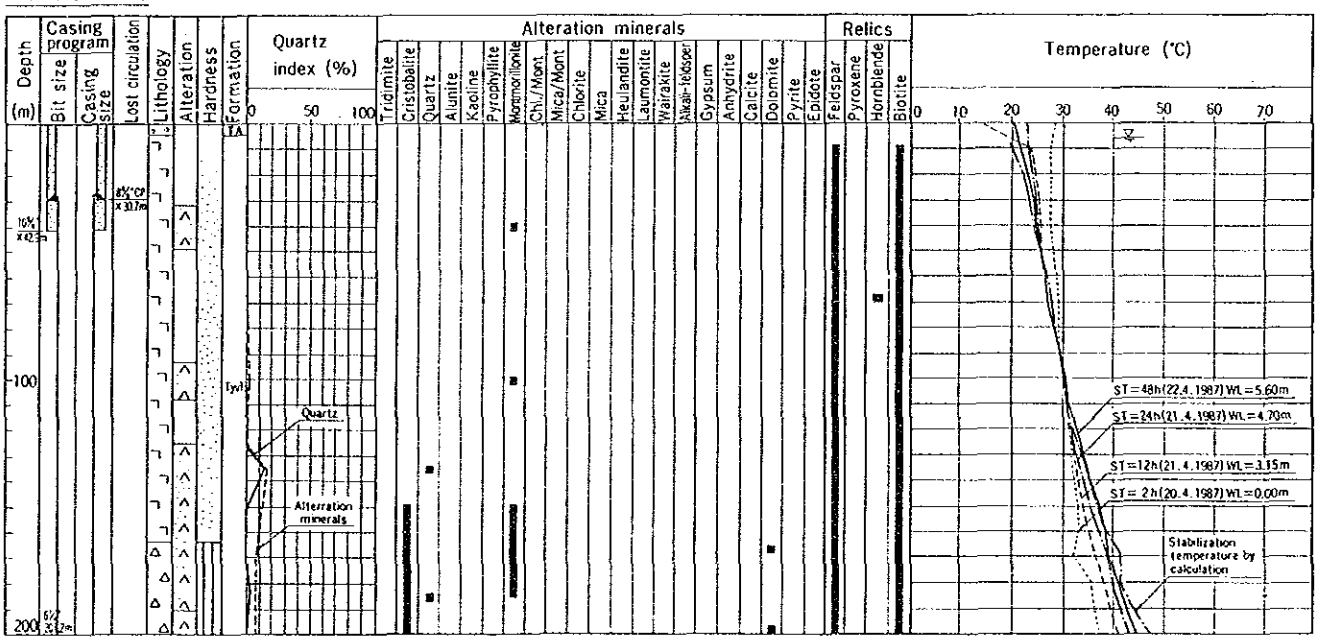

Fig. II.3.66 (2) Distribution of alteration in thermal gradient hole.

Table II.3.6(1) Results of X-ray analysis

Well No. DG-1			ALTERATION MINERALS																					RELICS			
			I			II	III		IV					V				Others										
Nos	Depth(m)	Alteration Type	Tridymite	Cristobalite	Quarts	Alunite	Kaolin	Pyrophyllite	Montmorillonite	Chl./Mont	Mica/Mont	Chlorite	Mica	Heulandite	Laumontite	Wairakite	Alkali-feldspar	Gypsum	Anhydrite	Calcite	Dolomite	Pyrite	Epidote	Feldspar	Pyroxene	Hornblende	Biotite
1	20			3																				4			
2	35	II			7	1			0.5													1		4			
3	49.7	IV′		4					4															3			2
4	65	↑		7					3															3			3
5	85			5					4															2			2
6	100.5			4					4													1		3			1
7	115.0			5					3															3			1
8	135			6					2													1		3			
9	149				9				3													1					
10	170			5	5				2															3			
11	186.2				6				4															3			
12	200.8				5				4													1		3			
13	215				4				2											2		1		3			
14	235				8				2											2	2			2			
15	250				6				1											5	2	1		2			
16	265	↓			7				2											4				3			1
17	285	IV′			9																2	0.5		1			
18	300.3	III			4		2														6	2		2			3
19	315	↑			8		1		1												3			2			2
20	335				26		4														2	1					1
21	349.5				16		3																				2
22	365.0				10		0.5													2	2						0.5
23	385				17		2														15						
24	399.1				16		3														4	2					
25	415				21		3						1								4	1					
26	435				16		1														6	2					
27	450.9	↓			17		1						0.5								5	2					
28	465	III			15		2														4						
29	485	IV′			19								1								5	1		4			
30	503.5	↕			13								0.5								3	1		5			
31	515	IV′			14								1								5	1		2			
32	535	III			16		0.5						0.5								5	1		1			
33	550	↕			12		1		0.5				1							1	2	1					
34	565	III			12		1		0.5				1							1	3	1					
35	585	IV′			13								0.5							1	6	3		1			
36	608	III			34		2						1									2					
37	625	IV			29								0.5							1	4	1					
38	640	III			15		1						0.5							1	3	1					
39	655	↕			21		0.5						0.5					0.5			5	1					
40	670	III			15		0.5						0.5								4	1		2			
41	682.3	IV′			18								1								2	1		4			

The Arabic numbers show Quartz Index and Roman numbers show Alteration Type by Hayashi (1979)

Table II. 3. 6 (2) Results of X-ray analysis

Well No. DG-2			ALTERATION MINERALS																					RELICS			
			I			II	III		IV					V				Others										
Nos	Depth (m)	Alteration Type	Tridymite	Cristobalite	Quarts	Alunite	Kaolin	Pyrophyllite	Montmorillonite	Chl. / Mont	Mica / Mont	Chlorite	Mica	Heulandite	La montite	Wairakite	Alkali-feldspar	Gypsum	Anhydrite	Calcite	Dolomite	Pyrite	Epidote	Feldspar	Pyroxene	Hornblende	Biotite
1	20	III			22		2		1													1		2			1
2	35	↑			15		3		1													1		2			2
3	50.7				24		6		1													2					3
4	65				31		2															2					1
5	85				27		2														3						1
6	101				10		1														5			1			
7	115				15		1														4						
8	135				25		1						1								2						
9	150				20		2						1								4						
10	165				26		2						1								3						
11	185	↓			27		2						1								2						
12	201.5	III			22		1						0.5								4						

Well No. DG-3			ALTERATION MINERALS																					RELICS			
			I			II	III		IV					V				Others										
Nos	Depth (m)	Alteration Type	Tridymite	Cristobalite	Quarts	Alunite	Kaolin	Pyrophyllite	Montmorillonite	Chl. / Mont	Mica / Mont	Chlorite	Mica	Heulandite	Laumontite	Wairakite	Alkali-feldspar	Gypsum	Anhydrite	Calcite	Dolomite	Pyrite	Epidote	Feldspar	Pyroxene	Hornblende	Biotite
1	20																							58			3
2	40	IV′							0.5															4			4
3	54																							12			2
4	70																							11		0.5	1
5	85																							13			3
6	101.0	IV′							1															4			5
7	115																							8			1
8	135	IV′			12																			14			1
9	149.4	↑		5					4															3			1
10	165	↓		3					1												2			3			1
11	185	IV′		5	2				0.5															4			1
12	200	PA		4																	2			20			

The Arabic numbers show Quartz Index and Roman numbers show Alteration Type by Hayashi (1979)

ing geothermal activity is presumed.

(a) The transition depth from low-cristobalite to quartz is about 170 m. The transition temperature is considered to be 100°C and it indicates that the temperature has not reached 100°C shallower than 170 m. However, quartz occurs locally at a depth of 35 m, it is considered that the hot water greater than 100°C is flowing into this area.

(b) Hot water around 35 m was acidic because alunite is found at this depth.

(c) An acidic alteration zone characterized by kaoline exists from 300 m to the bottom of the hole. This alteration zone develops usually above or around the hot water reservoir. In the acidic alteration zone in DG-1, much quartz, dolomite and calcite filled up the fractures with druse. As a result this zone seems to form an impermeable bed, and it is thought that it forms the cap rock in the geothermal structure.

2) Hydrothermal alteration in DG-2

Much quartz and kaoline are found at the surface to the bottom (200 m) of the hole and an acidic alteration zone exists. From the results of the temperature logging (temperature is fixed at about 30°C), however, it is presumed that this alteration zone was formed by past geothermal activity..

3) Hydrothermal alteration in DG-3

Hydrothermal alteration in DG-3 is weak, alteration minerals cristobalite, quartz and montmorillonite are sparse at depth greater than 135 m.

(4) Fracture analysis in the core

The dip and strike of the hydrothermal veins and the fractures with slickensides in the spot core in DG-1 were measured using the natural remanent magnetization of rocks. Four rock samples of the Yuntdağ volcanics I were taken from outcrops 2 km north of Kaynarca. Using

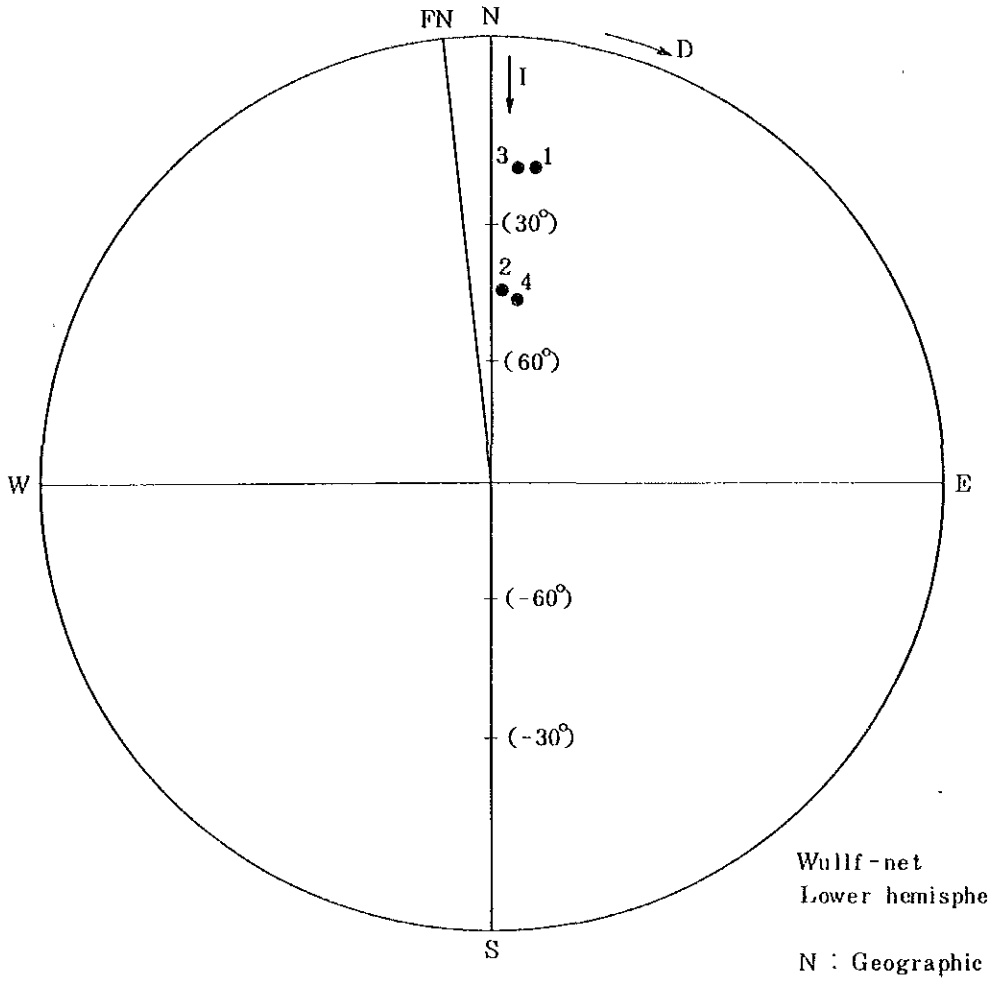

Wullf-net
Lower hemisphere

N : Geographic north

FN : Geomagnetic north
in Fukuoka

Sample nos.	Declination	Inclination
1	14°	20°
2	9°	44°
3	11°	20°
4	13°	45°

Data shows value of geomagnetic field in Fukuoka, Japan.
Direction of geomagnetic north in Fukuoka leans 6° west ward against geographic north.
Direction of geomagnetic north in Dikili is in accord with geographic north.

II 3.67 Distribution of declination and inclination of field rock sample

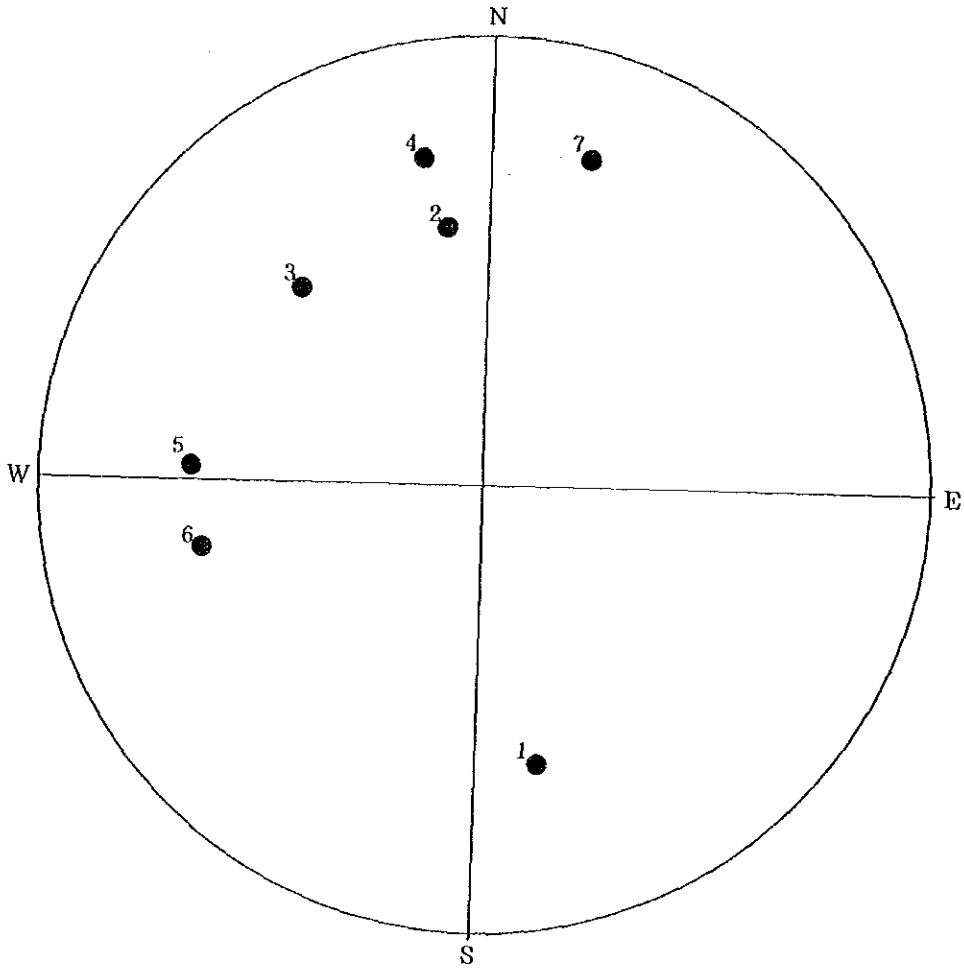

Wulif-net

Upper hemisphere

(The Arabic numbers represent sample numbers.)

Fig II 3.68 Stereonet plot of dip and strike of fracture in DG-1

Table Ⅱ.3.7 Results of measurement of fractures in core (DG—1)

Sample No.	Depth (m)	Rock name	Degree of alteration	Hydrothermal vein		Movement direction judged from slickenside	Dip and strike of fracture from temporary north	Direction of remanent magnetization		Dip and strike of fracture from direction of remanent magnetization
				Mineral	Width (mm)			Declination	Inclination	
1	150.8	Ho andesite (Tyu 3)	Intermediatly altered	Calcite, Pyrite	2 ~ 3	—	EW 65 S	−167	−6	N 77 E 65 SE
2	185.8	Ho andesite (Tyu 3)	Intermediatly altered	Calcite, Pyrite	2 ~ 3	—	EW 60 S	10	−40	N 80 E 60 NW
3	200.0	Ho andesite (Tyu 3)	Weakly altered	Calcite, Quartz	2 ~ 3	—	EW 62 S	44	−21	N 46 E 62 NW
4	250.9	Ho-Bi andesite (Tyu 1)	Strongly altered	Calcite	6 ~ 7	—	EW 73 S	−168	36	N 78 E 73 NW
5	399.5	Ho-Bi andesite (Tyu 1)	Intermediatly altered	Calcite, Quartz	1 ~ 2	—	EW 67 S	−93	22	N 3 E 67 NW
6	451.4	Ho-Bi andesite (Tyu 1)	Intermediatly altered	—	—	168	EW 65 S	−77	52	N 13 W 65 SW
7	608.2	Ho andesite (Tyu 1)	Strongly altered	—	—	115	EW 75 S	163	64	N 73 W 75 NE

these samples, the directions of the natural remanent magnetization of the Yuntdağ volcanics I were measured. As shown in Fig. II.3.67, it was confirmed that the directions of magnetization of 4 samples coincides with the geographic north.

Therefore the direction of magnetization of the core with the fracture are measured and on the presumption that this direction was north, the dip and strike of the fractures or veins was decided. The results of the measurement are shown in Table II.3.7 and Fig. II.3.68. The flow chart of this method is drawn in Appendix A.4.4.

Detailed discussion is impossible because of few data. The fractures and veins which have an east-west strike, dip 60° to 70° northward or southward and have north-south strike, dip 65° to 67° westward are abound-dant shown in Fig. II.3.68. East-west striking veins are rich at shallow depths. From the occurrence of the hydrothermal veins in section 5.(2), there is a possibility that the veins are related to the east-west fault forming the graben in the Kaynarca area.

(5) Homogenization temperature measurement of fluid inclusions

The measurement was carried out in order to estimate the temperature at which a hydrothermal mineral is formed and estimate the static formation temperature in the hole.

Quartz and calcite in the cores and cuttings were collected at 7 different depths from DG-1 as shown in the following table.

List of sample

Sampling depth (m)	Name of mineral	Occurrence
160.0	Calcite	Cuttings
250.0	Calcite	Vein in core
425.0	Quartz	Cuttings
608.0	Calcite	Vein in core
615.0	Calcite	Cuttings
655.0	Quartz	Cuttings
680.0	Calcite	Cuttings

The results are given in Table II.3.8. The distribution of homogenization temperature and the temperatures measured by a thermistor are shown in Fig. II.3.69. The details of the measurements are explained in Appendix A.4.5.

The lowest homogenization temperatures at depth substantially coincide with the present underground temperature at the same depth in the active geothermal field. In DG-1, the line which links the lowest value of the homogenization temperature is parallel to the logging temperature curve. The value of the homogenization temperature, however, is a little lower than the logging temperature. The underground temperature around DG-1 seems to be changeable because hot water from depth mixes with shallow cold water. Therefore, it is thought that the fluid inclusions which were formed at a lower temperature than present are located around DG-1. Moreover, homogenization temperature in DG-1 has a wide distribution ranging from 254.6°C to 79.9°C. These results suggest that vigorous geothermal activity, whose temperature reached 250°C existed in the area. The strong alteration zone around DG-1 is presumed to have been formed at that time.

(6) Rock property measurement

The rock property measurements were carried out on samples from spot cores taken from DG-1, 2, 3. The measurements consist of density (dry condition, wet condition), porosity, thermal conductivity, magnetic susceptibility and resistivity. The methods are shown in Appendix A.4.6.

Only two rock properties of DG-2 and DG-3 could be determined because most core from these holes was broken.

The results are shown in Table II.3.9 and the mean value of the original rocks which were collected during the 2nd stage survey are included in the table. Fig. II.3.70 shows a comparative diagram of rock properties against depth.

All core from DG-1 had undergone hydrothermal alteration, the density of the core is large and the effective porosity is small compared with the orignal rocks. Fig. II.3.70 indicates that the density increases and the effective porosity decreases with depth. The resistivity and thermal conductivity tend to increase proportionally with depth. The thermal conductivity of cores is used for the calculation of the heat flow.

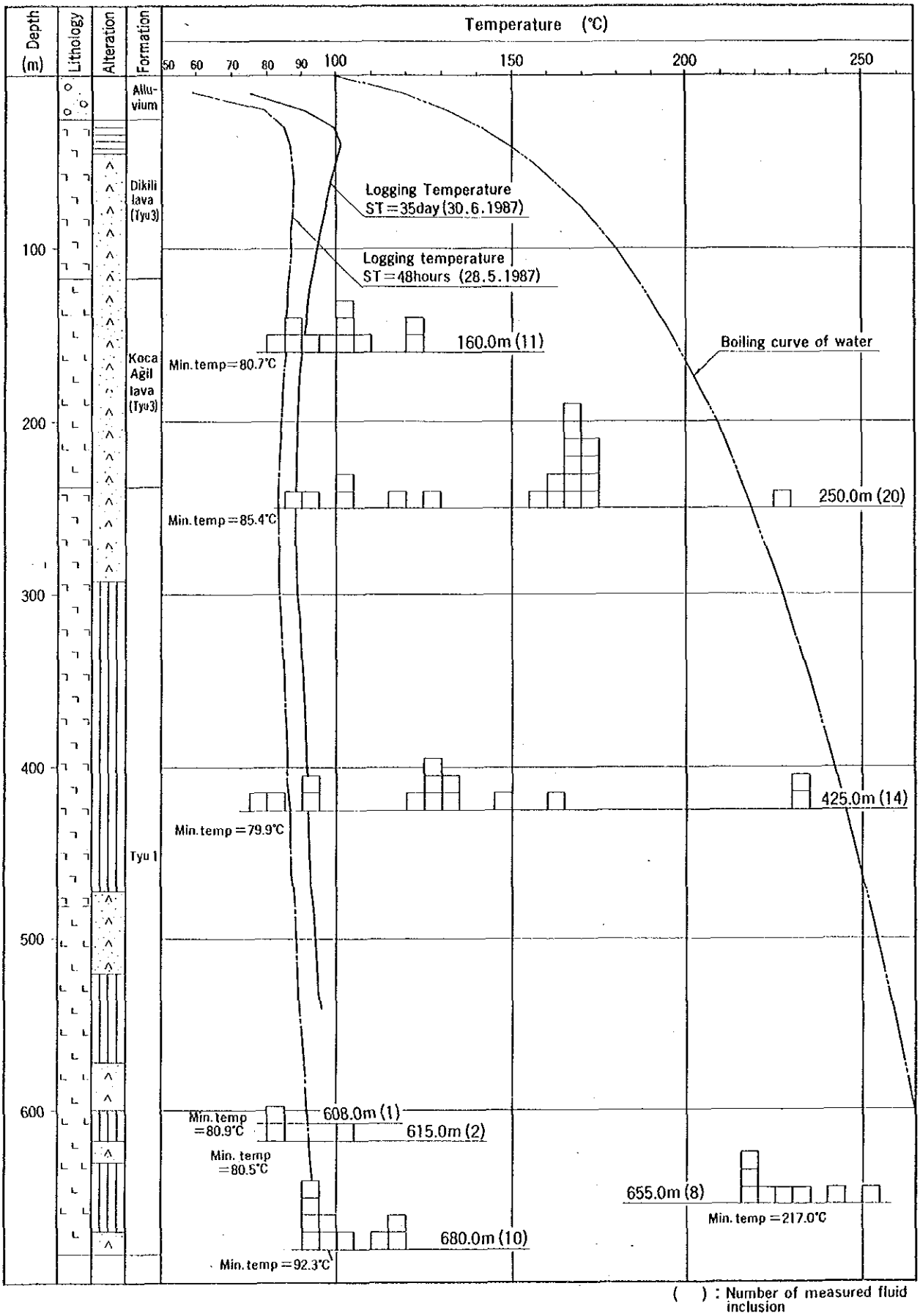

Fig.II.3.69 Homogenization temperature of fluid inclusions in DG-1

Well No. DG-1

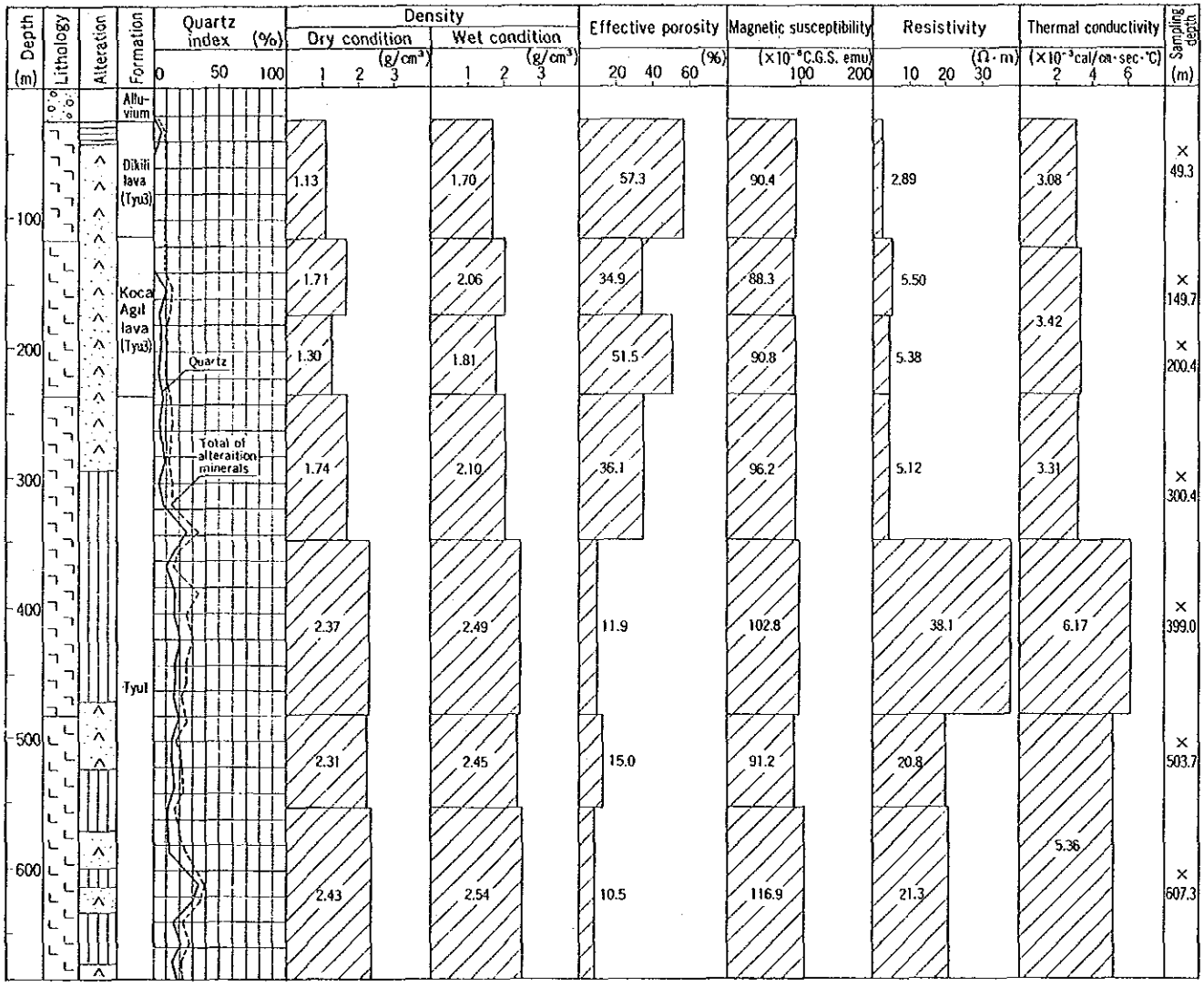

Fig. II.3.70 (1) Comparative diagram of rock properties against depth

Well No. DG-2

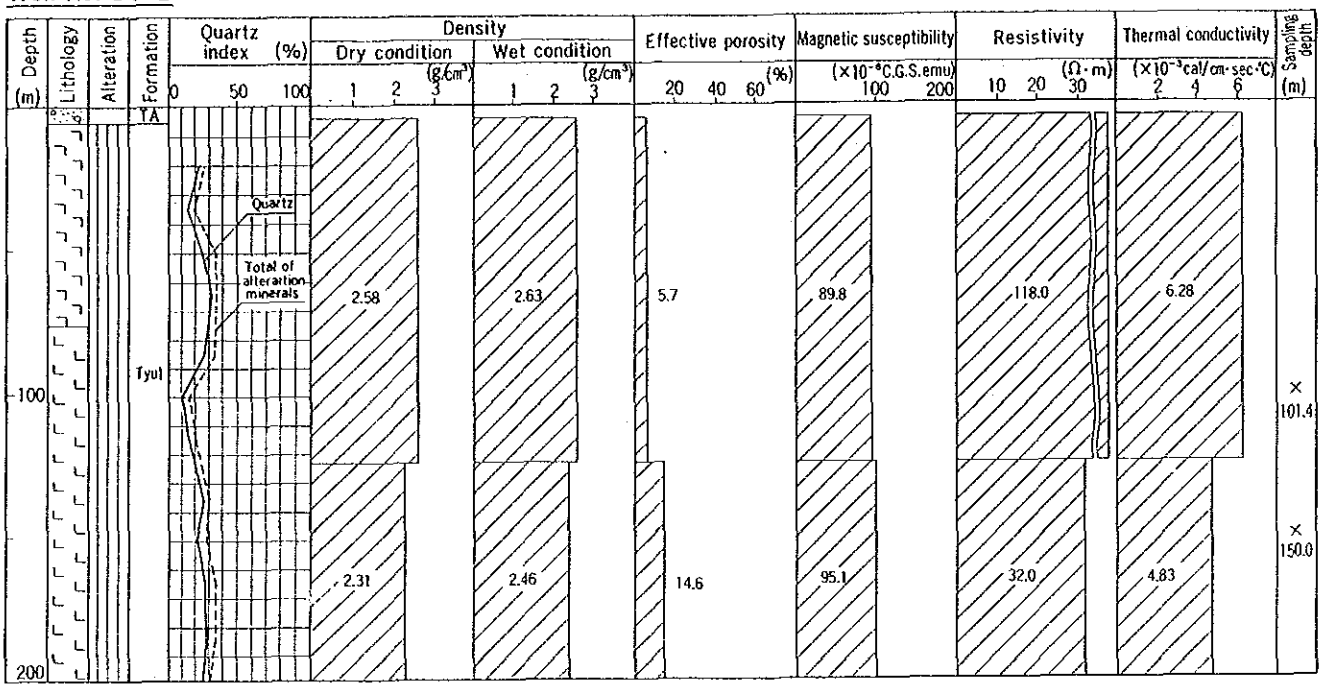

Well No. DG-3

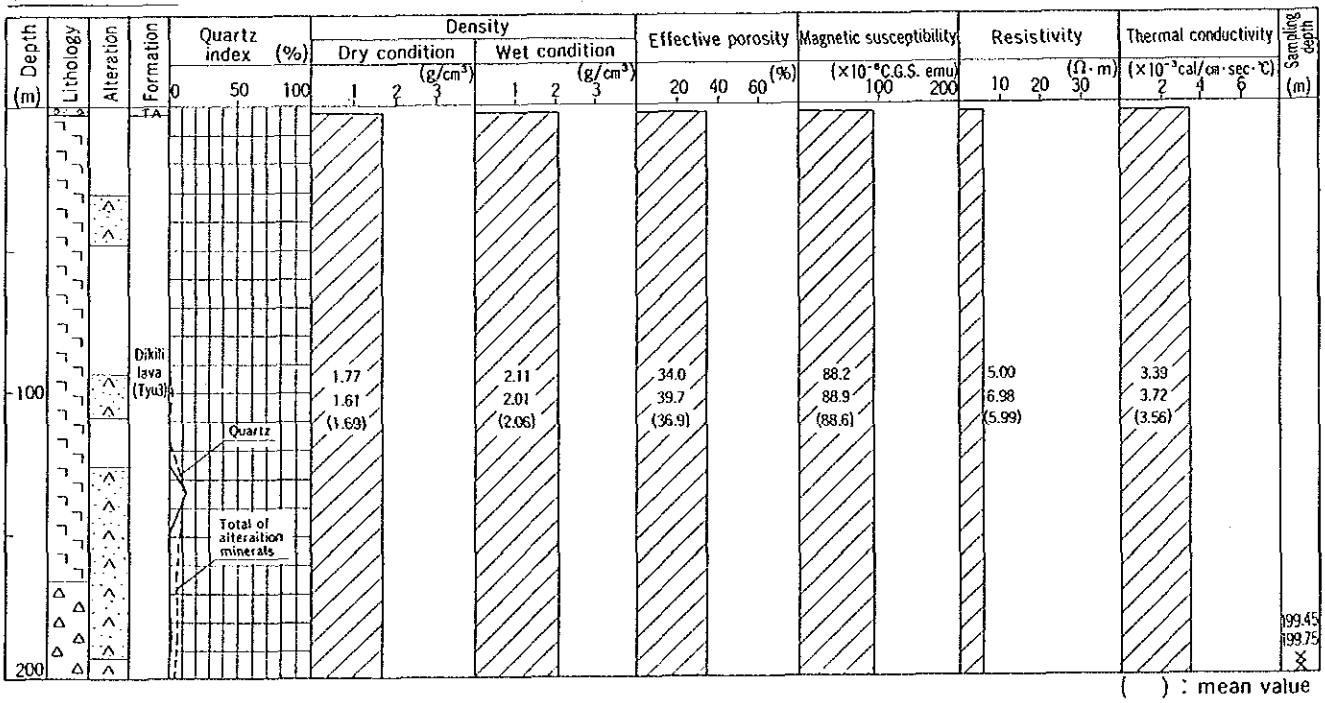

Fig. II.3.70 (2) Comparative diagram of rock properties against depth

Table II 3.8 (1) Fluid inclusion data

No 1

Well No.	D G − 1	Sampling depth	1 6 0.0 0 m	(core) cuttings)

Mineral	Occurrence	Fluid inclusion			Remarks	Mineral	Occurrence	Fluid inclusion			Remarks
		No.	Size (μm)	H.T. (℃)				No.	Size (μm)	H.T. (℃)	
Calcite		1 − a	2 × 2	100.2							
Calcite		2 − a	28 × 24	80.7							
Calcite		3 − a	60 × 20	123.6							
Calcite		4 − a	4 × 4	101.3							
Calcite		5 − a	40 × 40	98.2							
Calcite		6 − a	40 × 72	124.1							
Calcite		7 − a	12 × 24	87.6							
Calcite		8 − a	16 × 4	104.3							
Calcite		9 − a	20 × 8	107.1							
Calcite		10 − a	24 × 10	92.3							
		b	12 × 16	88.2							

H.T. : Homogenization temperature

Table II 3. 8 (2) Fluid inclusion data

No 2

Well No.	D G − 1	Sampling depth	2 5 0. 0 0 m	(core) cuttings)

Mineral	Occurrence	Fluid inclusion No.	Fluid inclusion Size (μm)	Fluid inclusion H.T. (℃)	Remarks	Mineral	Occurrence	Fluid inclusion No.	Fluid inclusion Size (μm)	Fluid inclusion H.T. (℃)	Remarks
Calcite		1 − a	4 × 6	92.5		Calcite		5 − g	4 × 4	169.4	
		b	10 × 14	173.0		Calcite		6 − a	12 × 8	164.2	
		c	10 × 16	174.9				b	6 × 10	166.3	
		d	10 × 4	229.3				c	30 × 4	166.0	
Calcite		2 − 9	28 × 10	127.3		Calcite		7 − a	18 × 6	168.3	
Calcite		3 − a	8 × 4	85.4							
		b	6 × 12	171.3							
Calcite		4 − a	4 × 14	101.3							
		b	2 × 4	104.7							
Calcite		5 − a	16 × 12	160.8							
		b	8 × 12	158.9							
		c	4 × 12	169.4							
		d	2 × 20	116.1							
		e	2 × 6	168.0							
		f	16 × 8	171.3							

H.T. : Homogenization temperature

Table II 3.8 (3) Fluid inclusion data

No 3

Well No.	D G − 1	Sampling depth	4 2 5.0 0 m	(core · cuttings)

Mineral	Occurrence	Fluid inclusion			Remarks	Mineral	Occurrence	Fluid inclusion			Remarks
		No.	Size (μm)	H.T. (℃)				No.	Size (μm)	H.T. (℃)	
Quartz		1 − a	12 × 28	160.1							
		b	8 × 20	132.4							
Quartz		2 − a	4 × 2	92.3							
		b	12 × 12	90.4							
Quartz		3 − a	12 × 28	125.0							
		b	28 × 16	79.9							
Quartz		4 − a	4 × 2	122.3							
		b	4 × 8	128.6							
Quartz		5 − a	16 × 8	231.3							
		b	8 × 4	231.3							
		c	24 × 2	128.3							
Quartz		6 − a	6 × 4	84.8							
Quartz		7 − a	8 × 4	134.4							
Quartz		8 − a	12 × 12	145.3							

H.T. : Homogenization temperature

Table Ⅱ 3. 8 (4) Fluid inclusion data

No 4

Well No.	D G − 1	Sampling depth	6 0 8.0 0 m	(core) cuttings)

Mineral	Occurrence	Fluid inclusion			Remarks	Mineral	Occurrence	Fluid inclusion			Remarks
		No.	Size (μm)	H.T. (℃)				No.	Size (μm)	H.T. (℃)	
Calcite		1 − a	70 × 56	80.9							

H.T. : Homogenization temperature

Table Ⅱ 3. 8 (5) Fluid inclusion data

No 5

Well No.	D G − 1	Sampling depth	6 1 5.0 0 m	(core・cuttings)

Mineral	Occurrence	Fluid inclusion			Remarks	Mineral	Occurrence	Fluid inclusion			Remarks
		No.	Size (μm)	H.T. (℃)				No.	Size (μm)	H.T. (℃)	
Calcite		1 − a	4 × 2	103.3							
Calcite		2 − a	40 × 8	80.5							

H.T. : Homogenization temperature

Table II 3. 8 (6) Fluid inclusion data

No 6

Well No.	D G − 1	Sampling depth	6 5 5.0 0 m (core·cuttings)

Mineral	Occurrence	Fluid inclusion No.	Fluid inclusion Size (μm)	Fluid inclusion H.T. (℃)	Remarks	Mineral	Occurrence	Fluid inclusion No.	Fluid inclusion Size (μm)	Fluid inclusion H.T. (℃)	Remarks
Quartz		1 − a	10 × 10	224.7							
		b	8 × 16	254.6							
		c	6 × 12	240.4							
		d	6 × 6	217.0							
		e	6 × 10	219.6							
		f	10 × 10	228.3							
		g	8 × 2	231.9							
		h	10 × 6	219.0							

H.T. : Homogenization temperature

Table Ⅱ 3. 8 (7) Fluid inclusion data

No 7

Well No.	D G − 1	Sampling depth	6 8 0.0 0 m	(core) cuttings)

Mineral	Occurrence	Fluid inclusion			Remarks	Mineral	Occurrence	Fluid inclusion			Remarks
		No.	Size (μm)	H.T. (℃)				No.	Size (μm)	H.T. (℃)	
Calcite		1 − a	14 × 10	94.8							
		b	2 × 6	94.8							
		c	20 × 4	92.3							
Calcite		2 − a	4 × 12	99.2							
		b	24 × 4	118.4							
		c	8 × 6	115.5							
		d	8 × 2	100.4							
Calcite		3 − a	20 × 36	113.6							
Calcite		4 − a	12 × 2	97.3							
		b	20 × 4	94.3							

H.T. : Homogenization temperature

Table II 3.9 Results of rock property measurement

Well No.	Depth (m)	Density: Dry Condition (g/cm³)	Density: Wet Condition (g/cm³)	Effective Porosity (%)	Magnetic Susceptibility ($\times 10^{-6}$ C.G.S.emu)	Resistivity (Ω・m)	Thermal Conductivity ($\times 10^{-3}$ cal/cm・sec・℃)
DG-1	49.3 m	1.13	1.70	57.3	90.4	2.89	3.08
	149.7 m	1.71	2.06	34.9	88.3	5.50	※ (1.16)
	200.4 m	1.30	1.81	51.5	90.8	5.38	3.42
	300.4 m	1.74	2.10	36.1	96.2	5.12	3.31
	399.0 m	2.37	2.49	11.9	102.8	38.1	6.17
	503.7 m	2.31	2.45	15.0	91.2	20.8	5.36
	607.3 m	2.43	2.54	10.5	116.9	21.3	※ (0.29)
DG-2	101.4 m	2.58	2.63	5.7	89.8	118.0	6.28
	150.0 m	2.31	2.46	14.6	95.1	32.0	4.83
DG-3	199.45 m	1.77	2.11	34.0	88.2	5.00	3.39
	199.75 m	1.61	2.01	39.7	88.9	6.98	3.72

※ ( ) : Sample was broken during measurement

〔Reference data (Mean value of fresh rock properties of Tyu1 and Tyu3〕

Yamtdag^{v} volcanics III (Hornblende Andesite)	2.41	2.47	6.27	35.80	191.9	4.09
Yamtdag^{v} volcanics I (Hornblende Andesite)	2.59	2.63	3.88	34.20	522.2	5.21

(7) Chemical analysis of core and cuttings

Chemical analysis was carried out (using the same samples for X-ray analysis) in order to understand the relation between the rock chemical composition and geothermal activity or hydrothermal alteration in the survey area.

Items of analysis are 25 components as follows:

(a) Main chemical composition of rock forming minerals
(9 components)
Si, Al, Mg, Ca, Na, K, Fe, Mn, Ti

(b) Chemical composition related to volcanic divergent material
(4 components)
As, Hg, B, S

(c) Chemical composition related to the hydrothermal deposit
(2 components)
Cu, Pb

(d) Others
(10 components)
Li, Rb, Sb, Sr, Be, Ba, Co, Ignition loss, H_2O, pH

The results of the chemical analysis are arranged in Table II.3.10. The chemical composition against depth is shown in Fig. II.3.71 and 3 component diagrams are shown in Fig. II.3.72 and Fig. II.3.73.

The broken line indicates the mean value of the original rocks in the Yuntdağ volcanics I and III. As compared with the chemical compositions of fresh rock and core,, cuttings and alteration minerals by X-ray analysis, the following features are mentioned.

1) Rock chemical component in DG-1

(a) The rocks in DG-1 show low contents of Al, Fe, Mg, Ca, Na which belong to the main component of rock forming minerals, rather than the original rocks.

These amounts become large in proportion to the strength of

Well No. DG-1

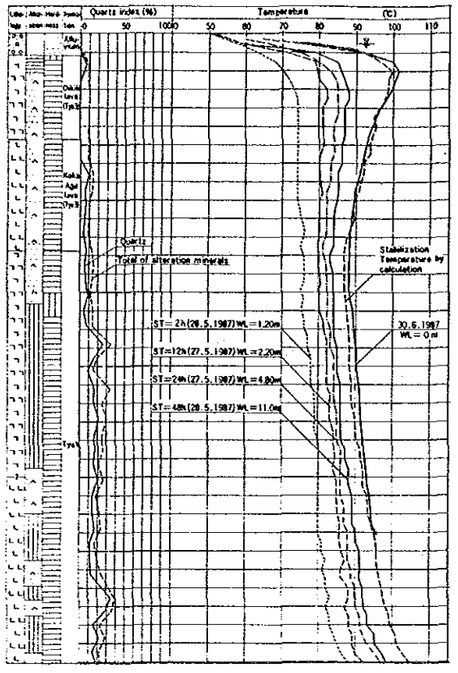

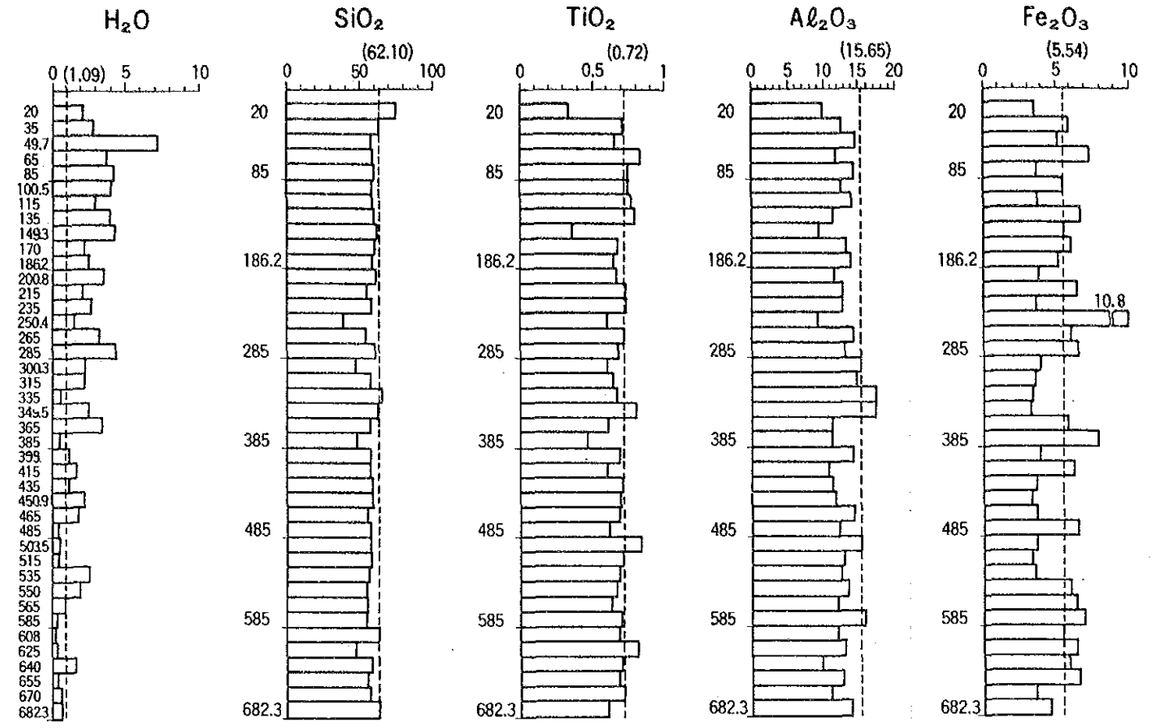

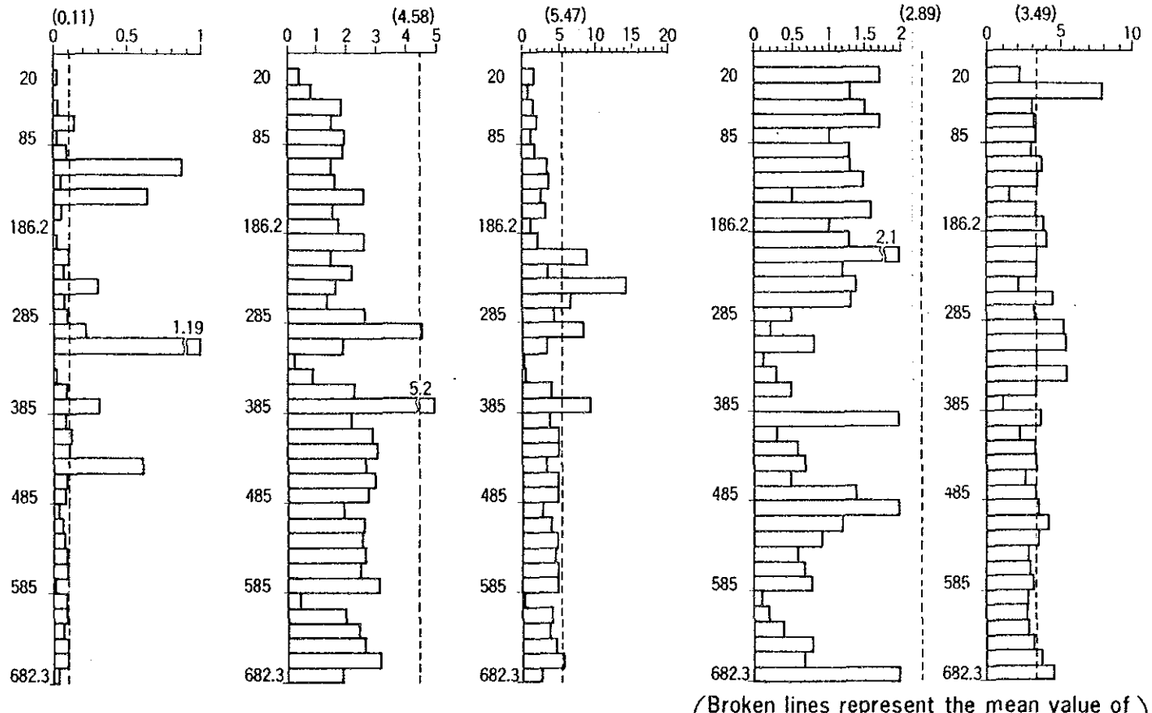

Fig. II.3.71 (1) Chemical composition of rock in thermal gradient hole.

Well No. DG-1

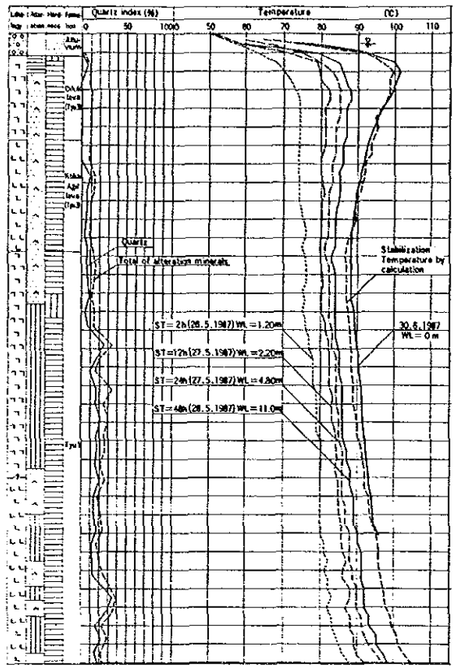

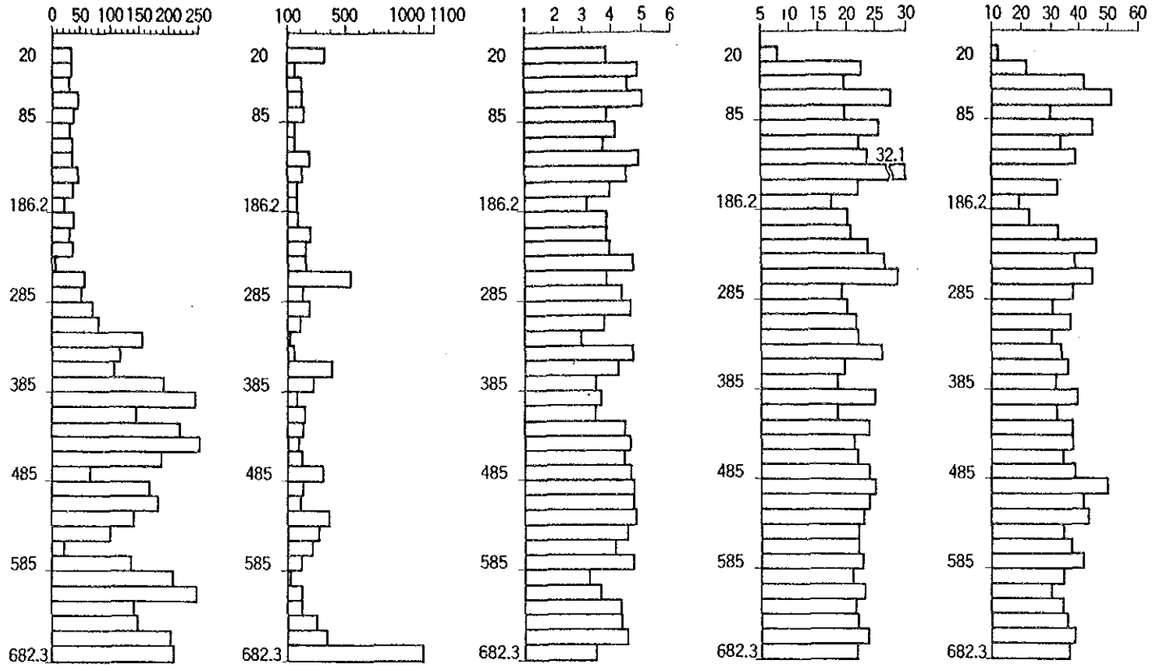

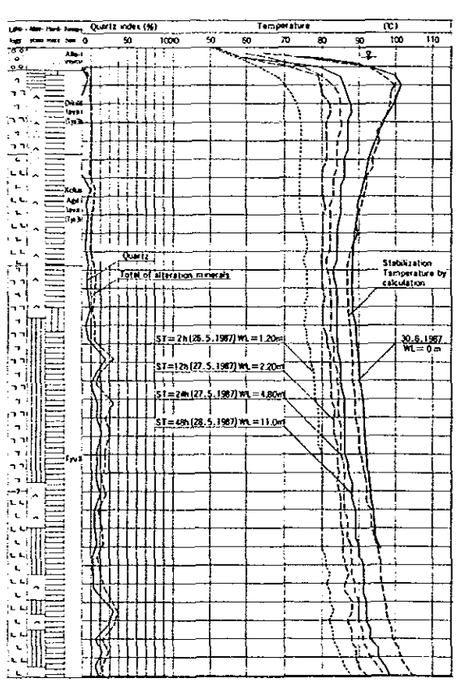

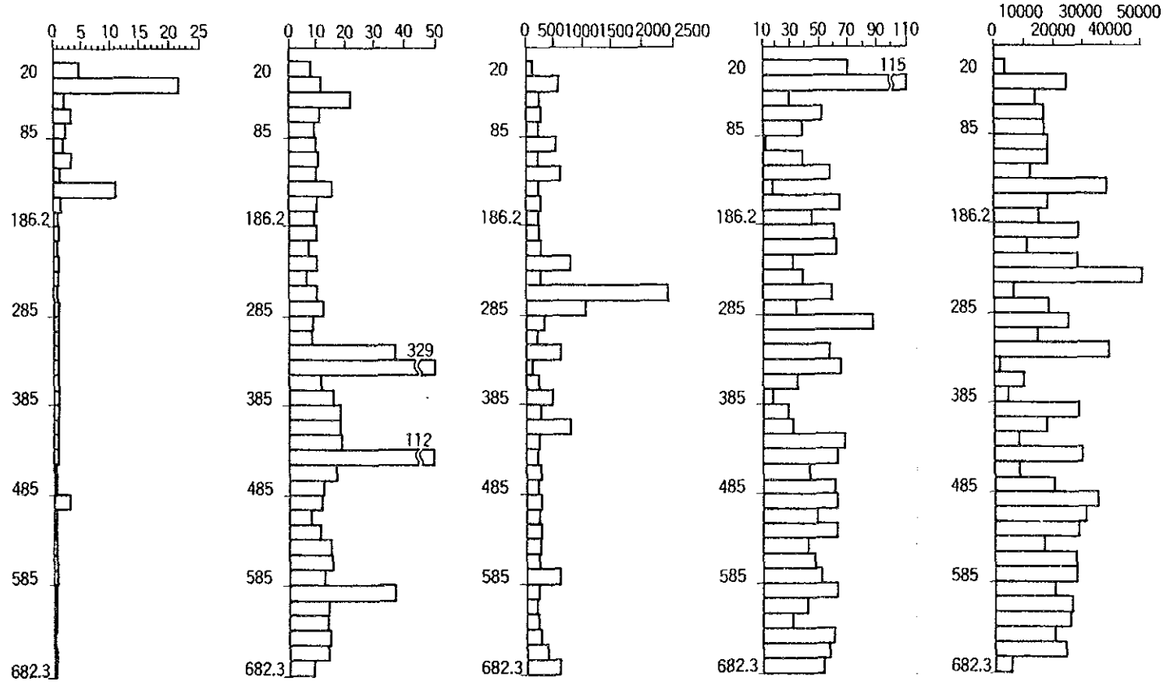

Fig. II.3.71 (2) Chemical composition of rock in thermal gradient hole.

Well No. DG-1

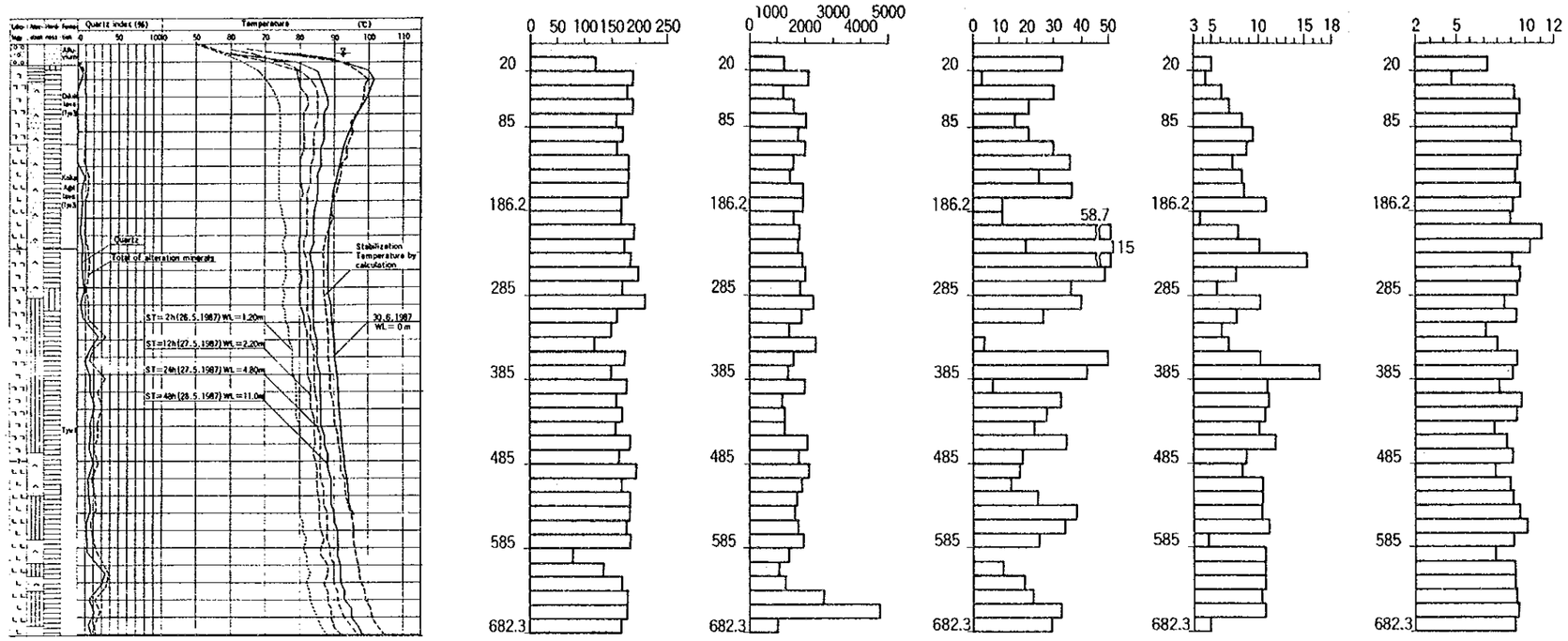

Fig. II.3.71 (3) Chemical composition of rock in thermal gradient hole.

Well No. DG-2

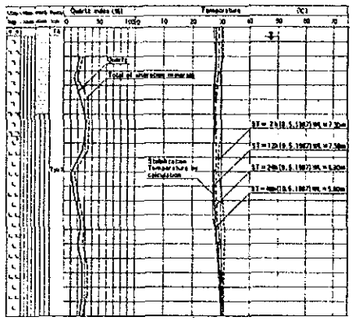

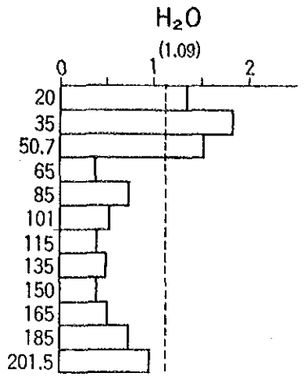

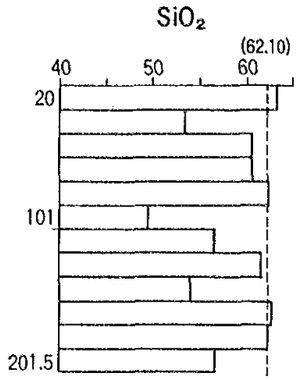

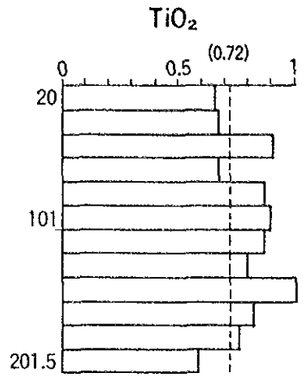

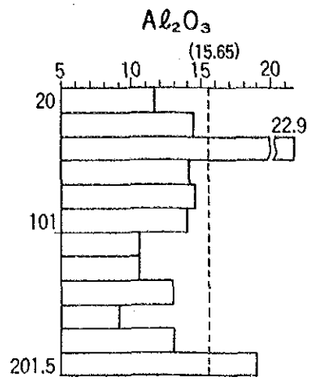

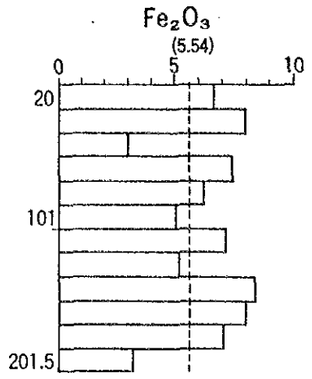

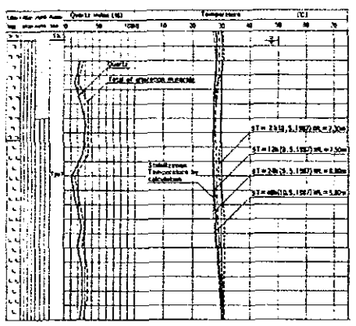

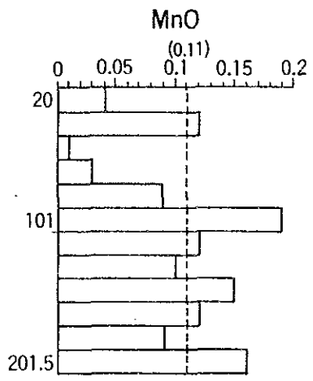

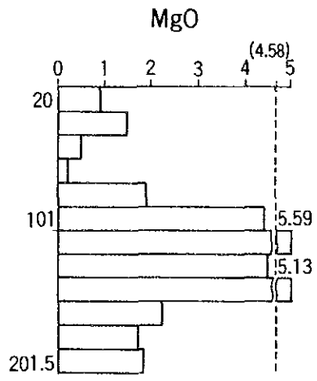

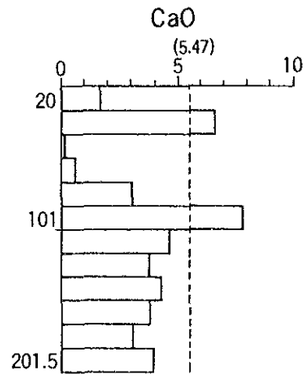

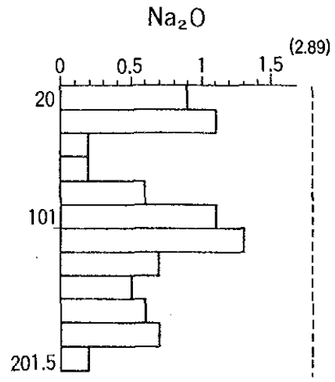

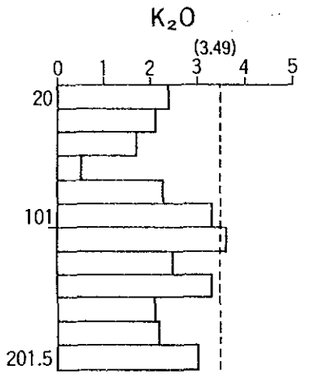

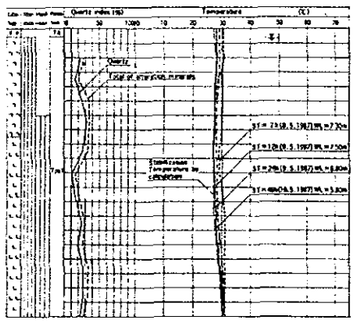

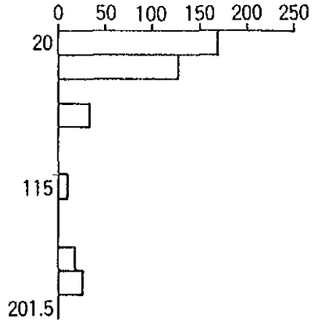

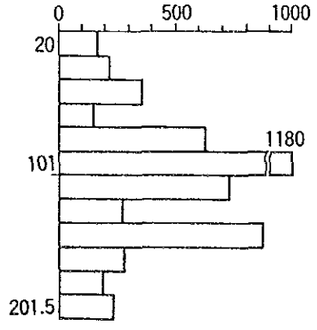

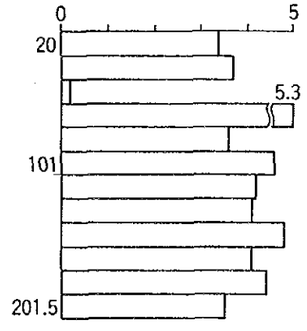

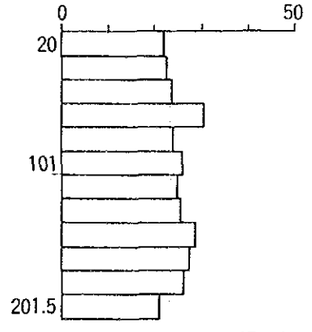

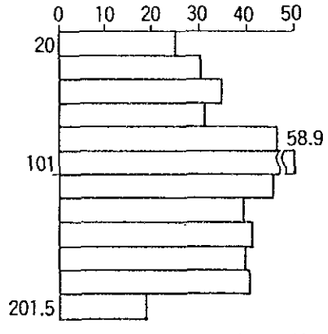

(Broken lines represent the mean value of fresh rocks in Tyu I and Tyu III)

Fig. II.3.71(4) Chemical composition of rock in thermal gradient hole.

Well No. DG-2

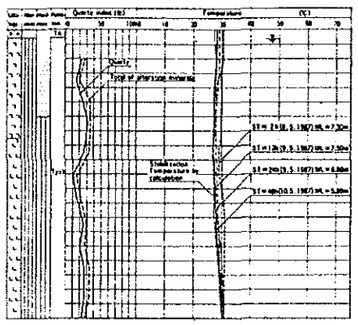

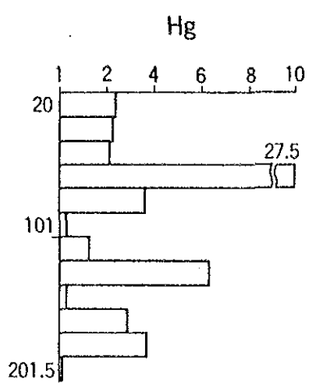

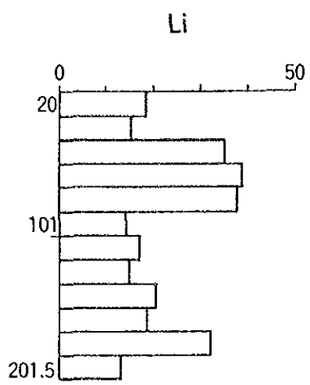

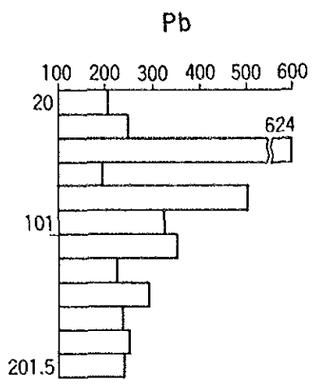

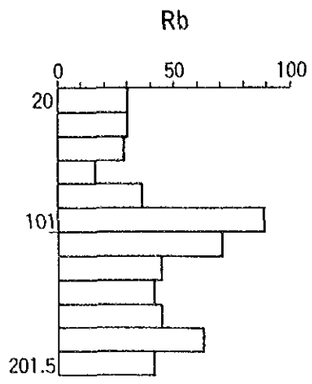

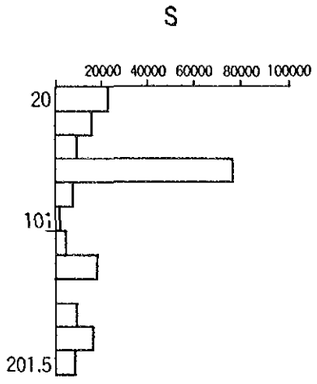

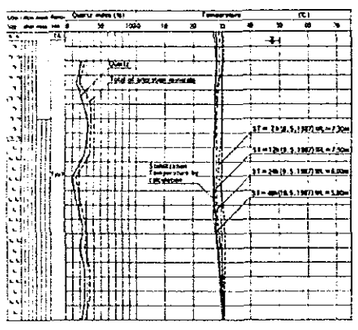

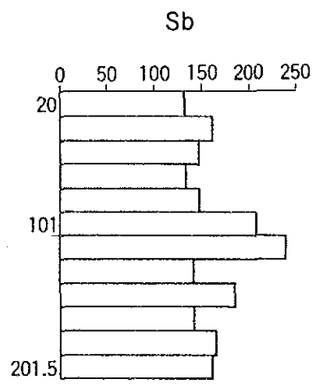

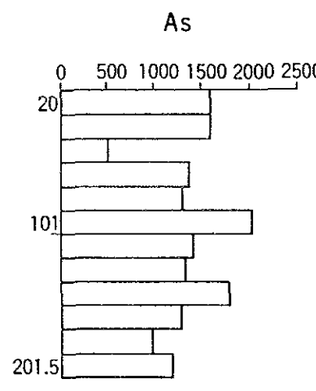

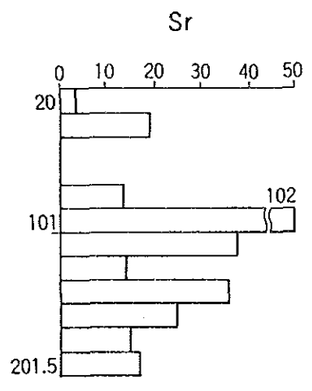

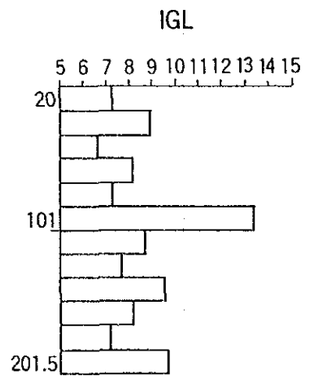

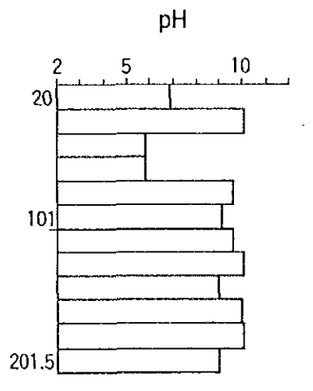

Fig. II.3.71(5) Chemical composition of rock in thermal gradient hole.

Well No. DG-3

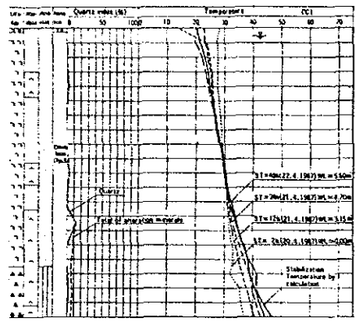

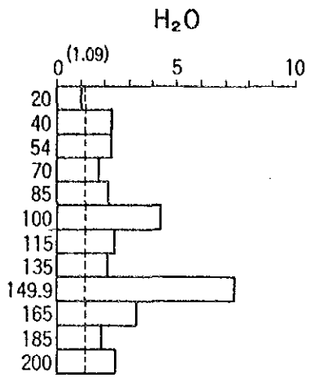

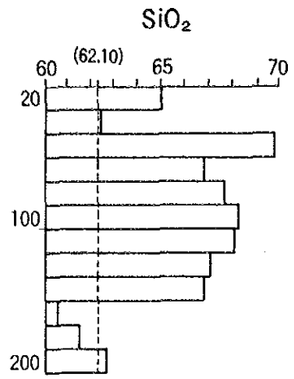

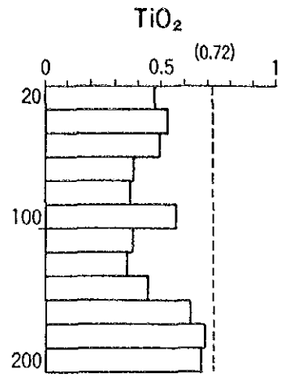

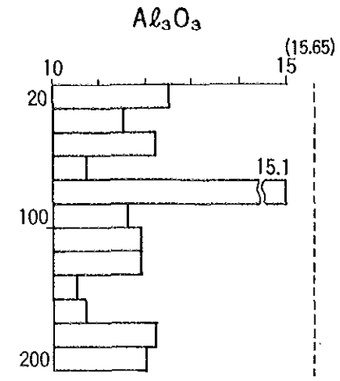

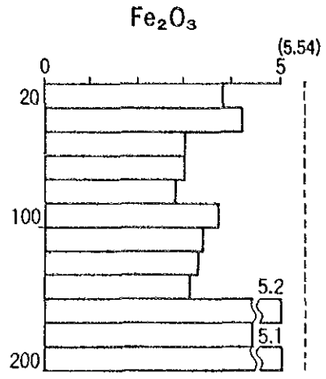

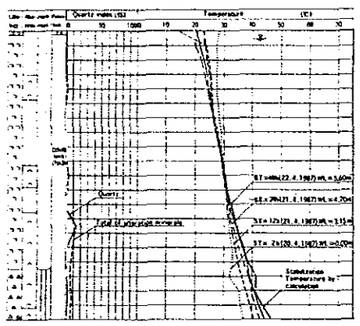

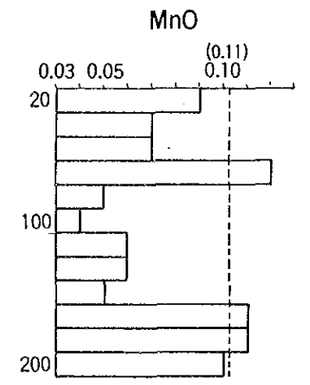

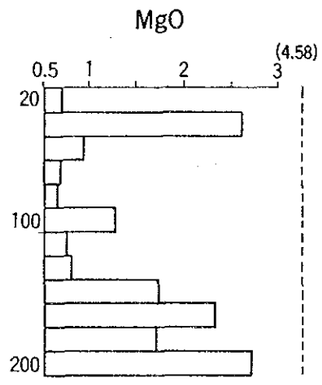

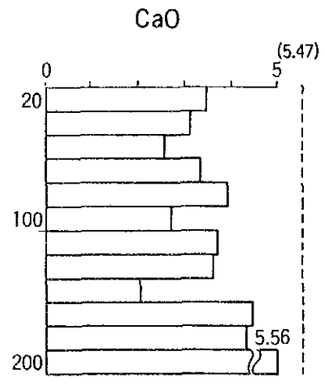

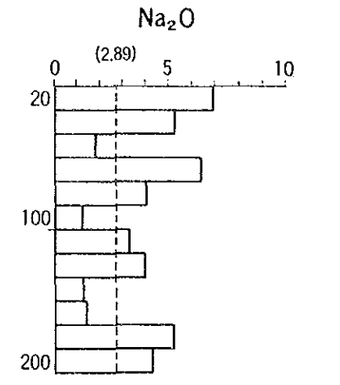

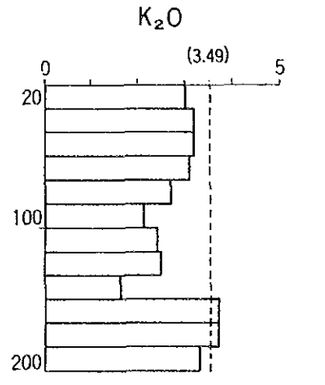

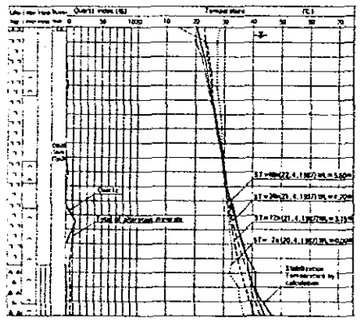

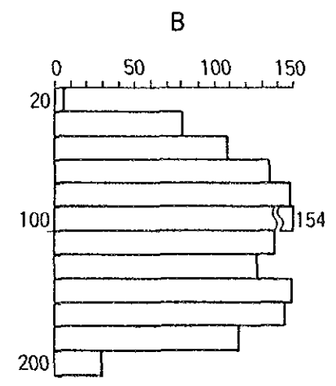

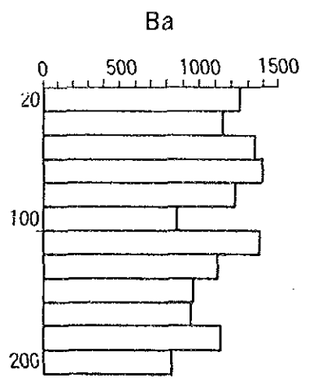

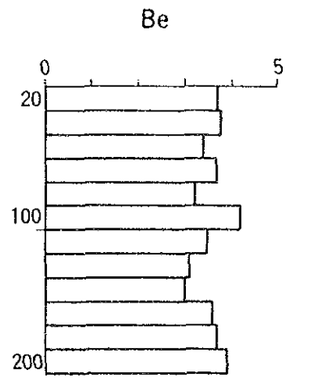

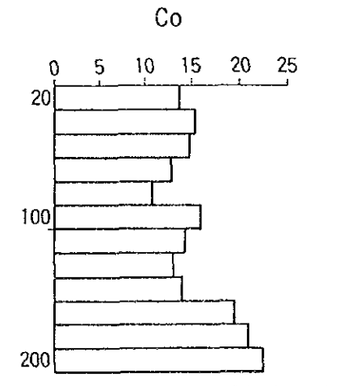

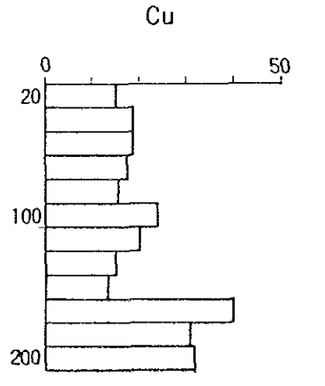

(Broken lines represent the mean value of fresh rocks in Tyu I and Tyu III)

Fig. II.3.71(6) Chemical composition of rock in thermal gradient hole.

Well No. DG-3

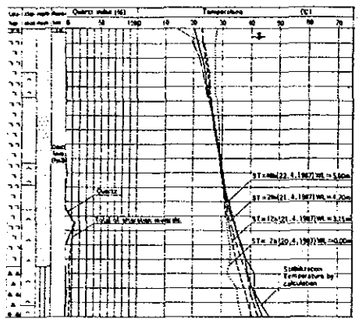

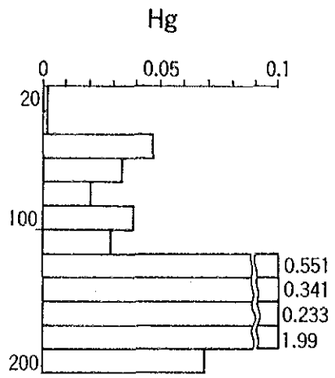

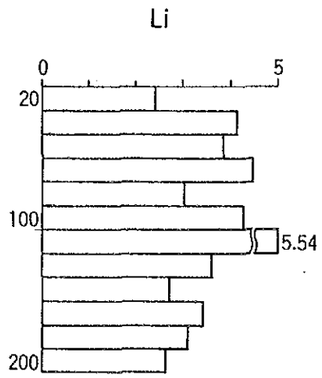

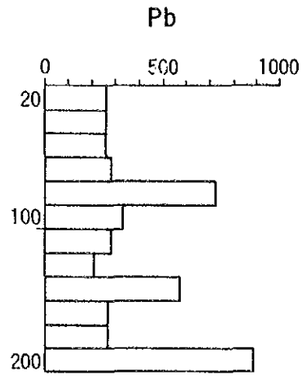

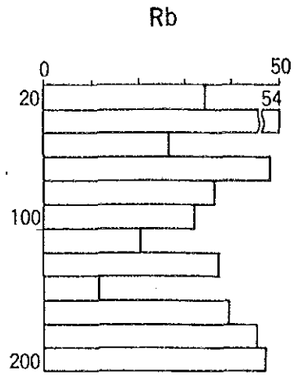

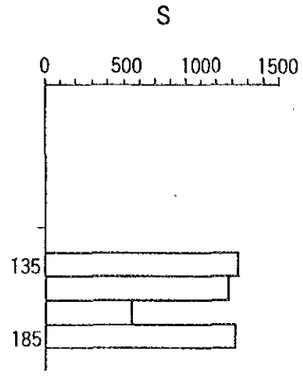

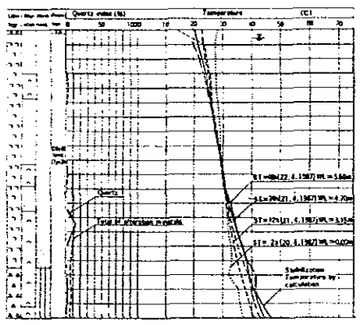

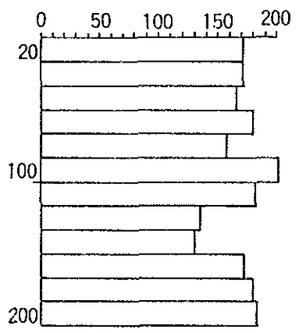

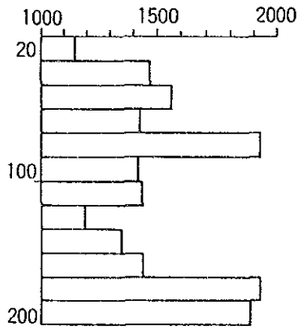

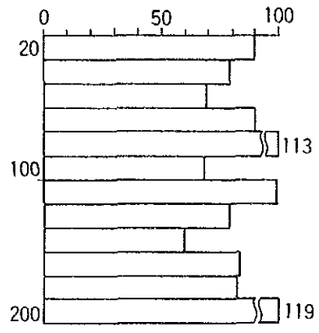

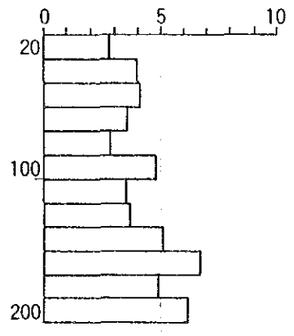

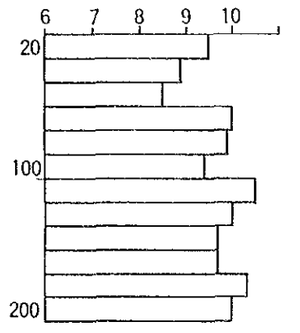

Fig. II.3.71 (7) Chemical composition of rock in thermal gradient hole.

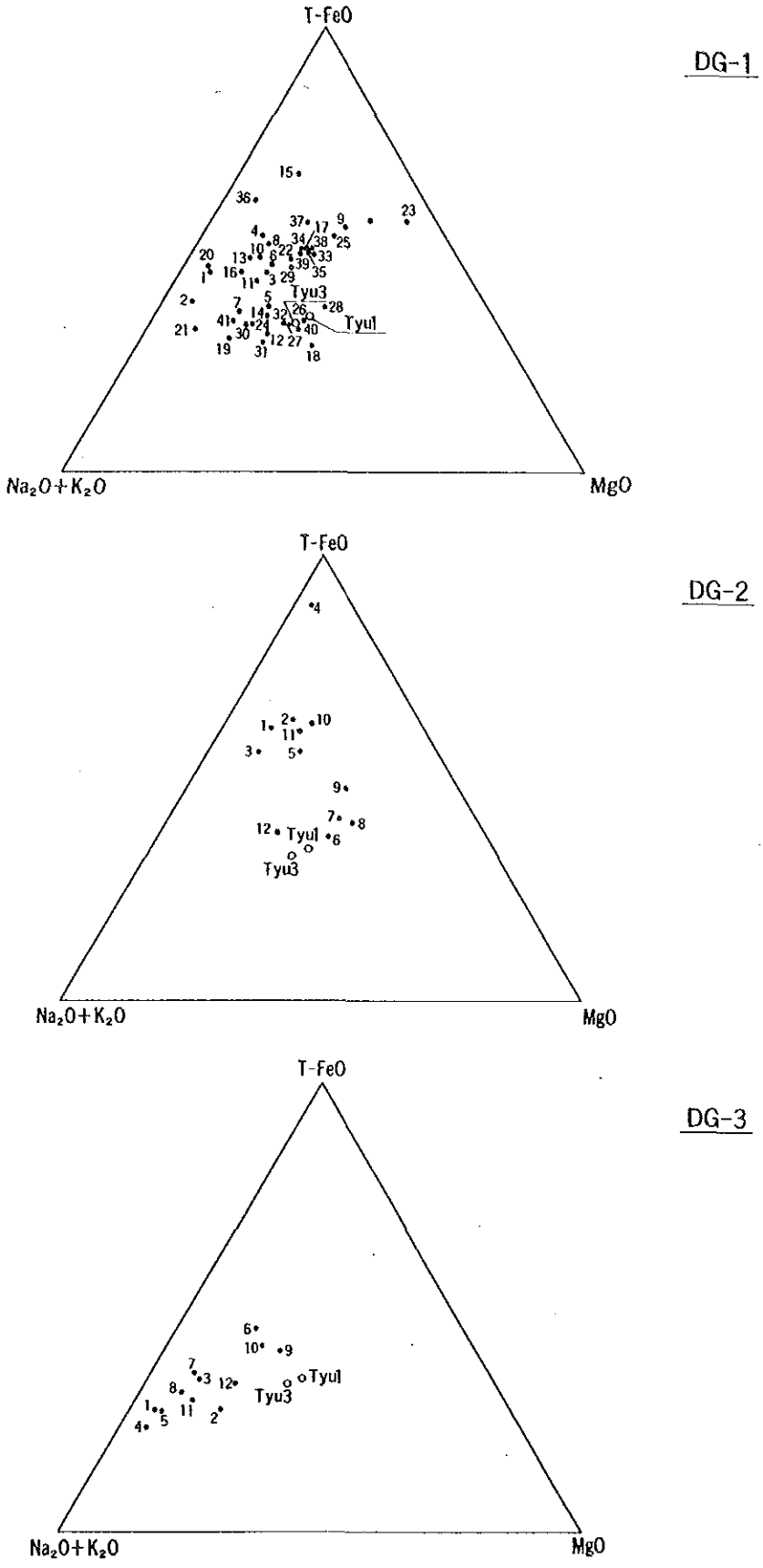

Fig.II.3.72 Chemical composition of core and cuttings plotted onto the AFM diagram.

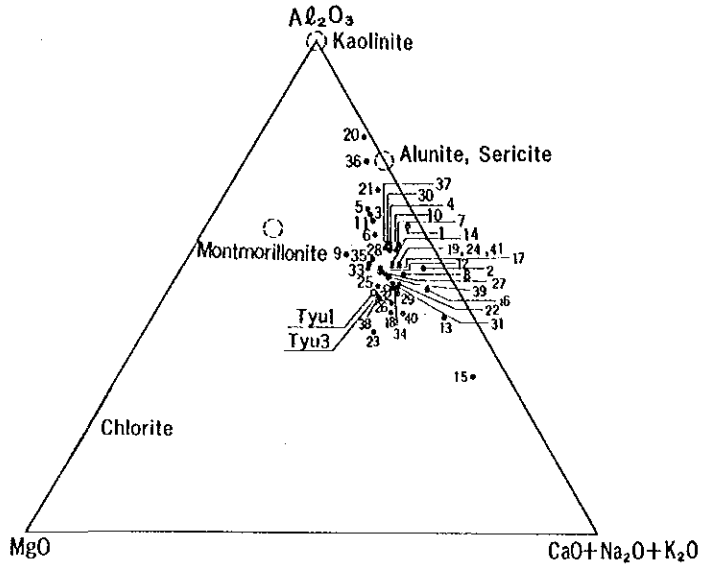

DG-1

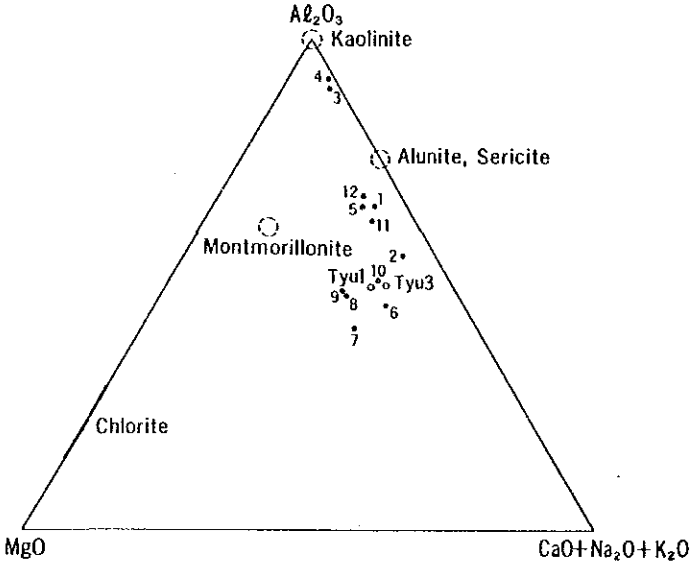

DG-2

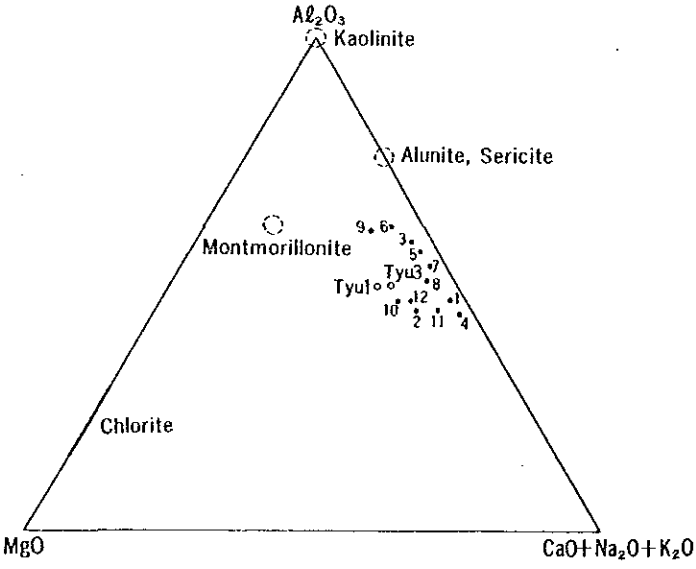

DG-3

Fig.II.3.73 Chemical composition of core and cuttings plotted onto the Aℓ-(Ca+Na+K)-Mg diagram

Table II.3.10 (1) Chemical composition of core and cuttings

Well No. DG－1

Sample nos	Depth (m)	H_2O	SiO_2	TiO_2	Al_2O_3	Fe_2O_3	MnO	MgO	CaO	Na_2O	K_2O	B	Ba	Be	Co	Cu	Hg	Li	Pb	Rb	S	Sb	As	Sr	IGL	pH (29℃)
		%										mg/Kg (ppm)													%	
1	20	2.07	75.0	0.34	9.5	3.4	0.02	0.390	1.47	1.7	2.1	33	348	3.8	8.2	12.6	4.89	8.35	166	68.9	3730	120	1240	32.5	3.82	7.3
2	35	2.83	62.7	0.71	12.4	5.8	N.D	0.809	0.68	1.3	7.7	34	147	4.9	22.5	21.8	21.7	12.1	594	115	24700	188	2080	3.0	4.25	3.6
3	49.7	7.22	57.5	0.65	14.3	5.1	0.03	1.84	1.44	1.5	3.0	31	189	4.5	19.6	41.6	2.31	21.9	266	29.0	13900	178	1190	29.5	5.78	9.2
4	65	3.71	58.6	0.83	11.4	7.3	0.15	1.54	1.86	1.7	3.2	44	198	5.0	27.3	50.8	3.44	11.6	283	52.5	16800	188	1590	20.3	6.59	9.6
5	85	4.20	59.6	0.75	14.3	3.6	0.02	1.94	1.29	1.0	3.3	34	217	3.8	19.6	29.6	2.58	9.58	250	38.3	16700	160	2010	15.2	8.10	9.4
6	100.5	4.07	58.2	0.74	12.5	5.4	0.09	1.90	1.74	1.3	3.0	31	155	4.1	25.4	44.5	2.05	9.88	541	13.2	18200	172	1740	20.3	9.23	9.1
7	115	2.90	58.1	0.77	14.0	3.7	0.87	1.51	3.39	1.3	3.7	36	154	3.7	21.9	33.2	3.38	11.3	243	39.2	18100	162	1990	29.4	8.60	9.6
8	135	3.94	58.6	0.79	11.3	6.7	0.05	1.66	3.50	1.5	3.4	37	240	4.9	23.6	38.5	1.39	10.2	616	57.4	12300	181	1560	35.6	7.18	9.4
9	149.3	4.23	60.9	0.36	9.3	5.5	0.64	2.58	2.48	0.5	1.5	47	199	4.5	32.1	10.4	10.9	15.5	252	19.4	38400	182	1460	23.9	8.05	9.3
10	170	2.25	59.0	0.67	13.3	6.0	0.06	1.57	3.15	1.6	3.3	34	167	3.9	21.9	32.2	1.68	10.5	274	63.8	17900	180	1970	36.1	8.25	9.6
11	186.2	2.48	58.2	0.65	14.1	5.1	N.D	1.75	1.23	1.0	3.9	18	166	3.1	16.9	19.0	0.944	9.21	250	45.6	15300	168	1920	10.7	10.6	9.1
12	200.8	3.49	60.6	0.67	11.5	3.7	0.02	2.66	2.26	1.3	4.1	42	170	3.8	20.1	22.6	1.04	10.4	257	59.9	28500	169	1630	10.7	3.61	9.0
13	215	2.14	54.5	0.73	12.4	6.4	0.11	1.50	8.70	2.1	3.4	32	258	3.8	20.6	32.4	0.997	7.55	293	61.0	11000	192	1800	58.7	7.68	11.1
14	235	2.72	58.0	0.73	12.7	3.6	0.08	2.21	3.69	1.2	3.4	37	233	3.9	23.4	45.7	1.07	10.6	800	32.0	28000	174	1780	19.1	9.88	10.3
15	250.4	1.47	38.3	0.60	9.1	10.8	0.31	1.71	14.4	1.4	2.1	6	230	4.7	26.5	38.3	1.02	7.19	286	39.2	50100	186	1940	115	15.1	9.1
16	265	3.26	54.3	0.72	14.3	6.0	0.08	1.42	6.80	1.3	4.6	55	532	3.8	28.7	44.0	0.986	10.5	2480	58.4	6670	199	2070	47.9	7.34	9.6
17	285	4.33	60.0	0.67	12.9	6.5	0.10	2.65	4.38	0.5	3.3	50	201	4.3	18.7	37.4	1.07	12.3	1050	34.4	18000	169	1850	35.7	5.42	9.4
18	300.3	2.29	46.0	0.59	15.1	3.9	0.23	4.58	8.38	0.2	5.3	69	245	4.6	19.9	30.1	1.04	9.06	354	87.2	24700	210	2300	39.6	10.0	8.5
19	315	2.25	57.3	0.64	14.7	3.5	1.19	1.93	3.60	0.8	5.5	79	190	3.7	21.5	36.6	1.04	8.81	247	60.5	14800	159	1890	25.9	7.52	9.3
20	335	0.67	64.8	0.67	17.2	3.3	N.D	0.309	0.25	0.1	3.4	154	116	2.9	21.9	30.2	1.07	37.1	633	56.9	39000	152	1430	N.D	5.91	7.1

Table II.3.10 (2) Chemical composition of core and cuttings

Well No. DG-1

Sample nos	Depth (m)	H_2O	SiO_2	TiO_2	AL_2O_3	Fe_2O_3	MnO	MgO	CaO	Na_2O	K_2O	B	Ba	Be	Co	Cu	Hg	Li	Pb	Rb	S	Sb	As	Sr	IGL	pH (29℃)
		%										mg/Kg (ppm)													%	
21	349.5	2.53	62.4	0.81	17.2	3.2	0.02	0.909	0.43	0.3	5.7	116	153	4.7	26.1	33.4	1.03	329	146	64.0	2250	119	2420	3.80	6.87	8.0
22	365	3.43	57.3	0.61	11.1	5.8	0.10	2.28	4.48	0.5	3.4	106	413	4.2	19.3	35.7	1.05	11.8	262	35.3	10200	174	1620	49.3	10.2	9.4
23	385	0.56	47.5	0.46	11.2	7.9	0.32	5.20	9.61	N.D	1.1	189	285	3.4	18.2	31.6	1.06	15.7	485	18.5	4750	150	1380	41.6	16.6	9.1
24	399	1.22	57.4	0.69	14.3	3.9	0.10	2.22	3.83	2.0	3.8	245	160	3.6	24.8	39.2	1.03	18.0	265	28.6	28700	177	2040	7.3	10.7	8.1
25	415	1.70	57.0	0.60	10.8	6.3	0.14	2.96	5.29	0.3	2.3	146	219	3.4	18.3	32.1	1.06	18.1	780	31.5	17400	162	1610	31.8	11.0	9.7
26	435	1.18	58.6	0.71	11.1	3.6	0.13	3.10	5.28	0.6	3.4	222	206	4.4	23.8	37.6	1.06	18.4	275	67.4	3100	173	1690	26.9	10.6	9.4
27	450.9	2.16	58.8	0.69	11.7	3.3	0.62	2.65	3.36	0.7	3.5	251	171	4.6	21.3	37.8	1.06	112	247	62.9	30700	159	1670	22.5	9.93	7.8
28	465	1.80	55.6	0.68	14.5	3.6	0.11	2.99	5.29	0.5	2.6	187	198	4.4	21.9	34.1	0.738	17.0	288	43.7	8400	186	2090	33.8	11.6	8.7
29	485	0.39	56.8	0.61	12.2	6.5	0.10	2.85	5.20	1.4	3.4	65	344	4.6	23.7	38.6	0.653	12.4	256	59.9	20600	166	1790	18.1	8.50	9.1
30	503.5	0.56	57.5	0.84	15.4	3.7	0.05	2.04	2.98	2.0	3.6	163	199	4.7	25.0	49.6	3.18	11.9	287	62.0	35200	194	2150	17.1	8.01	7.9
31	515	0.51	57.0	0.71	13.1	3.3	0.08	2.69	4.31	1.2	4.3	179	186	4.7	24.1	41.5	0.629	8.41	268	48.2	31200	172	1900	13.7	10.0	9.0
32	535	2.47	56.1	0.69	12.4	3.6	0.09	2.65	5.21	0.9	3.6	141	385	4.8	22.8	43.1	0.586	11.5	284	62.6	28500	185	1700	23.4	10.2	9.2
33	550	1.90	54.8	0.67	13.4	6.0	0.11	2.76	4.95	0.6	2.9	98	305	4.5	21.9	33.9	0.883	15.3	287	43.5	16900	184	1640	37.8	10.3	9.6
34	565	0.93	55.3	0.63	12.0	6.4	0.11	2.60	5.49	0.7	3.0	23	260	4.1	22.0	36.8	0.997	15.7	276	47.5	27800	178	1750	33.5	11.1	10.1
35	585	0.43	55.3	0.70	15.8	7.0	0.02	3.14	5.70	0.8	3.3	134	195	4.7	23.3	41.2	0.789	12.7	623	52.8	27800	184	1940	24.5	4.61	9.2
36	608	0.33	64.3	0.69	12.1	5.5	0.11	0.565	0.42	0.1	2.8	207	109	3.2	21.3	33.8	0.517	37.2	263	62.4	20700	80.5	1420	N.D	10.6	7.9
37	625	0.44	47.1	0.82	13.1	6.5	0.11	2.12	4.53	0.2	2.8	246	200	3.6	23.0	30.8	0.635	14.3	223	40.7	26300	137	1110	10.8	10.5	9.3
38	640	1.67	58.4	0.70	9.6	5.9	0.08	2.54	4.09	0.4	2.9	140	200	4.3	21.5	33.8	0.692	14.5	266	31.5	25700	170	1320	18.6	10.5	9.3
39	655	0.41	55.2	0.69	12.9	6.6	0.11	2.74	5.09	0.8	3.3	147	294	4.3	21.8	35.4	0.272	14.8	287	60.4	20300	181	2680	22.0	9.79	9.4
40	670	0.65	57.4	0.72	11.0	3.6	0.11	3.19	5.92	0.7	3.9	199	357	4.5	23.6	38.9	0.438	14.2	397	57.5	23500	183	4680	32.3	10.5	9.5
41	682.3	0.67	62.9	0.61	14.1	4.6	0.05	1.98	2.70	2.0	4.8	207	1020	3.4	21.8	35.9	0.102	9.23	620	53.4	5680	168	1060	28.8	4.73	9.3

Table II.3.10 (3) Chemical composition of core and cuttings

Well № DG-2

Sample nos	Depth (m)	H_2O	SiO_2	TiO_2	Al_2O_3	Fe_2O_3	MnO	MgO	CaO	Na_2O	K_2O	B	Ba	Be	Co	Cu	Hg	Li	Pb	Rb	S	Sb	As	Sr	IGL	pH (29℃)
		%										mg/Kg (ppm)													%	
1	20	1.35	63.2	0.66	11.6	6.7	0.04	0.932	1.70	0.9	2.4	168	169	3.4	22.1	25.3	2.42	18.7	206	30.1	23300	132	1604	3.4	7.27	6.9
2	35	1.83	53.5	0.68	14.3	8.0	0.12	1.47	6.57	1.1	2.1	127	226	3.7	22.5	30.3	2.28	15.3	250	30.5	15900	162	1600	19.0	8.96	10.9
3	50.7	1.54	60.7	0.91	22.9	3.0	0.01	0.492	0.16	0.2	1.7	N.D	360	0.2	23.7	35.0	2.17	34.9	624	28.7	9810	147	524	N.D	6.64	5.8
4	65	0.37	60.7	0.68	14.2	7.5	0.03	0.246	0.34	0.2	0.5	33	150	5.3	30.6	31.4	27.5	38.7	195	16.0	76900	133	1380	N.D	8.18	5.8
5	85	0.74	62.3	0.87	14.6	6.2	0.09	1.90	2.89	0.6	2.3	N.D	636	3.6	24.2	46.6	3.66	37.8	504	37.3	7930	148	1320	13.7	7.28	9.6
6	101	0.53	49.5	0.90	14.0	5.1	0.19	4.38	7.81	1.1	3.3	N.D	1180	4.6	26.3	58.9	0.295	14.5	326	89.5	2200	207	2040	102	13.4	9.1
7	115	0.42	56.6	0.87	10.5	7.2	0.12	5.59	4.71	1.3	3.6	12	730	4.2	24.9	45.6	1.28	16.9	350	71.0	5600	239	1420	38.1	8.77	9.6
8	135	0.50	61.4	0.80	10.6	5.2	0.10	4.46	3.76	0.7	2.5	N.D	279	4.1	25.3	39.5	6.28	14.8	225	44.6	18000	142	1340	14.1	7.72	10.5
9	150	0.39	53.8	1.01	12.9	8.4	0.15	5.13	4.32	0.5	3.3	N.D	871	4.8	28.7	41.4	0.320	20.7	293	41.6	372	184	1790	36.2	9.60	9.0
10	165	0.51	62.6	0.83	9.2	8.0	0.12	2.23	3.83	0.6	2.1	19	283	4.1	27.5	39.8	2.85	18.6	237	45.2	9700	141	1320	25.0	8.19	10.2
11	185	0.74	62.4	7.76	13.0	7.1	0.09	1.72	3.12	0.7	2.2	25	191	4.4	26.5	40.8	3.69	32.3	252	63.4	16300	165	988	15.2	7.18	10.6
12	201.5	0.86	56.6	0.59	19.0	3.2	0.16	1.84	3.88	0.2	3.0	N.D	239	3.5	20.0	18.8	0.108	13.3	240	41.6	9640	162	1190	17.1	9.71	9.0

Well № DG-3

Sample nos	Depth (m)	H_2O	SiO_2	TiO_2	Al_2O_3	Fe_2O_3	MnO	MgO	CaO	Na_2O	K_2O	B	Ba	Be	Co	Cu	Hg	Li	Pb	Rb	S	Sb	As	Sr	IGL	pH (29℃)
		%										mg/Kg (ppm)													%	
1	20	1.00	55.0	0.47	12.5	3.8	0.09	0.887	3.47	6.9	3.0	4	1240	3.7	13.7	15.1	0.002	2.44	266	34.4	N.D	172	1150	89.9	2.79	9.5
2	40	2.30	62.4	0.53	12.5	4.2	0.07	2.60	3.11	5.3	3.2	81	1150	3.8	15.4	18.8	0.002	4.15	269	54.0	N.D	172	1470	78.8	4.00	8.9
3	54	2.29	69.8	0.49	12.2	3.0	0.07	0.934	2.56	1.8	3.2	108	1350	3.4	14.8	18.7	0.047	3.84	261	26.6	N.D	164	1560	68.9	4.12	8.5
4	70	1.78	66.8	0.38	10.7	3.0	0.12	0.887	3.36	6.4	3.1	135	1400	3.7	12.7	17.5	0.034	4.45	279	48.1	N.D	180	1430	90.5	3.54	10.0
5	95	2.14	67.7	0.36	15.1	2.8	0.05	0.645	3.91	4.1	2.7	147	1210	3.2	10.7	15.4	0.020	3.00	731	36.4	N.D	157	1930	113	2.83	9.9
6	100	4.28	68.2	0.56	11.6	3.7	0.04	1.27	2.69	1.2	2.1	154	876	4.2	16.2	24.0	0.039	4.25	331	32.0	N.D	203	1420	68.0	4.83	9.4
7	115	2.38	68.1	0.37	11.9	3.4	0.06	0.749	3.72	3.3	2.4	138	1380	3.5	14.4	20.5	0.029	5.54	290	20.4	N.D	182	1440	99.6	3.52	10.5
8	135	2.14	67.1	0.35	11.9	3.3	0.06	0.804	3.62	4.0	2.5	127	1110	3.1	13.0	15.2	0.551	3.60	214	37.4	1240	135	1190	78.7	3.64	10.0
9	149.9	7.39	66.8	0.44	10.5	3.1	0.05	1.74	2.04	1.3	1.6	148	954	3.0	13.8	13.4	0.341	2.69	567	11.3	1180	130	1350	59.6	5.11	9.7
10	165	3.31	60.5	0.62	10.7	5.2	0.11	2.33	4.47	1.4	3.7	144	949	3.6	19.5	40.1	0.233	3.39	271	39.3	546	173	1440	83.1	6.69	9.7
11	185	1.83	61.5	0.68	12.2	4.4	0.11	1.70	4.33	5.2	3.7	116	1130	3.7	21.0	30.9	1.99	3.10	277	45.6	1220	179	1930	82.7	4.92	10.3
12	200	2.41	62.7	0.67	12.0	5.1	0.10	2.69	5.56	4.3	3.3	29	815	3.9	22.5	32.0	0.069	2.65	891	47.1	N.D	182	1892	119	6.22	10.0

hydrothermal alteration. From these facts, it is thought that plagioclase, biotite and hornblende of primary mineral were decomposed and these chemical components were leached out.

(b) At various depths, it is found that the values of Fe, Mn, Mg, Ca are high. The depth corresponds to the depth of appearance of calcite and dolomite. These components seem to precipitate in the rocks as thermal veins.

(c) High concentrations of K are found at 35 m and is thought to be related to the formation of alunite. Concentration of K is high at depth where biotite which escaped alteration has remained.

(d) The change in B concentration corresponds well with the degree of alteration. Therefore, B seems to concentrate in altered rocks.

(e) Hg and Rb concentrations are high in the high temperature part of DG-1. These components indicate the existance of a geothermal fluid.

(f) Concentrations of metal elements such as Pb deposited in hydrothermal veins at 200 m to 270 m.

(g) Concentration of S appears high as a whole. S appears to be derived from volcanic activity. Therefore it is thought that the area around DG-1 has been active geothermally from the past to present.

2) Rock chemical component in DG-2

(a) Much Si, Al, Mn, Mg, Ca, Na, K were leached out from rocks in DG-2, because alteration is strong as a whole.

(b) The Hg component shows a high value at 65 m. Judging from the temperature in the hole, 30°C, Hg seems to be concentrated in altered rock formed in the past.

3) Rock chemical component in DG-3

(a) The value of H_2O is high, therefore the rocks in DG-1 are presumed to be highly porous.

(b) Thee concentration of Hg and S increases with depth. Therefore, there is a possibility of geothermal activity at depth around DG-3.

As shown in Fig. II.3.72 AFM diagram, the strongly altered rocks in DG-1 and DG-3 have lower contents of $Na_2O + K_2O$ than the original rocks and show a slight increase in T-FeO. It is thought that rock forming minerals such as plagioclase, hornblende and so on were decomposed and Na, K were leached out and Fe deposited in hydrothermal veins.

Fig. II.3.73 Al-(Ca+Na+K)-Mg shows that the changes of chemical compositions are controlled by formation of the secondary minerals such as kaoline, mica, alunite and silica minerals. In DG-1 and DG-2, much mica clay minerals and kaoline were formed by geothermal alteration.

7. Chemical analysis of hot water sampled from holes DG-1, 2 and 3

On the basis ofthe chemical analysis data of hot water sampled from holes DG-1, 2 and 3, the subsurface condition of the geothermal fluid was discussed from a geochemical viewpoint. The chemical compositions of the water samples are shon in Table II.3.11.

(1) On the water sampled from DG-1:

1) The sampled water was of weakly alkaline SO_4-HCO_3 type (Table II.3.11)

2) The contents of mainly dissolved chemical components except for SiO_2 are very similar to those dissolved in the hot water discharging in the Kaynarca hot spring.

3) The temperature of the reservoir which provided mainly the water sampled from DG-1 is calculated to be between 33°C and 67°C using a silica thermometer. However, the temperatures calculated using a Na-K-Ca-Mg thermometer and SO_4-H_2O (oxygen-18) thermometer are relatively high (180 to 194°C). Therefore, it seems tthat the water discharging from DG-1 was composed of low temperature water and high temperature water.

4) Isotopic characteristics (Figs. II.3.74 and 75) of the water from DG-1 are very similar to that of the Kaynarca hot-spring. Therefore, it is reasonable to consider that geothermal fluids originate

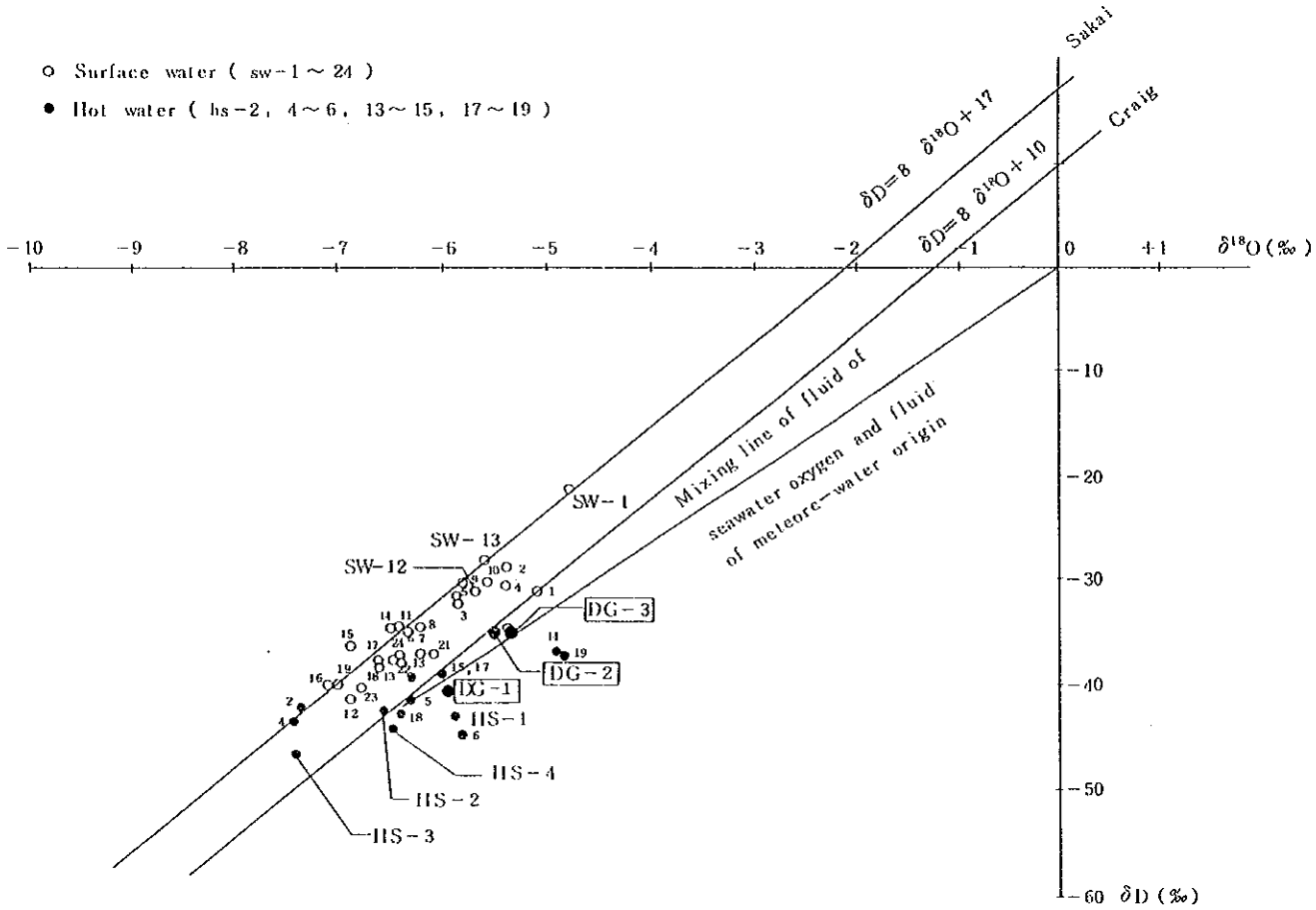

Fig II 3.74 Deuterium and oxygen-18 isotope ratios of hot spring and cold water(surface water) in the Dikili-Bergama geothemal field

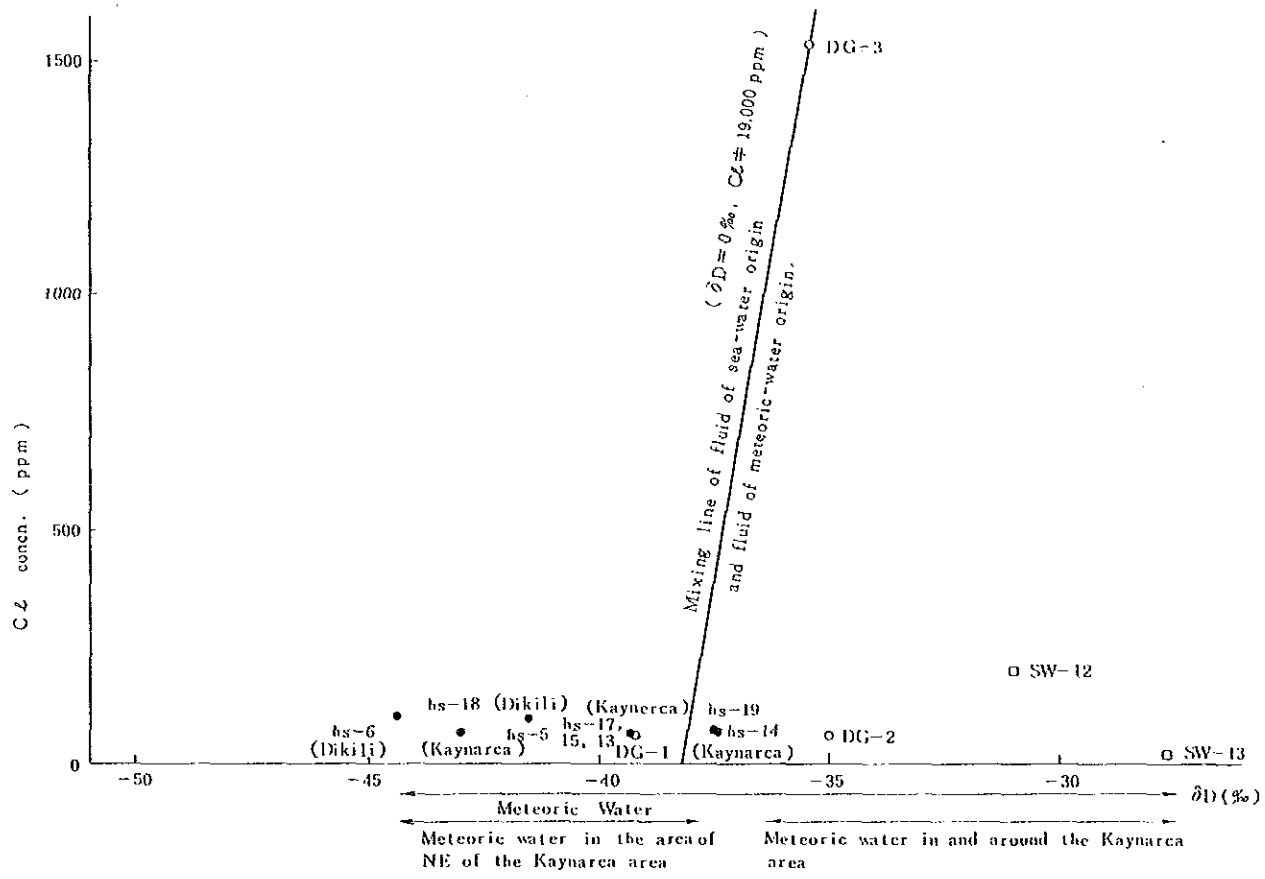

Fig II 3.75 Relationship between Cℓ concentration and δD value in geothermal water in the Dikili−Bergama geothermal field.

Table Ⅱ 3.11 Chemical composition of hot water from thermal gradient hole

Items		DG－1	DG－2	DG－3
pH	－	9.0(25℃)	7.6(25℃)	7.7(25℃)
COND	μs/cm	1800	1170	5500
T－S	mg/ℓ	1180	912	3500
Na	mg/ℓ	363	115	737
K	mg/ℓ	32.1	8.18	87.0
Li	mg/ℓ	0.533	0.077	0.143
Ca	mg/ℓ	10.8	129	313
Mg	mg/ℓ	2.29	28.3	63.0
F	mg/ℓ	4.23	1.68	0.27
Cℓ	mg/ℓ	51.2	63.1	1530
SO_4	mg/ℓ	553	320	131
HCO_3	mg/ℓ	282	281	251
HBO_2	mg/ℓ	6.7	0.7	3.7
T-SiO_2	mg/ℓ	21.6	56.5	96.1
H_2S	mg/ℓ	＜0.03	＜0.03	＜0.03
T－Fe	mg/ℓ	6.90	10.3	0.95
Aℓ	mg/ℓ	0.53	8.53	4.30
Br	mg/ℓ	＜3.0	＜3.0	4.7
I	mg/ℓ	＜0.30	＜0.30	0.48
As	mg/ℓ	0.0061	0.0153	0.0570
NH_4	mg/ℓ	0.67	0.22	0.20
δD (H_2O)	‰	－39.2	－35.0	－35.5
$\delta^{18}O$ (H_2O)	‰	－5.9	－5.6	－5.4
$\delta^{34}S$ (SO_4)	‰	16.3	10.9	13.4
$\delta^{18}O$ (SO_4)	‰	3.2	4.0	10.1
Tritium	T. R	＜0.8	＜0.8	＜0.8
T-CO_2	mg/ℓ	169	189	171

from meteoric water recharged from the northern area and its circulation time from the recharge area to the discharge area is long because of the very low concentration of tritium in the sampled water, as well as the hot water in the Kaynarca hot-spring.

5) The chloride concentration and the Cl/B ratio of the water from DG-1 (Fig. II.3.76) are thought to indicate that the sampled water consists of a mixture of high temperature water discharging from the Kaynarca hot spring and cold groundwater flowing in from the vicinity of Kaynarca at shallow depth. Therefore, it is reasonable to consider that the water discharging from DG-1 is not provided directly from the conduit connecting the Kaynarca hot-spring and the deep reservoir as shown in Fig. II.3.77.

(2) On the water sampled from DG-2:

1) The sampled water was of neutral SO_4-HCO_3 type (Table II.3.11).

2) Contents of dissolved chemical components except for Ca, SO_4 and HCO_3 are low but Cl content in the water is relatively high as compared with those in groundwater recharged from the northern area of the Kaynarca hot spring.

3) Subsurface temperatures calculated with a silica thermometer and a Na-K-Ca-Mg thermometer are 77°C and 50°C, respectively and are considered to be relatively low. However, the SO_4-H_2O (oxygen-18) thermometer giving 185°C, indicates that reservoir at deeper level or far from this well is relatively high temperature.

4) Judging from the isotope ratio data (Figs. II.3.74 and 74), the water sampled from DG-2 is considered to be of meteoric origin. Furthermore, considering the low concentration of tritium in the water and relatively lower delta-D values of the water compared with those of groundwater around this well, the water from DG-2 is considered to be ground water recharged from the northern area of the Kaynarca hot spring.

5) The main water in DG-2 seems to be of meteoric water origin. Deep geothermal water or sea water is considered to mit slightly, because the Cl content in the water is relatively high in com-

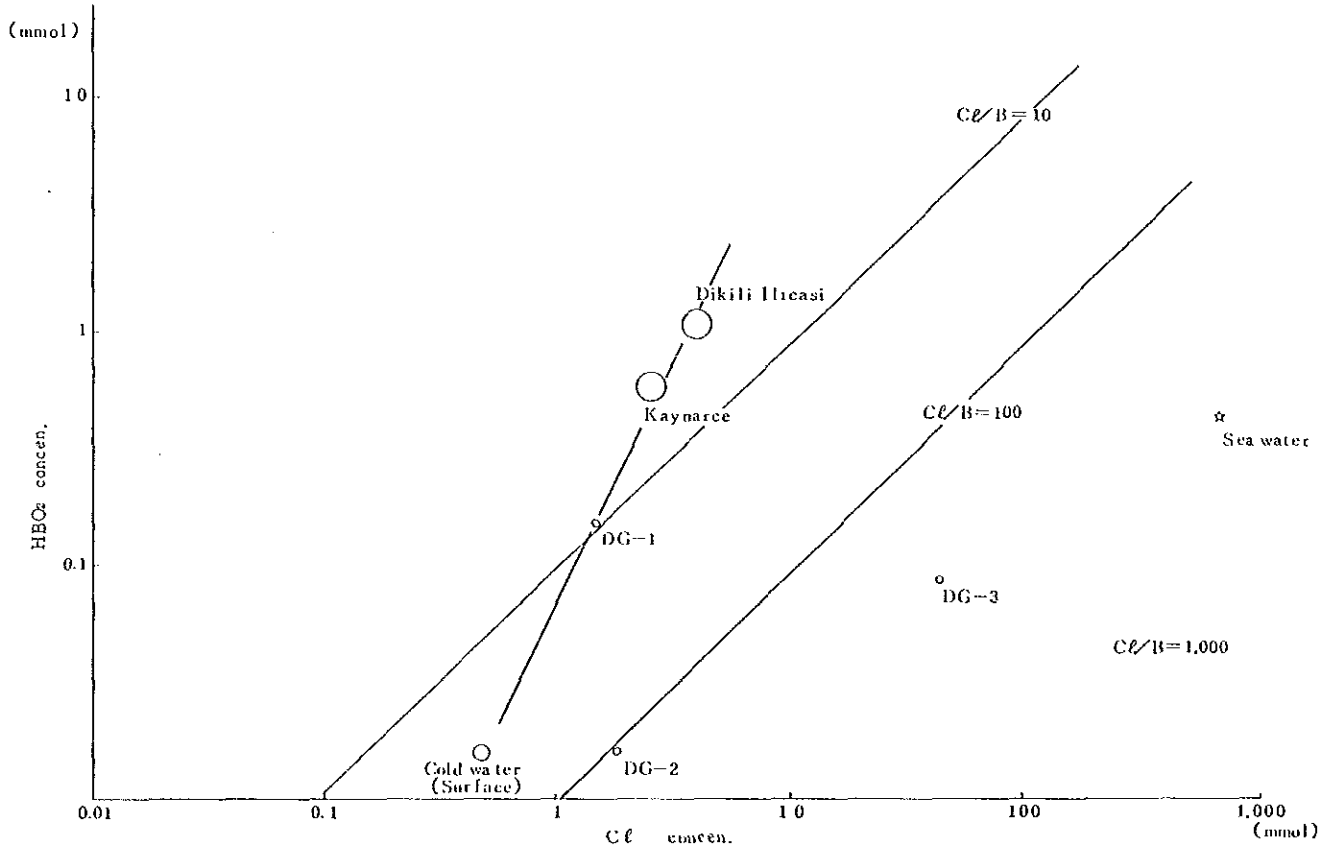

Fig II 3.76 Relationship between Cℓ and HBO_2 Concentration.

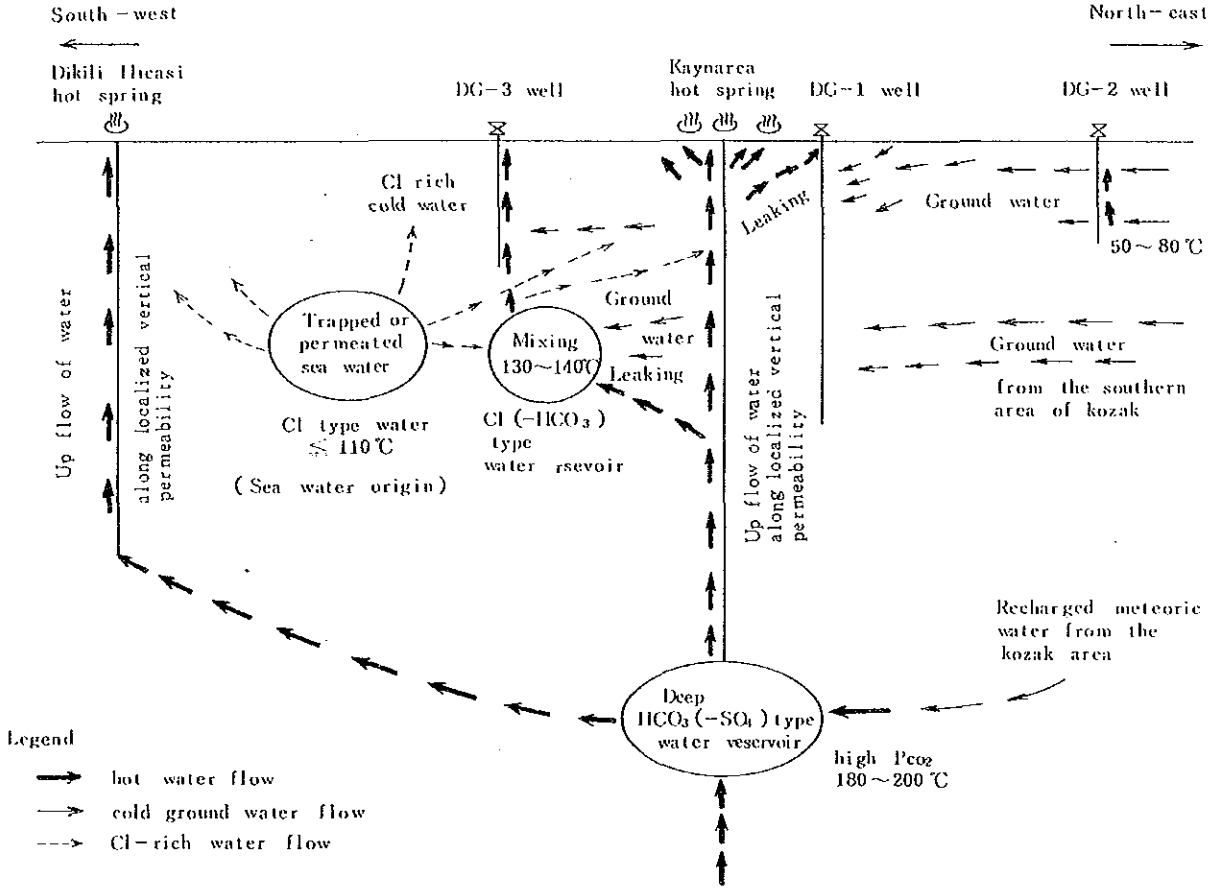

Fig II 3.78 Simplified modal of geothermal fluid estimated from chemical analysis data of temperature gradient holes

parison with that in groundwater in the vicinity as shown in Fig. II.3.76.

(3) On the water sampled from DG-3:

1) The sampled water was of neutral Cl-HCO_3 type (Table II.3.11).

2) Mainly dissolved chemical components such as Na, Ca, Cl, SO_4 and so on in the water have a high concentration.

The concentrations of the dissolved chemical components in the water are considerably high in comparison with those in the hot water discharging from Kaynarca and Dikili Ilıcasi.

3) The temperature of the reservoir which provided the water in hole DG-3 directly are calculated to be 132 to 135°C using a silica thermometer (Quartz) and Na-K-Ca-Mg thermometer. Its temperature is the highest of the drilled holes (DG-1 to 3) in this area. However, the SO_4-H_2O (oxygen-18) thermometer with which the reservoir temperature of deeper level or far from the DG-3 well can be obtained, indicates a relatively low temperature (111°C).

4) Considering Figs. II.3.74, II.3.75 and II.3.76 and Table II.3.12, the hot water from DG-3 seems to be a mixture of hot water discharging from Kaynarca and Dikili Ilıcasi (meteoric water origin) and water of sea-water origin. However, it is reasonable to consider that direct mixing between hot water and sea water does not occur, because of the different characters of delta-$^{34}S(SO_4)$, Cl/B atomic ratio, Cl/As atomic ratio and so on between the DG-3 water and sea water. Containing plenty of SO_4 ion, sea-water origin fluid is considered to be less than 111°C.

5) According to the results' of geochemical survey performed in 1986, there was a possibility that the Cl-rich water contained in hot water discharging from Kaynarca and Dikili Ilıcasi originated from a deep water reservoir. However, judging from the results of this survey using chemical data of the holes, it is possible that the Cl-rich water originates from sea water and its chemical-characteristics have changed by water-rock interaction.

Table II.3.12 Geochemical temperatures and Cℓ/B and Cℓ/As atomic ratios in the waters sampled from DG—1, DG—2, DG—3 and others

		Geochemical Temperature (℃)				Cℓ/B	Cℓ/As
		Quartz	Chalcedony	Na-K-Ca-Mg	SO_4-H_2O		
well	DG—1	67	33	180	194	9.4	17,700
	DG—2	108	77	50	185	111	8,720
	DG—3	135	107	132	111	511	56,700
hot spring	Kaynarca	172 ∫ 200	149 ∫ 182	147 ∫ 178	797 ∫ 218	3.4 ~ 4.5	927 ~ 1270
	Dikili Ilıcasi	136 ∫ 142	108 ∫ 115	148 ∫ 162	229 ∫ 231	2.4 ~ 3.0	218 ~ 366
Cold Spring		—	—	—		34 ~ 49	126,000 ~ 222,000
Present Sea water		—	—	—		1207	4.0×10^7

6) Assuming subsurface dilution of silica with low temperature groundwater, the reservoir temperature is estimated to be approximately 200°C, as shown in Fig. II.3.78.

7) As a results of the survey on the water sampled from holes DG-1, 2 and 3 and previously performed geochemical surveys, the target for future development is considered not to be Cl type but water reservoir but to be SO_4-HCO_3 type hot water reservoir in and around the Kaynarca hot spring and its temperature can be expected to be approximately 200°C (Fig. II.3.78). Furthermore, unfortunately, because of the high content of CO_2 in the water, its depth seems to be considerably deep.

8. Geological structure and geothermal activity in Kaynarca geothermal area

Based on the results of the geological analysis of core and cuttings from the thermal gradient holes and the previous surveys, the geological cross section was drawn in Fig. II.3.79.

From the detailed geological mapping, the depression zone which was located from west to east around Kaynarca was presumed to be filled up by effusive materials from the Demirtas felsic volcanism and Soma formation. However, the core and cuttings in the thermal gradient holes have revealed that the Yuntdağ volcanics III overlie the Yuntdağ volcanics I thickly in the depression zone as shown in the geological cross section.

Many fractures and hydrothermal veins are found at depths of 100 m to 250 m in the spot core of DG-1. The direction of many fractures in this zone is east-west. It is presumed that these fractures and veins accompany the east-west fault. DG-1 seems to cut the fault or was drilled near the fault at shallow part, because this fault near DG-1 is presumed to dip south from the gravity survey and the geological survey. Therefore, DG-1 was drilled on the horst side in the depression zone.

The isothermal line in the subsurface around the thermal gradient holes is shown in Fig. II.3.80. The temperature in the subsurface increases along the fault. In DG-1, the temperature increases rapidly from the surface to a depth of 40 m and the heat flow is large, 12.75 HFU.

The hot water reservoir of about 100°C is presumed to exist in Alluvium and the upper part of the Dikili lava from a depth of 10 m to 100 m around DG-1

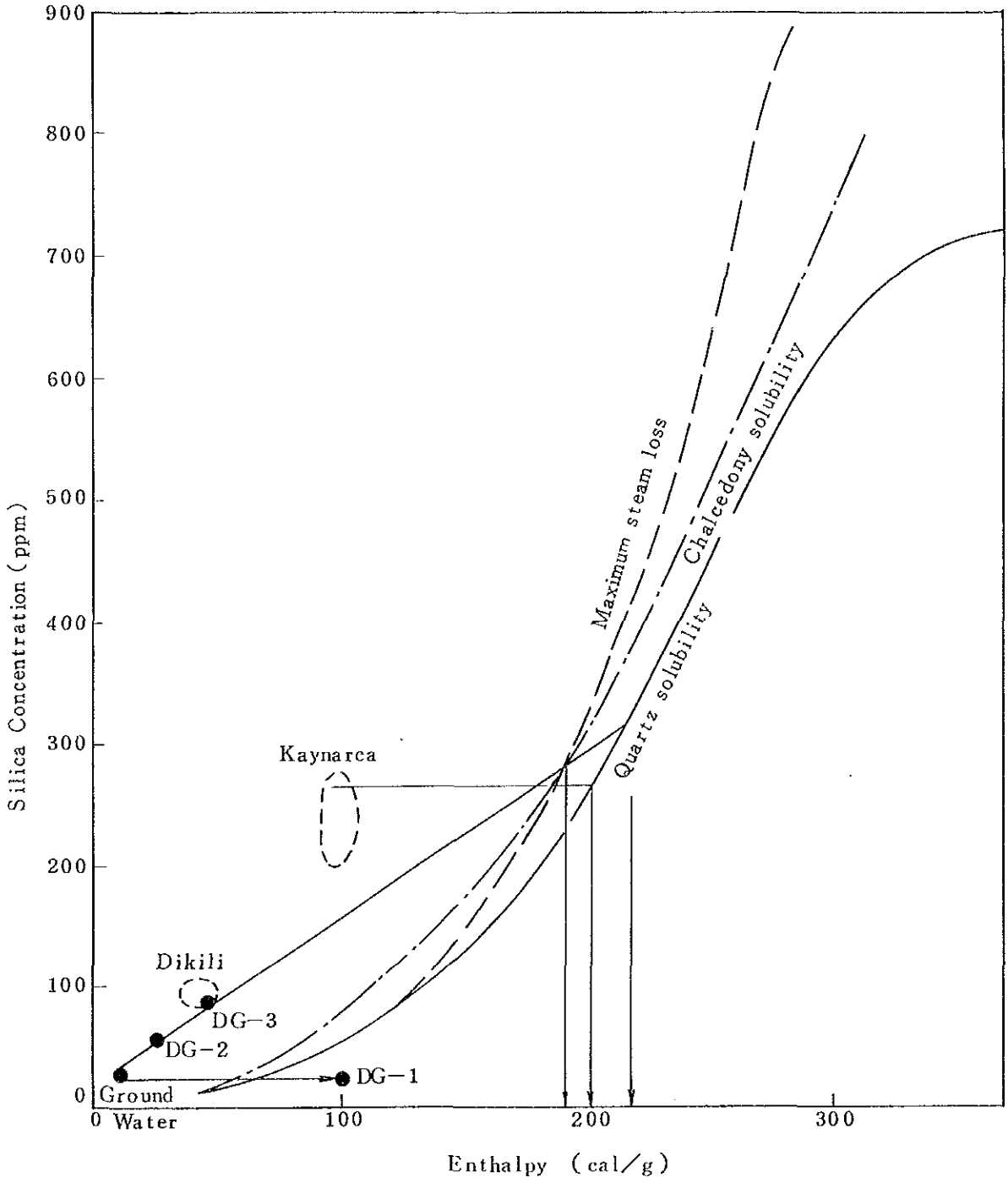

Fig II 3.77 Silica temperature using mixing model

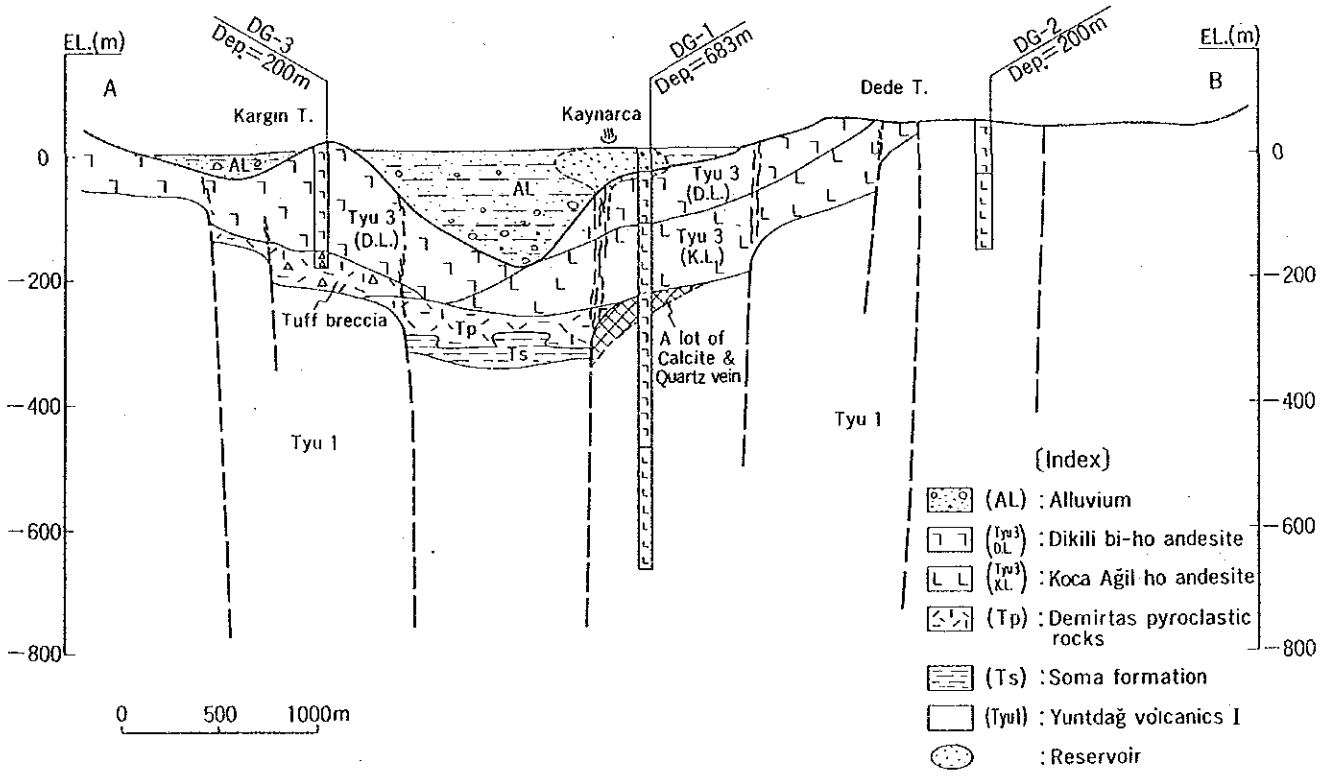

Fig. II.3.79 Geological cross section of the Kaynarca geothermal area.

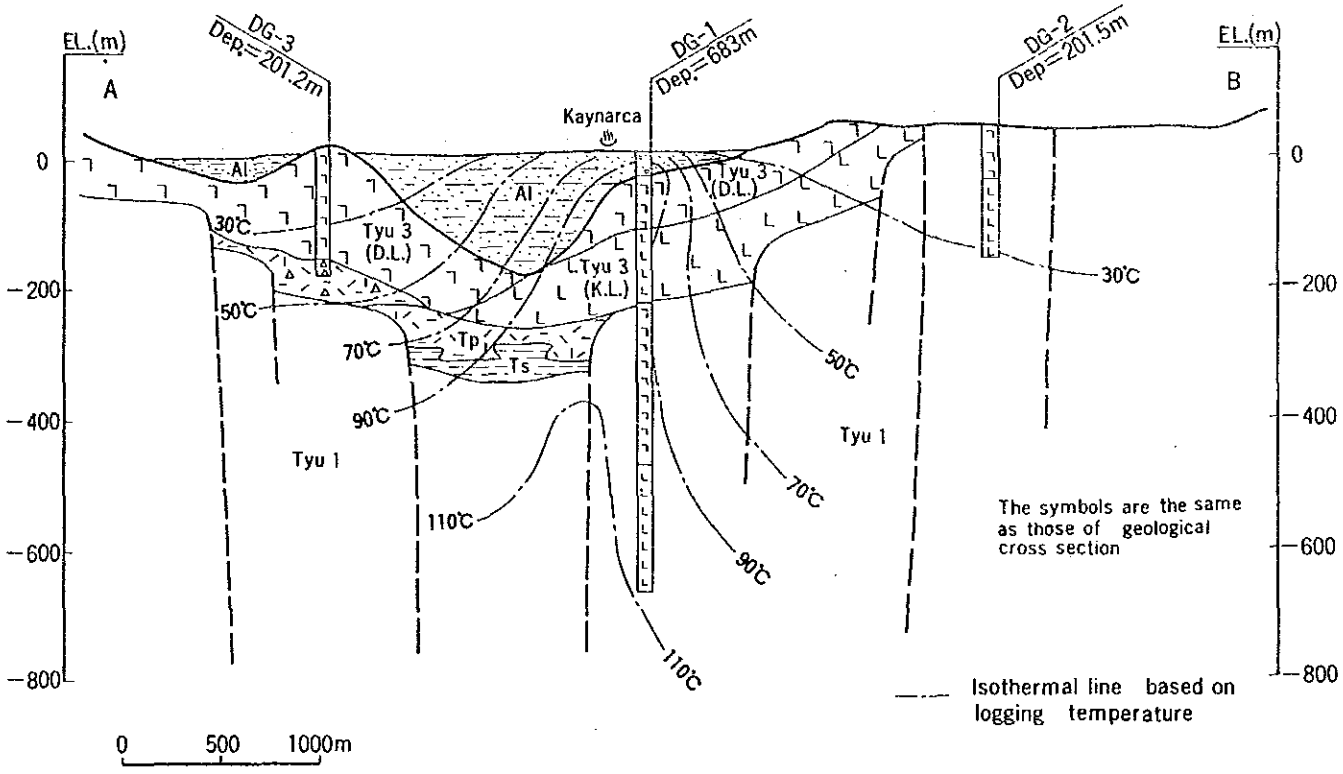

Fig. II. 3. 80 Isothermal line of the Kaynarca geothermal area.

because cristobalite changes to quartz, Hg concentration is high and a small lost circulation was confirmed at 95 m.

From 100 m to 500 m, the temperature gradient is small and the temperature is fixed. The lost circulation was not confirmed deeper than 100 m. This part corresponds to the massive and impermeable rocks of the Yuntdağ volcanics I.

At depths greater than 500 m, the temperature in the hole increases gradually. From the results of the chemical analysis of the thermal gradient hole, the existence of a hot water reservoir of 180°C to 200°C is expected at depth below Kaynarca.

Judging from the mean temperature gradient (5 to 10°C/100 m) in the hole, it is presumed that the depth of the hot water reservoir is greater than 1,000 m.

CHAPTER III. INTEGRATED ASSESSMENT

CHAPTER III. INTEGRATED ASSESSMENT

III.1 Delimitation of the geological reservoir and modelling of the geothermal system

III.1.1 Delimitation of the geothermal reservoir

The shallow reservoir in Kaynarca which was observed as low resistivity zones probably extends into the alluvial deposits near the surface, while, there is a high possibility that a deep reservoir is formed in the fracture zones in the Tertiary volcanic rocks.

It is considered that the resistivity values in the Tertiary volcanic rocks are not so low compared with those of shallow reservoir and sedimentary rocks.

A deep reservoir was roughly delimited by elucidating the existence of the faults as a passage of geothermal fluid from the geological survey, geochemical survey, CSAMT survey and Misc-á-la-masse survey.

In Fig. III.1.1, the shallow reservoir in the Kaynarca area is presumably shown as a high longitudinal conductance extending in the southern part of the Kaynarca. It is correlated with the high anomaly zone of Hg content in soil and soil air. Accordingly, it is defined that the shallow reservoir is formed to the south of the Kaynarca hot spring.

From the results of geological survey and geophysical explorations, the reservoir is through to extend southward from NW-SE tending faults through the Kaynarca.

On the other hand, a deep reservoir in and around Kaynarca is considered to be developed in fracture zones along the following three faults; NE-SW, NW-SE and E-W trends. As shown in Fig. II.3.57, a low residual potential zone detected by the Mise-á-la-masse survey extends roughly from the NE to the SW. That is, Kaynarca is situated at the intersection of the NE-SW trending fault and NW-SE trending falult. Besides, the area 200 m southeast from well DG-1 is not only of obviously high longitudinal conductance zone but also of low residual potential anomaly zone. Accordingly, there is a high possibility that the anomaly area represents a conduit for geothermal fluid from the deep reservoir.

III.1.2 Conceptual geothermal model

From the results of three stage explorations, the geothermal system model in and around the Kyanarca area is illustrated as shown in Fig. III.1.2.

In the Dikili-Bergama geothermal area, an E-W trending basin extends from Kiriklar to Dikili. There are two hot spring, one at Kaynarca characterized by boiling hot spring and one at Dikili Ilıcasi characterized by relatively high Cl content in the hot spring. The basin is formed by the movements of the WNW-ESE trending fault and the NW-SE fault, it is observed as a district low gravity anomaly.

In addition to the abovementioned E-W trending fault, there are two kinds of faults trending NW-SE and NE-SW. Hot springs and hydrothermal altered zone tend to arrange along those faults. Therefore, it is clear that geothermal fluid is coming up along the faults and must be partially reserved in fracture zones.

As to fracture in outcrops of Tertiary to Quaternary volcanic rocks, the NW-SE trending fractures are predominant. Especially most of the fractures which are filled with secondary minerals trend in a NW-SE direction. It is concluded that near surface geothermal activity is caused by thermal fluid that has flowed up in fractures along faults.

In Kaynarca, the NE-SW trending fault was determined by Hg concentrations in the soil and soil air, distribution of high longitudinal conductance zone and low residual potential zone as shown in Fig. III.1.1. The fact implies that there is a NE-SW fault trend besides the NW-SE trending fault. Kaynarca is situated at the intersection of these two faults.

The geological structure of the pre-Tertiary rocks and Kozak pluton that make up the basement is characterized by small grabens and horsts formed mainly by NW-SE and E-W trending faults. Hot springs at Dikili Ilıcasi and Kaynarca are distributed on the south and north margins of a graben respectively.

The geothermal reservoir in the Kaynarca area is expected in the fracture zone of the Yuntdağ volcanics I lava flow. Moreover, there is a possibility that a reservoir seats in limestone intercalated with pre-Tertiary basement. Tuff and tuff breccia which are interbedded with the Yuntdağ volcanics I and Demirtas pyroclastic rocks may form sealing layer for the deep reservoir. These sealing layers are overlain by the Yuntdağ volcanics III and alluvial deposits. The shallow reservoir must be developed in a permeable zone of them.

The Sulu Kaya lava and the Koca Tepe lava which resulted from the latest volcanism in the survey area are distributed between the Kaynarca and Kocaoba hot springs. There is a great possibility that the post volcanism in the heat source for the present geothermal activity. In fact, a low residual potential zone is situates at the southern slope of Mt. Sulu Kaya, and it supports the above possibility.

From the results of hydrothermal alteration survey, it is made clear that the

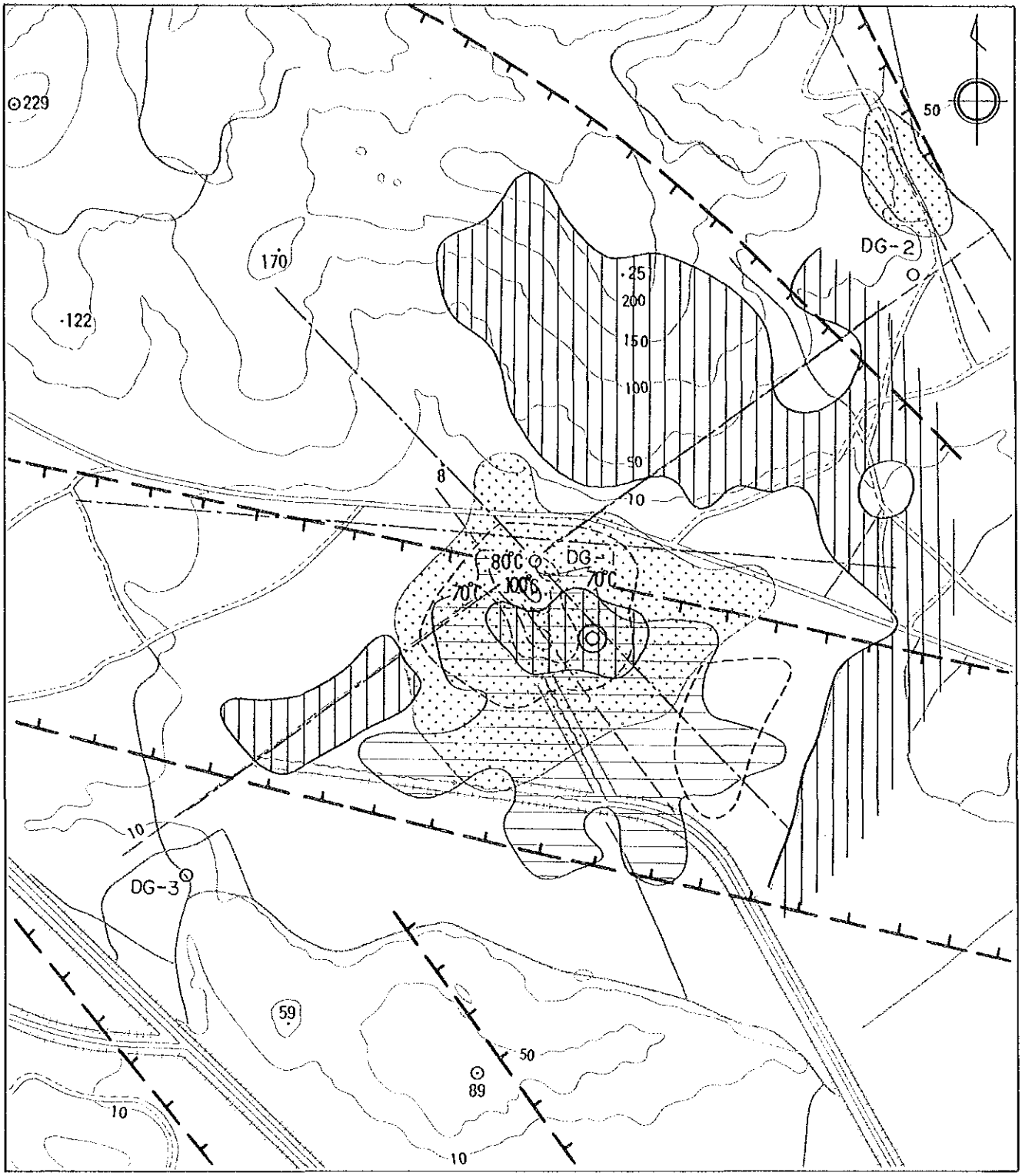

Legend

- : Kaynarca hot spring area
- O : Thermal gradient hole (DG-1～DG-3)
- : Estimated faults from geological survey and gravity anomaly
- 100℃ : Temperature contour of hot spring and fumarole
- : Recommended site for deep exploratory well
- : Overlapped area of high Hg contents in soil and soil-gas
- : Estimated faults from geochemical survey
- : High longitudial conductance zone (more than 130 mho, CSAMT)
- : Low residual potential zone (less than −0.5×10 mV/A, mise-a-la-mase)
- : Estimated faults from CSAMT

Fig. III.1.1 Synthetic interpretation map

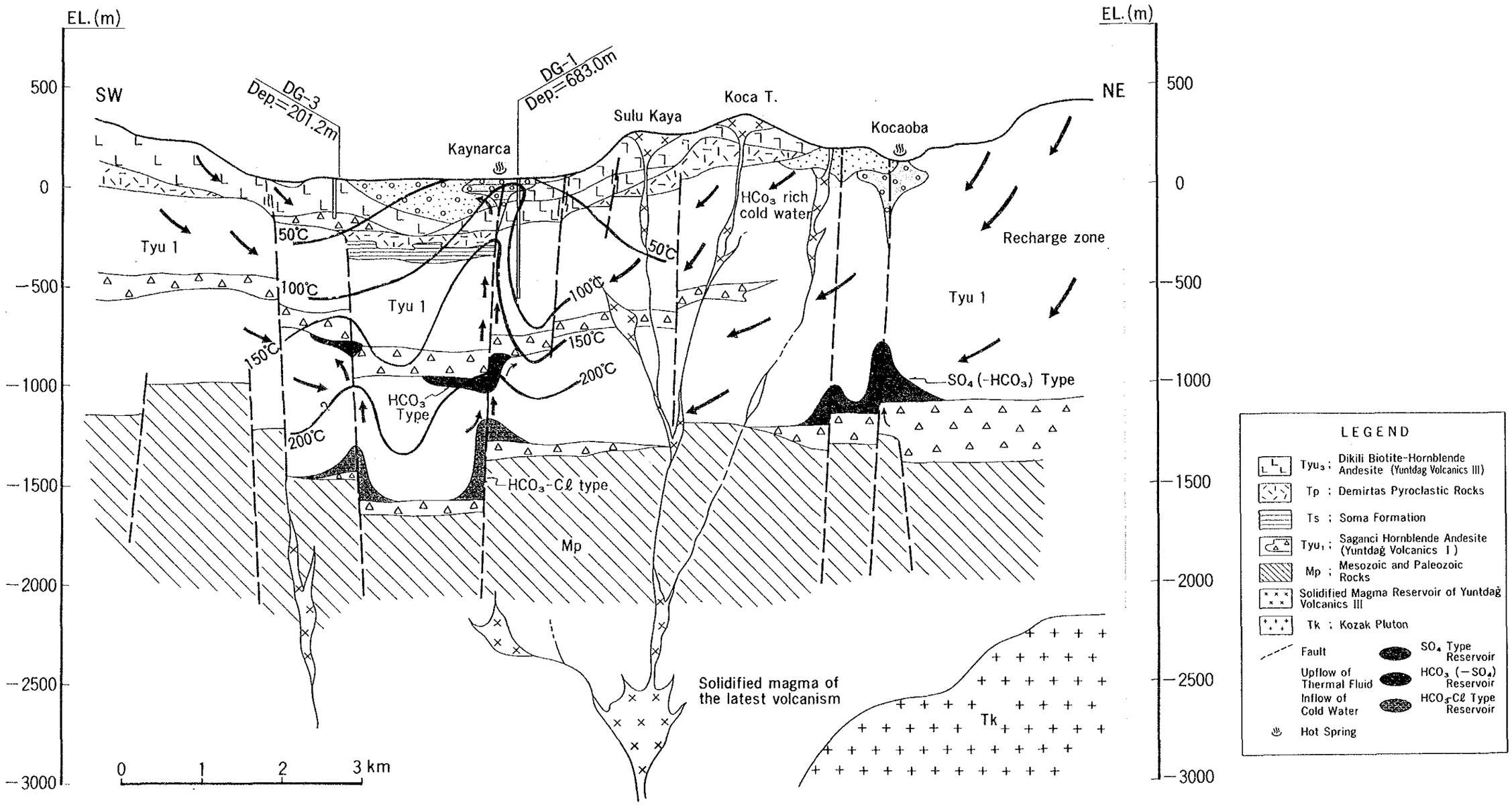

Fig. III.1.2 Conceptual model of the Kaynarca geothermal area

geothermal activity was affected by the volcanism of Miocene age to Piocene age and has continued.

The geothermal system (the Kaynarca system) of the most prospective area in the Dikili-Bergama geothermal area was interpreted on the basis of the chemical characteristics of hot springs and surface water. Geothermal fluid in the Kaynarca system is of water-dominated type and originated from meteroric water.

In the Kaynarca geothermal area, there are presumably two kinds of reservoirs; a shallow reservoir and a deep reservoir. The former is formed mainly in alluvial deposits, and the latter is formed in fracture zones of Tertiary volcanic rocks, Yuntdağ I. Hot water in the both reservoirs is mainly of neutral HCO_3 type.

The reservoir temperature of the water reserved at depth is thought to be 180 to 200°C. Furthermore, a 220 to 230°C reservoir at greater depth is inferred from the isotope thermometer results. Considering water-rock reaction, it is possible to assume that this water at deeper level is of neutral HCO_3-Cl type. Besides, neutral Cl type water of relatively low temperature (lower than 110°C) and of sea water origin is reserved around this system. The hot water discharging in Kaynarca and Dikili Ilıcasi is formed by mixing of these waters and ground water. The neutral $HCO_3(-SO_4)$ type water seems to be common in the both waters and must be main constituent water in the Kaynarca system. The neutral $HCO_3(-SO_4)$ water higher than 180°C is considered to be restricted to the area in and around Kaynarca and to be reserved at considerably deep level due to high PCO_2. Besides, judging from the results of the CSAMT survey, the prospective reservoir is estimated to exist at the depth of more than 800 m. It is concluded that the depth of the reservoir is relatively deep for approximately 200°C water in comparison with other active geothermal systems.

The circulating time of water recharged from the surface to the northwest of Kaynarca in this system is relatively long (more than 75 years). Therefore, similar to other active geothermal systems, this hydrothermal system is considered to be broadened considerably.

This water of high temperature is considered to be up-flowing in the fracture zone developed at the intersection of the NW-SE trending fault and NE-SW trending one from the results of CSAMT survey, Mise-á-la-masse survey and geochemical survey. Unfortunately, well DG-1 (683 m in depth) could not encounter the fracture zone along the fault, and the high temperature reservoir could not be confirmed. However, the drilling did revealed that the high temperature water is flowing up in limited conduit and does not spread out horizontally to a depth of 700 m. These results are supported by the Mise-á-la-masse survey.

As described above, a geothermal fluid of higher than 200°C is expected to be reserved at great depth in the Kaynarca area. However, it is difficult to consider that the fluid is reserved at a depth shallower than 1,000 m and is broadened considerably at depths.

III.2 Assessment of the geothermal potential (feasibility of electric power development)

III.2.1 Assessment of geothermal potential

In this section, the major conclusions arising from each result, that are of particular geothermal significance, are summarized. These conclusions are combined to construct an overall concept of the resource for assessment on the feasibility of electric power development in the Kaynarca area in the Dikili-Bergama geothermal area.

1. The heat source of the geothermal activity in the Kaynarca area is considered to be related to the post-volcanism of the Sulu Kaya lava and the Koca Tepe lava which were the latest volcanism in the Dikili-Bergama geothermal area. But, unfortunately it is presumed that the geothermal activity following a vigorous period in the study area has been declining, because, the latest volcano in the area erupted before 2 million years BP in Pliocene time and its activity must be small.

2. The chemical characteristics of hot water discharging from the Kaynarca hot spring indicate that geothermal fluid of 180°C to 200°C is reserved in fracture zones in the Tertiary volcanic rocks, Yuntdağ volcanics I at depth. However, a isotope thermometer gives temperature higher than 220°C which is presumed to represent a deeper reservoir but is not confirmed.

3. Judging from the Hg anomaly in the geochemical survey, the extent of high longitudinal conductance zones by the CSAMT survey and low residual potential zones by the Mise-á-la-masse survey, the geothermal reservoir (1 km^2) is probably located to the south of the Kaynarca. High temperature water from deep level is considered to be flowing up through limited conduits at the intersection of NE-SW trending and NW-SE trending faults.

4. The thickness of low resistivity zones around the discontinuities in the electrical basement ranges between 600 and 800 m from the results of electrical surveys. Considering that the geothermal reservoirs are mostly formed in the electrical basement, the expected reservoir in the survey area is estimated to exist at depths greater than 800 m.

5. The problems of calcium carbonate scale deposition in production wells (expensive steam supply system) and low quality of steam containing a high

content of non-condensable gas (low efficiency of generation of electric power) will cause difficulties in the future development in the Kaynarca area.

As described above, it is scarcely expected that a geothermal fluid of higher than 200°C is reserved at depths shallower than 1,000 m in the Kaynarca area which is considered to be the most active in the Dikili-Bergama geothermal area. The activity (geothermal potential) of this area seems to be relatively low, compared with those of other geothermal areas, even with those of the Kızıldere and Germencik geothermal areas in Turkey.

III.2.2 Feasibility of electric power development in the Kaynarca area

Geothermal activity (geothermal potential) in the Kaynarca area, such as temperature of reservoir fluid, depth and size of the reservoir and predicted problems in the future development (carbonate scale and noncondensable gas troubles) was discussed in the previous section. From the results of the prefeasibility study, it is judged that the economical development for electric power generation in the Dikili-Bergama geothermal area is not feasible at present.

CHAPTER IV. FUTURE DEVELOPMENT PLAN

CHAPTER IV. FUTURE DEVELOPMENT PLAN

IV.1 Plan of the future development

For the development of geothermal resource, it is recommended to prepare an exploration strategy by considering peculiarities of the study area, and to proceed with the exploration step by step. For instance, it is recommended to make a flow chart for the development such as that shown at the beginning of the Study, to understand the purpose and applicable limitation of each exploration method, and then evaluate the results of each step by integrated analysis. In accordance with the evaluation of each step, it will be necessary to decide to proceed or interrupt the project, or to modify the exploration strategy.

As a result of the Study, the geothermal potential of the Kaynarca area which was selected as the most prospective area in the Dikili-Bergama geothermal area is not so high to develop a geothermal power plant from an economical point of view. There is, however, a possibility that a deep reservoir exists at the Kaynarca geothermal area from the results of the Study and by comparing to other geothermal fields in Turkey. For example the temperature of production well in the Germancik-Omerbeyli geothermal field is around 90°C at a depth of 600 m. 1,100 m depth, the temperature reaches 206°C. The potential of the Kaynarca geothermal area will be evaluated as feasible to utilize for power generation by new devices in the future. Deep exploratory wells (1,500 to 2,000 m in depth) should be drilled to confirm the reservoir.

The site for the deep exploratory well is recommended at about 200 m south of DG-1, and is shown in Fig. III.1.1.

Considering the peculiarities of the project area, there is a possibility to develop the deep reservoir at the Kaynarca geothermal area for multi purpose utilization.

IV.2 Multi-purpose utilization of the geothermal resource

Collection of mineral matters and heating applications are the main subjects of multi purpose utilization of geothermal resources in general. CO_2 gas collection to produce dry ice is one possible utilizations of the geothermal resource of the Kaynarca geothermal area.

The project area is not a residential area or an industrial area, but is used only for sheep pasturage in winter. Therefore, for the planning of multi purpose utilizations of geothermal resource at the survey area, it is recommended to keep high load factor by combining applications in winter and in summer. For example, a combination of green-

house heating and cattle house heating in winter, and grass drying and refrigeration using a heat pump in summer. Other utilizations are process heating for the leather industry and carpet industry which are a special product of Turkey.

It is necessary to carry out a demand study and an economic study to make a firm plan of the multi purpose utilization.

IV.3 Prediction of scale deposition in future geothermal utilization scheme and recommendation on scale prevention method

In general, there are two kinds of scales deposited in equipment of geothermal power plants. Scale in the steam supply system such as production wells, two phase fluid transportation pipes, etc. and in the reinjection system such as transportation pipes of hot water after separation of steam, reinjection wells etc. are mostly constituted of calcium carbonate ($CaCO_3$) and silica (SiO_2) respectively. If a separator with insufficient capacity is used, scale such as silica and sodium chloride sometimes deposits on turbine blades in the power plant.

The mechanism of each scale deposition is not uniform and factors effecting on the scale deposition depend on each reaction of scale formation. Therefore, in case of considering countermeasures against the scale troubles in a geothermal power plant, the objective scale formation mechanism has to be fully understood. Then, the most suitable countermeasure has to be selected.

It is difficult to predict the scale troubles from the results of surface surveys such as geological survey, geochemical survey and geophysical surveys. Especially, scaling in the steam supply system can not be predicted without understanding accurate physical and chemical conditions of the subsurface fluid. If the conditions of the subsurface fluid is revealed by an exploratory well, the scale deposition in the future development can be predicted easily. During the Study, unfortunately geothermal fluid could not discharge successfully from the wells of DG-1, 2 and 3, and therefore, the characteristics of the subsurface fluid for future development could not be determined. Therefore, assuming that chemical characteristics of hot water discharging from the Kaynarca hot spring are the same as those of reservoir water at depths, scale deposition in this area is predicted. On the basis of the predicted results, a reasonable and the most suitable countermeasure is recommended.

IV.3.1 Prediction of scale deposition

As described in the previous reports (Progress Report II) the subsurface fluid of the Dikili-Kaynarca system is composed of Na-Ca-SO_4 (-HCO_3) type water and Na-Ca-

HCO_3 (-Cl) type water containing relatively rich-Cl ion. It is considered that hot waters discharging from DG-2 and from DG-3 mainly consist of the former water and of the latter water, respectively.

The water discharging from the Kaynarca hot spring is of neutral (pH 7.4 to 8.7) Na-Ca-SO_4 (-HCO_3) type and its subsurface temperature was estimated to be a maximum of 220 to 230°C. Since bubbling gas composed of CO_2 is the main components in the Kaynarca hot spring, the PCO_2 of reservoir fluid must be high compared with those of other geothermal systems. The chemical characteristics of hot waters discharging from hot springs in Kaynarca are analogous to each other. Regarding the chemical components related to scaling, HCO_3 ion and T-CO_2 contents are high, but Ca ion and SiO_2 content are low in concentration.

On the basis of the chemical characteristics of hot water discharging form the Kaynarca hot spring scale deposition in the future development is predicted.

At present, there are two methods to predict calcium carbonate scale formation using chemical data of the hot water. One is the method of saturation index S_{IC} (S_{IC} = [practically measured activity product]/[thermodynamic activity product]) and the other is the method of Langelier saturation index S (S = pH [measured] – pHs [calculated]). Quantitative prediction of scaling can not be performed using these two methods. However calcium carbonate scale tends to deposit from the waters having high S_{IC} and S values. These indexes of S_{IC} and S seem to be excellent qualitative indicators. In this study, scale deposition of the Kaynarca geothermal system was discussed using the Langelier saturation index.

The calculated results are described in Progress Reports I and II. The value of the Langelier saturation index of each hot water discharging from the Kaynarca hot spring is not high. However, all S values of the hot water are positive and the hot water are considered to be supersaturated with $CaCO_3$. Empirically, $CaCO_3$ scale tends to deposit from hot water having more than +1.0 S and 60°C. In practice, scale deposition from the water of more than +2.0S seems to be troublesome. In the case of the boiling hot-spring in Kaynarca, S value indicated to be +1.8. Therefore, it is assumed from the S value of the boiling hot spring that the carbonate scale troubles will occur in the steam supply system in the future development at Kaynarca. If the reservoir of high PCO_2, namely hot water containing Ca and CO_3 ions is developed, there is a high possibility of $CaCO_3$ scale deposition.

In the case of prediction on silica scaling, the possibility of silica scale is generally judged from the supersaturated concentration of monosilicic acid and the pH of hot water. Prediction for the hot water in the Kaynarca system was performed using

estimated silica content assuming the reservoir temperature calculated with geochemical thermometers. If the production wells tap the 200°C reservoir, the concentration of monosilicic acid in discharging hot water after the separation of steam is calculated to be about 340 ppm SiO_2. Silica in water above 99°C does not tend to deposit due to the concentration being lower than the solubility of silica. Therefore, it is not necessary to pre-treat the hot water after steam separation for reinjection. In the case of tapping the 220°C reservoir by production wells, however, concentration of monosilicic acid in discharging water after the separation of steam is about 450 ppm SiO_2. Therefore, in order to avoid scale trouble, it is necessary to pretreat the hot water after steam separation or to keep the water-temperature higher than 120°C for reinjection. If open-air type channels or pipelines and reinjection wells for the reinjection water are adopted without pretreatment of the reinjection water, silica scale must deposit in them and the flow rate in the channel or pipeline and reinjection capacity of the well must decrease. Concerning the reservoir of relatively low temperature in this area, it is considered that there is no terrible silica scale trouble but there is calcium carbonate scale. For development of the Kaynarca area, calcium carbonate scale in production wells has to be noted.

IV.3.2 Scale prevention method

Since deposition of calcium carbonate scale in the steam supply system is anticipated, countermeasures against the carbonate scale are described in detail here.

Formation of $CaCO_3$ is expressed by the following chemical reaction.

$$Ca^{2+} + CO_3^{2-} \rightarrow CaCO_3 \text{ (ppt)}$$

The concentration of carbonate ion [CO_3^{2-}] relating to the above reaction is increased and the reaction rate is accelerated by the following degassing reactions.

$$2HCO_3^- \rightarrow CO_2 \text{ (Aq)} + CO_3^{2-} + H_2O$$

$$HCO_3^- + H^+ \rightarrow CO_2 \text{ (Aq)} + H_2O$$

$$CO_2 \text{ (Aq)} \rightarrow CO_2 \text{ (Vap)}$$

Therefore, if the above reactions can be prevented, scaling in the steam supply system can be mitigated.

The following reaction tends to occur at a flashing point in the production well. Practically, the scale deposited in a few meter length from flashing point and tapers upwards in shape, as shown in Fig. IV.3.1. Therefore, treatment for scale prevention has

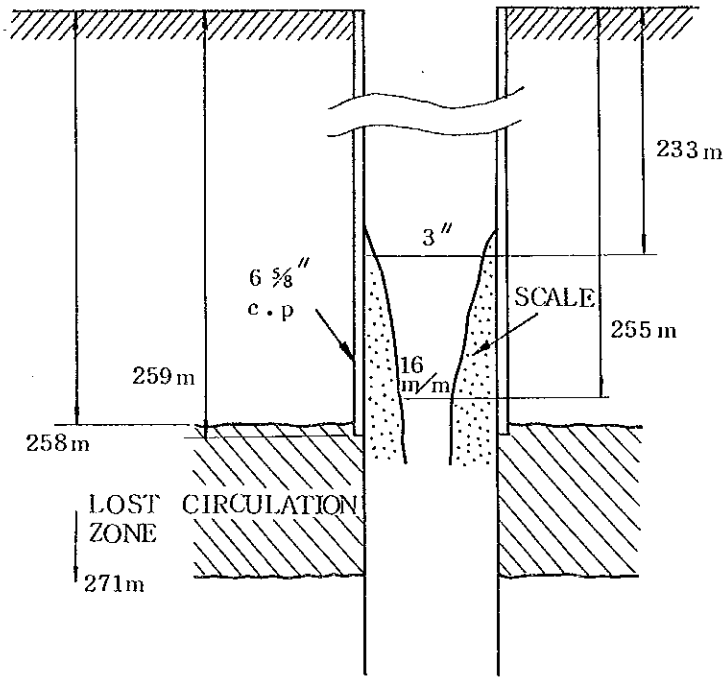

Fig. Ⅳ. 3. 1 An example of carbonate scale deposited in a production well
(Otake geothemal field)

to be performed below the flashing point. In the case of flashing in the reservoir, $CaCO_3$ deposits clog cracks in rocks. In this case, flashing point has to be controlled for the treatment by operating the wellhead valve.

So far, various prevention methods against carbonate scaling such as wellhead pressure controlling, water injection, downhole mechanical pump, carbonic acid equilibrium system, injection of chemicals and so on have been developed. At present, considering successful cases in Japan (the Mori and Noya geothermal fields) and theory on chemical reaction of scaling, the injection of chemicals such as polyacrylate, etc. are recommended. Adding a slight amount of sodium polyacrylate into the geothermal water (less than a few ppm) decreases the carbonate scale formation rate. This method does not effect the surrounding environment because of the low concentration. According to the report on carbonate scaling investigation, it is advisable to inject sodium polyacrylate into a production well.

Besides, the injection of phosphate reagent or mineral acid is expected to be effective. Acidification by acid injection is considered to be effective for prevention of not only calcium carbonate but also silica. The efficiency of inhibitor against corrosion, however, has not been proven under injection conditions at high temperature. So, for adoption of the acid injection, test work is required to confirm materials and down-hole chemical-problems at a depth.

The chemicals have to be injected below the flashing point in a production well using injection pipes as shown in Fig. IV.3.2. As change of physical characteristics (enthalpy, pressure and flow rate) of discharge from the well is probably caused by the installation of a chemical injection pipe in the well and the injection pipe is possibly eroded in strongly discharging well, the injection pipe should be installed outside of the well. As described previously, superior techniques for the injection of chemicals are required, because the chemicals have to be injected at a depth below the flashing point of high pressure and temperature from the surface. Various factors relating to this method have to be investigated in detail. The procedure of this method is considered as follows.

(1) Estimation of the depth of the flashing point in advance of installation work of the chemicals injection pipe.

(2) Check on adequate materials for injection pump and pipe.

(3) The choice of effective chemicals and their injection pressure and flow rate from the surface on the basis of estimated chemical and physical characteristics of subsurface fluid.

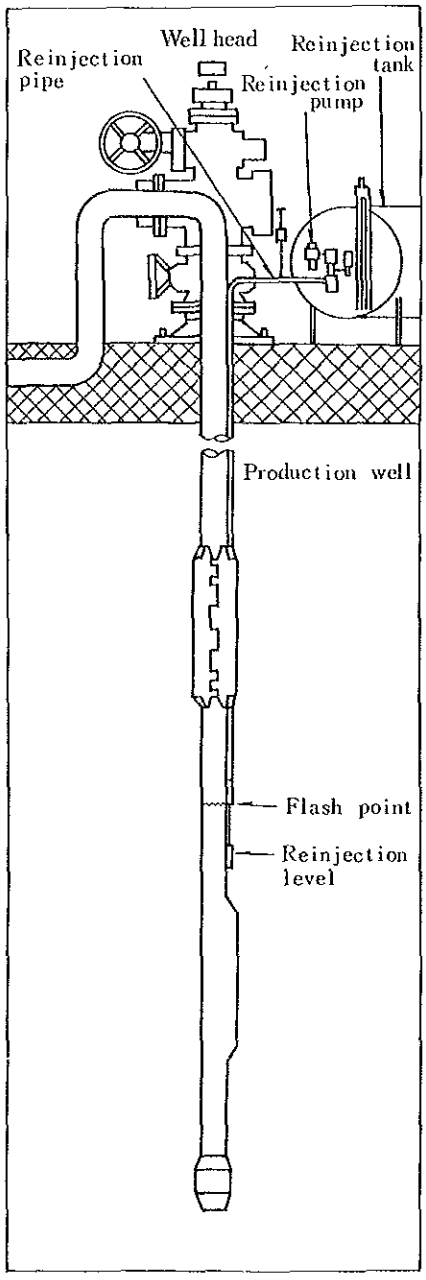

Fig. Ⅳ. 3. 2 Injection system of chemicals for carbonate scale prevention

Regarding the cleaning of production wells clogged with calcium carbonate scale, the scale can be removed mechanically because the deposition of carbonate scale is around the flashing point in the wells, but dissolution of the scale by injection of acid solution with corrosion inhibitor seems to be effective. In case of adopting the acid injection method, the efficiency of the inhibitor and handling of the strong acid solution should be noted.

Neglecting the cost of the removal and prevention methods, it is recommended that the calcium carbonate scale problems in wells and pipes in Turkey are solved by using the above methods.